FUNDAMENTALS OF PHOTONICS

THIRD EDITION

SOLUTIONS MANUAL

FOR EXERCISES†

† A solutions manual is not available for the end-of-chapter problems

FEBRUARY 20, 2019

BAHAA E. A. SALEH
University of Central Florida
Boston University

MALVIN CARL TEICH
Boston University
Columbia University

JOHN WILEY & SONS, INC.

This edition first published 2019

Registered Office
John Wiley & Sons, Inc., 111 River Street, Hoboken, NJ 07030, USA

Editorial Office
111 River Street, Hoboken, NJ 07030, USA

For details of our global editorial offices, customer services, and more information about Wiley products visit us at www.wiley.com.

Wiley also publishes its books in a variety of electronic formats and by print-on-demand. Some content that appears in standard print versions of this book may not be available in other formats.

Library of Congress Cataloging-in-Publication Data is available.
Volume Set ISBN: 9781119506874
Volume I ISBN: 9781119506867
Volume II ISBN: 9781119506898

Printed in the United States of America

10 9 8 7 6 5 4 3 2 1

CHAPTER
1

RAY OPTICS

1.1 POSTULATES OF RAY OPTICS

EXERCISE 1.1-1

Proof of Snell's Law

The pathlength is given by $n_1 d_1 \sec\theta_1 + n_2 d_2 \sec\theta_2$. (1)

The pathlength is a function of θ_1 and θ_2, which are related by

$$d_1 \tan\theta_1 + d_2 \tan\theta_2 = d. \quad (2)$$

The pathlength is minimized when $\dfrac{\partial}{\partial\theta_1}[n_1 d_1 \sec\theta_1 + n_2 d_2 \sec\theta_2] = 0$,
i.e., when $n_1 d_1 \sec\theta_1 \tan\theta_1 + n_2 d_2 \sec\theta_2 \tan\theta_2 (\partial\theta_2/\partial\theta_1) = 0$. (3)

From (2), we have $\dfrac{\partial}{\partial\theta_1}[d_1 \tan\theta_1 + d_2 \tan\theta_2] = 0$,

so that $d_1 \sec^2\theta_1 + d_2 \sec^2\theta_2 (\partial\theta_2/\partial\theta_1) = 0$ and $\dfrac{\partial\theta_2}{\partial\theta_1} = -\dfrac{d_1 \sec^2\theta_1}{d_2 \sec^2\theta_2}$.

Substituting into (3), we have $n_1 d_1 \sec\theta_1 \tan\theta_1 - n_2 \dfrac{d_1 \sec^2\theta_1 \tan\theta_2}{\sec\theta_2} = 0$,
whereupon $n_1 \tan\theta_1 = n_2 \sec\theta_1 \sin\theta_2$, from which $n_1 \sin\theta_1 = n_2 \sin\theta_2$, which is Snell's law.

1.2 SIMPLE OPTICAL COMPONENTS

EXERCISE 1.2-1

Image Formation by a Spherical Mirror

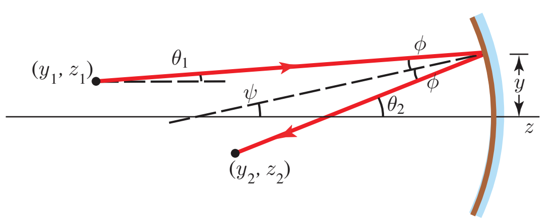

A ray originating at $P_1 = (y_1, z_1)$ at angle θ_1 meets the mirror at height
$y \approx y_1 + \theta_1 z_1$. (1)

The angle of incidence at the mirror is $\phi = \psi - \theta_1 \approx \dfrac{y}{-R} - \theta_1$.
The reflected ray makes angle θ_2 with the z axis:

$$\theta_2 = 2\phi + \theta_1 = 2\left[\frac{y}{-R} - \theta_1\right] + \theta_1 = \frac{2y}{-R} - \theta_1 = \frac{2(y_1 + \theta_1 z_1)}{-R} - \theta_1.$$

Substituting $f = \dfrac{-R}{2}$, we have $\theta_2 = \dfrac{y_1 + \theta_1 z_1}{f} - \theta_1$. (2)

The height y_2 can be determined from $\dfrac{y + (-y_2)}{z_2} \approx \theta_2$. (3)

Substituting from (1) and (2) into (3), we have $y_1 + \theta_1 z_1 - y_2 = z_2 \left[\dfrac{y_1 + \theta_1 z_1}{f} - \theta_1\right]$

and $y_2 = y_1 - \dfrac{z_2\, y_1}{f} + \theta_1 \left[z_1 - \dfrac{z_1\, z_2}{f} + z_2\right]$.

If $\left[z_1 - \dfrac{z_1\, z_2}{f} + z_2\right] = 0,$ or $\dfrac{1}{z_1} + \dfrac{1}{z_2} = \dfrac{1}{f}$, we have

$$y_2 = y_1 \left(1 - \frac{z_2}{f}\right), \tag{4}$$

which is independent of θ_1.

From (4) it is clear that $\dfrac{z_2}{f} = 1 - \dfrac{y_2}{y_1}$, so that $y_2 = -\dfrac{z_2}{z_1} y_1$.

EXERCISE 1.2-2

Image Formation

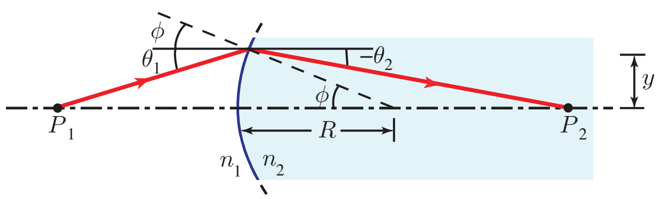

a) From Snell's law, we have $n_1 \sin(\theta_1 + \phi) = n_2 \sin[\phi - (-\theta_2)]$. Since all angles are small, the paraxial version of Snell's Law is $n_1(\theta_1 + \phi) \approx n_2(\phi + \theta_2)$, or $\theta_2 \approx (n_1/n_2)\theta_1 + [(n_1 - n_2)/n_2]\phi$.
Because $\phi \approx y/R$, we obtain $\theta_2 \approx \dfrac{n_1}{n_2}\,\theta_1 - \dfrac{n_2 - n_1}{n_2 R}\,y$, which is (1.2-8).

b) Substituting $\theta_1 \approx y/z_1$ and $(-\theta_2) \approx y/z_2$ into (1.2-8),
we have $-y/z_2 \approx \dfrac{(n_1/n_2)\,y}{z_1} - \dfrac{n_2 - n_1}{n_2 R}\,y$, from which (1.2-9) follows.

c) With reference to Fig. 1.2-13(b), for the ray passing through the origin 0, we have angles of incidence and refraction given by y_1/z_1 and $-y_2/z_2$, respectively, so that the paraxial Snell's Law leads to (1.2-10). Rays at other angles are also directed from P_1 to P_2, as can be shown using a derivation similar to that followed in Exercise 1.2-1.

EXERCISE 1.2-3

Aberration-Free Imaging Surface In accordance with Fermat's principle, we require

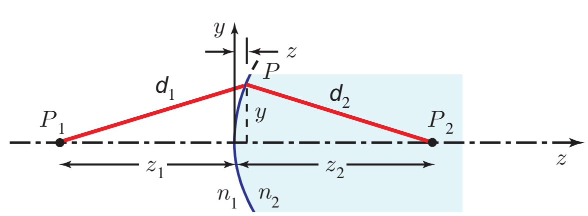

that the optical path length obey $n_1 d_1 + n_2 d_2 =$ constant $= n_1 z_1 + n_2 z_2$. This constitutes an equation defining the surface, which can be written in Cartesian coordinates as

$$n_1\sqrt{(z+z_1)^2+y^2}+n_2\sqrt{(z_2-z)^2+y^2}=n_1z_1+n_2z_2. \quad (1)$$

Given z_1 and z_2, (1) relates y to z and thus defines the surface.

EXERCISE 1.2-4

Proof of the Thin Lens Formulas

A ray at angle θ_1 and height y refracts at the first surface in accordance with (1.2-8) and its angle is altered to $\theta = \dfrac{\theta_1}{n} - \dfrac{n-1}{nR_1}\,y\,,$ (1)

where R_1 is the radius of the first surface $(R_1 < 0)$.

At the second surface, the angle is altered again to $\theta_2 = n\theta - \dfrac{1-n}{R_2}\,y\,,$ (2)

where R_2 is the radius of the second surface $(R_2 > 0)$. We have assumed that the ray height is not altered since the lens is thin.

Substituting (1) into (2) we obtain:

$$\theta_2 = n\left[\frac{\theta_1}{n} - \frac{n-1}{nR_1}\,y\right] - \frac{1-n}{R_2}\,y = \theta_1 - (n-1)\,y\left[\frac{1}{R_1} - \frac{1}{R_2}\right].$$

Using (1.2-11), we invoke $\theta_2 = \theta_1 - (y/f)$. (3)

If $\theta_1 = 0$, then $\theta_2 = (-y/f)$, and $z_2 \approx (y/-\theta_2) = f$, where f is the focal length. In general $\theta_1 \approx \dfrac{y}{z_1}$ and $-\theta_2 = \dfrac{y}{z_2}$. Therefore from (3), $\dfrac{-y}{z_2} = \dfrac{y}{z_1} - \dfrac{y}{f}$, from which (1.2-13) follows. Equation (1.2-14) can be proved by use of an approach similar to that used in Exercise 1.2-1.

EXERCISE 1.2-5

Numerical Aperture and Angle of Acceptance of an Optical Fiber

Applying Snell's law at the air/core surface:

$\sin\theta_a = n_1\sin\bar\theta_c = n_1\cos\theta_c$ (1)

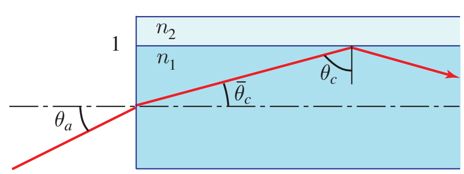

Since $\sin\theta_c = n_2/n_1,\ \cos\theta_c = \sqrt{1-(n_2/n_1)^2}\,.$

Therefore, from (1), NA $\equiv \sin\theta_a = n_1\sqrt{1-(n_2/n_1)^2} = \sqrt{n_1^2 - n_2^2}\,.$

For silica glass with $n_1 = 1.475$ and $n_2 = 1.460$, the numerical aperture NA = 0.21 and the acceptance angle $\theta_a = 12.1°$.

EXERCISE 1.2-6

Light Trapped in a Light-Emitting Diode

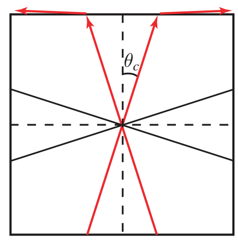

a) The rays within the six cones of half angle $\theta_c = \sin^{-1}(1/n)$ $(= 16.1^\circ$ for GaAs) are refracted into air in all directions, as shown in the illustration. The rays outside these six cones are internally reflected. Since $\theta_c < 45^\circ$, the cones do not overlap and the reflected rays remain outside the cones and continue to reflect internally without refraction. These are the trapped rays.

b) The area of the spherical cap atop one of these cones is $A = \int_0^{\theta_c} 2\pi r \sin\theta \, r \, d\theta = 2\pi r^2(1 - \cos\theta_c)$, while the area of the entire sphere is $4\pi r^2$. Thus, the fraction of the emitted light that lies within the solid angle subtended by one of these cones is $A/4\pi r^2 = \frac{1}{2}(1 - \cos\theta_c)$ (see Sec. 18.1B). Thus, the ratio of the extracted light to the total light is $6 \times \frac{1}{2}(1 - \cos\theta_c) = 3(1 - \cos\theta_c)$ $(= 0.118$ for GaAs). Thus, 11.8% of the light is extracted for GaAs.
Note that this derivation is valid only for $\theta_c < 45^\circ$ or $n > \sqrt{2}$.

1.3 GRADED-INDEX OPTICS

EXERCISE 1.3-1

The GRIN Slab as a Lens

Using (1.3-11) and (1.3-12), with $\theta_0 = 0$ and $z = d$, we have $y(d) = y_0 \cos(\alpha d)$ and $\theta(d) = -y_0 \alpha \sin(\alpha d)$. Rays refract into air at an angle $\theta' \approx n_0|\theta(d)| = n_0 y_0 \alpha \sin(\alpha d)$.

Therefore, $\overline{\text{AF}} \approx \dfrac{y(d)}{\theta'} = \dfrac{y_0 \cos(\alpha d)}{n_o y_0 \alpha \sin(\alpha d)} = \dfrac{1}{n_0 \alpha \tan(\alpha d)}$ and

$f = \dfrac{y_0}{\theta'} = \dfrac{1}{n_0 \alpha \sin(\alpha d)}$, so that

$$\overline{\text{AH}} = f - \overline{\text{AF}} = \frac{1}{n_0\alpha}\left[\frac{1}{\sin(\alpha d)} - \frac{1}{\tan(\alpha d)}\right] = \frac{1}{n_0\alpha}\,\frac{1 - \cos(\alpha d)}{\sin(\alpha d)}$$

$$= \frac{1}{n_0\alpha}\,\frac{2\sin^2(\alpha d/2)}{2\sin(\alpha d/2)\cos(\alpha d/2)} = \frac{1}{n_0\alpha}\tan(\alpha d/2).$$

Trajectories:

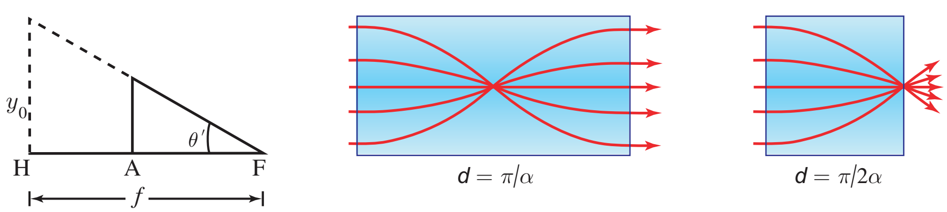

EXERCISE 1.3-2

Numerical Aperture of the Graded-Index Fiber

Using (1.3-11) with $y_0 = 0$, we obtain $y(z) = (\theta_0/\alpha)\sin(\alpha z)$. The ray traces a sinusoidal trajectory with amplitude θ_0/α that must not exceed the radius a. Thus $\theta_0/\alpha = a$. The acceptance angle is therefore $\theta_a \approx n_0\theta_0 = n_0\alpha a$.

For a step-index fiber (Exercise 1.2-5),
$\theta_a = \sqrt{n_1^2 - n_2^2} = \sqrt{(n_1 + n_2)(n_1 - n_2)}$.
If $n_1 \approx n_2,\ \theta_a \approx \sqrt{2n_1(n_1 - n_2)}$.
If $n_1 = n_0$ and $n_2 = n_0(1 - \alpha^2 a^2/2)$,
$\theta_a \approx \sqrt{2n_0(\alpha^2 a^2 n_0/2)} = \alpha\, a\, n_0$, which is the same acceptance angle as for the graded-index fiber.

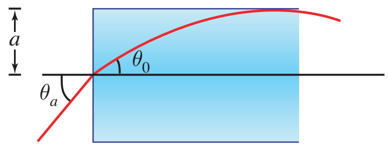

1.4 MATRIX OPTICS

EXERCISE 1.4-1

Special Forms of the Ray-Transfer Matrix

Using the basic equations
$y_2 = Ay_1 + B\,\theta_1$ and $\theta_2 = C\,y_1 + D\,\theta_1$, we obtain:

• If $A = 0$, then $y_2 = B\theta_1$, i.e., for a given θ_1, we see that y_2 is the same regardless of y_1.
This is a focusing system.

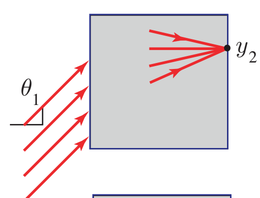

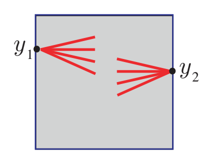

• If $B = 0$, then $y_2 = A\,y_1$, i.e., for a given y_1, we see that y_2 is the same regardless of θ_1.
This is an imaging system.

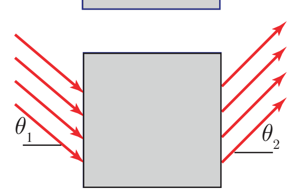

• If $C = 0$, then $\theta_2 = D\,\theta_1$, i.e., we see that all parallel rays remain parallel.

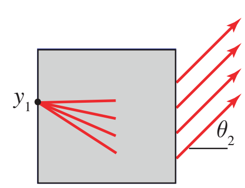

• If $D = 0$, then $\theta_2 = C\,y_1$, i.e., we see that all rays originating from a point become parallel.

EXERCISE 1.4-2

A Set of Parallel Transparent Plates

The first plate has ray transfer matrix: $\begin{bmatrix} 1 & d_1 \\ 0 & 1 \end{bmatrix} \begin{bmatrix} 1 & 0 \\ 0 & 1/n_1 \end{bmatrix} = \begin{bmatrix} 1 & d_1/n_1 \\ 0 & 1/n_1 \end{bmatrix}$.

The second plate has ray transfer matrix: $\begin{bmatrix} 1 & d_2 \\ 0 & 1 \end{bmatrix} \begin{bmatrix} 1 & 0 \\ 0 & n_1/n_2 \end{bmatrix} = \begin{bmatrix} 1 & d_2 n_1/n_2 \\ 0 & n_1/n_2 \end{bmatrix}$.

The first and second plates together have a ray transfer matrix:

$$\begin{bmatrix} 1 & d_2 n_1/n_2 \\ 0 & n_1/n_2 \end{bmatrix} \begin{bmatrix} 1 & d_1/n_1 \\ 0 & 1/n_1 \end{bmatrix} = \begin{bmatrix} 1 & d_1/n_1 + d_2/n_2 \\ 0 & 1/n_2 \end{bmatrix}.$$

Similarly N plates have a ray transfer matrix: $\begin{bmatrix} 1 & \sum_i d_i/n_i \\ 0 & 1/n_N \end{bmatrix}$.

Including the interface between the N^{th} plate and air, the overall ray transfer matrix becomes:

$$\begin{bmatrix} 1 & 0 \\ 0 & n_N \end{bmatrix} \begin{bmatrix} 1 & \sum_i d_i/n_i \\ 0 & 1/n_N \end{bmatrix} = \begin{bmatrix} 1 & \sum_i d_i/n_i \\ 0 & 1 \end{bmatrix}.$$

The ray transfer matrix of an inhomogeneous plate with refractive index $n(z)$ and width d is:

$$\begin{bmatrix} 1 & \int_0^d dz/n(z) \\ 0 & 1 \end{bmatrix}.$$

EXERCISE 1.4-3

A Gap Followed by a Thin Lens

$$\mathbf{M} = \begin{bmatrix} 1 & 0 \\ -1/f & 1 \end{bmatrix} \begin{bmatrix} 1 & d \\ 0 & 1 \end{bmatrix} = \begin{bmatrix} 1 & d \\ -1/f & 1 - d/f \end{bmatrix}.$$

EXERCISE 1.4-4

Imaging with a Thin Lens

$$\mathbf{M} = \begin{bmatrix} 1 & d_2 \\ 0 & 1 \end{bmatrix} \begin{bmatrix} 1 & d_1 \\ -1/f & 1 - d_1/f \end{bmatrix} = \begin{bmatrix} 1 - d_2/f & d_1 + d_2(1 - d_1/f) \\ -1/f & 1 - d_1/f \end{bmatrix}.$$

For imaging, the matrix element B must vanish (see Exercise 1.4-1), so that $d_1 + d_2(1 - d_1/f) = 0$. Dividing this by $d_1 d_2$ yields $1/d_2 + 1/d_1 - 1/f = 0$.

For all parallel rays to be focused onto a single point, the matrix element A must vanish (see Exercise 1.4-1), so that $1 - d_2/f = 0$ or $d_2 = f$.

EXERCISE 1.4-5

Imaging with a Thick Lens

a) This system is composed of 5 subsystems:
1) A distance d_1 in air, followed by
2) An air/glass refracting surface, followed by
3) A distance d in glass, followed by
4) An glass/air refracting surface, followed by
5) A distance d_2 in air.

The ray transfer matrix of subsystem 2) is:

$$\begin{bmatrix} 1 & 0 \\ -(n-1)/nR & 1/n \end{bmatrix} = \begin{bmatrix} 1 & 0 \\ -1/nf_1 & 1/n \end{bmatrix}, \qquad \text{where } f_1 = R/(n-1).$$

The ray transfer matrix of subsystems 2) and 3) is:

$$\begin{bmatrix} 1 & d \\ 0 & 1 \end{bmatrix} \begin{bmatrix} 1 & 0 \\ -1/nf_1 & 1/n \end{bmatrix} = \begin{bmatrix} 1-d/nf_1 & d/n \\ -1/nf_1 & 1/n \end{bmatrix}.$$

The ray transfer matrix of subsystems 2), 3), and 4) (the lens) is:

$$\begin{bmatrix} 1 & 0 \\ -(n-1)/R & n \end{bmatrix} \begin{bmatrix} 1-d/nf_1 & d/n \\ -1/nf_1 & 1/n \end{bmatrix} = \begin{bmatrix} 1-d/nf_1 & d/n \\ -(1-d/nf_1)/f_1 - 1/f_1 & -d/nf_1 + 1 \end{bmatrix}.$$

The ray transfer matrix of the entire system is:

$$\begin{bmatrix} 1 & d_2 \\ 0 & 1 \end{bmatrix} \begin{bmatrix} 1-d/nf_1 & d/n \\ -2/f_1 + d/nf_1^2 & 1-d/nf_1 \end{bmatrix} \begin{bmatrix} 1 & d_1 \\ 0 & 1 \end{bmatrix}.$$

For this system to be an imaging system, the B element of its ray transfer matrix must vanish, $i.e.$, $B = d_1(1-d/nf_1) + d/n + d_2\,[d_1(-2/f_1 + d/nf_1^2) + (1-d/nf_1)] = 0$.

Grouping together the terms proportional to d_1, d_2, and $d_1 d_2$, we have
$(d_1+d_2)(1-d/nf_1) - d_1 d_2(2/f_0 - d/nf_1^2) + d/n = 0.$ (1)

Using the definitions
$1/f = 2/f_1 - d/nf_1^2$ (2)
and $h = (fd/nf_1)$, (3)

(1) becomes: $(d_1+d_2)(1-h/f) - d_1 d_2/f + d/n = 0.$ (4)

We now rewrite (4) in terms of z_1 and z_2 by substituting $d_1 = z_1 - h$ and $d_2 = z_2 - h$. The results is: $z_1 + z_2 - z_1 z_2/f + b = 0,$ (5)

where $$\begin{aligned} b &= d/n - h^2/f - 2h(1-h/f) = d/n + h^2/f - 2h \\ &= d/n + (h/f)(h-2f). \end{aligned} \qquad (6)$$

If $b = 0$, (5) gives the desired result, $1/z_1 + 1/z_2 = 1/f$. To prove that $b = 0$, we use (2) and (3) to write $1/f = (2f-h)/f_1 f$, from which $2f - h = f_1$. Substituting this into (6), we obtain $b = d/n - hf_1/f$. We now use (3) to write $d/n = hf_1/f$, so that $b = hf_1/f - hf_1/f = 0$, as promised.

b) We show below that a ray parallel to the optical axis at height y_1 must pass through the point F_2, a distance $f - h$ from the right surface of the lens, regardless of the height y_1. This can be easily shown if we consider the ray transfer matrix of the system composed of the thick lens (subsystems 2, 3, and 4 above) followed by a distance

$f-h$ in air. This composite system has ray transfer matrix

$$\begin{bmatrix} 1 & f-h \\ 0 & 1 \end{bmatrix} \begin{bmatrix} 1-d/nf_1 & d/n \\ -2/f_1 + d/nf_1^2 & 1-d/nf_1 \end{bmatrix}.$$

If the element $A=0$, then $y_2 = B\theta_1$ so that for $\theta_1 = 0$ (for rays parallel to the optical axis), we have $y_2 = 0$, i.e., the rays pass through the point F_2.

We now examine $A = (1-d/nf_1) + (f-h)(-2/f_1 + d/nf_1^2)$, and show that it is 0. Using (2), we have $A = (1-h/f) + (f-h)(-2+h/f)/f_1$. Using the relation $2f-h = f_1$, we obtain $A = (1-h/f) + (f-h)/(-f) = 0$, as promised.

EXERCISE 1.4-6

A Periodic Set of Pairs of Different Lenses

Here, the unit cell is composed of 2 subsystems, each comprising a distance d of free space followed by a lens. The ray transfer matrix of the unit cell is therefore given by the product

$$\begin{bmatrix} 1 & d \\ -1/f_2 & 1-d/f_2 \end{bmatrix} \begin{bmatrix} 1 & d \\ -1/f_1 & 1-d/f_1 \end{bmatrix}.$$

The A and D elements of this product are:

$$A = 1 - d/f_1, \quad D = -d/f_2 + (1-d/f_2)(1-d/f_1)$$

so that

$$b = (A+D)/2 = 1 - d/f_1 - d/f_2 + d^2/2f_1 f_2 = 2(1-d/2f_1)(1-d/2f_2) - 1.$$

The condition $|b| \le 1$ is equivalent to $-1 \le b \le 1$ or $0 \le b+1 \le 2$, which leads to the desired condition

$$0 \le (1-d/2f_1)(1-d/2f_2) \le 1.$$

EXERCISE 1.4-7

An Optical Resonator

The resonator may be regarded as a periodic system whose unit system is a single round trip between the pair of mirrors. In a resonator of length d, a paraxial ray starting at the position y_0 travels a distance d in free space, is reflected from the mirror 2, then travels again backward through the same distance of free space, and finally is reflected from the mirror 1 at position y_1. The process is repeated periodically. The unit cell therefore consists of a cascade of two subsystems, each comprising propagation in free space followed by reflection from a mirror. The condition of stability may determined by writing the ray transfer matrix of the unit cell, as in the previous exercise. Since a mirror with radius of curvature R has the same ray transfer matrix as a lens with focal length f, if $f = -R/2$, the stability condition determined for the periodic set of pairs of lenses considered in the previous exercise may be directly used to obtain:

$$0 \le (1+d/R_1)(1+d/R_2) \le 1.$$

The same result is set forth in (11.2-5).

CHAPTER 2

WAVE OPTICS

2.2 MONOCHROMATIC WAVES

EXERCISE 2.2-1

Validity of the Fresnel Approximation

Given: $\lambda = 633 \times 10^{-9}$ m, $d = 1$ m.
The Fresnel approximation is valid when $\dfrac{N_F\theta_m^2}{4} \ll 1$, where $N_F = \dfrac{a^2}{\lambda d}$ and $\theta_m = \dfrac{a}{d}$.
The condition is, therefore, $\dfrac{a^4}{4\lambda d^3} \ll 1$ or $a \ll \left(4\lambda d^3\right)^{1/4} = 0.04$ m. Thus the radius a must be much smaller than 4 cm. When $a = 4$ cm, $N_F = \dfrac{a^2}{\lambda d} = 2514$ and $\theta_m = \dfrac{a}{d} = 0.04$ rad.

EXERCISE 2.2-2

The Paraboloidal Wave and the Gaussian Beam

$$A = (A_0/z)\exp[-jk(x^2+y^2)/2z], \tag{1}$$

$$\frac{\partial A}{\partial x} = -jxA\frac{k}{z},$$

$$\frac{\partial^2 A}{\partial x^2} = -j\frac{k}{z}\left(x\frac{\partial A}{\partial x} + A\right) = -j\frac{k}{z}\left(-jx^2A\frac{k}{z} + A\right) = -jA\frac{k}{z} - \left(\frac{k}{z}\right)^2 x^2 A.$$

Similarly, $\dfrac{\partial^2 A}{\partial y^2} = -jA\dfrac{k}{z} - \left(\dfrac{k}{z}\right)^2 y^2 A$,

so that $$\nabla_T^2 A = -j2A\frac{k}{z} - \left(\frac{k}{z}\right)^2 (x^2+y^2)\,A. \tag{2}$$

Now,

$$\frac{\partial A}{\partial z} = -\frac{A_0}{z^2}\exp\left[\frac{-jk\,(x^2+y^2)}{2z}\right] + \frac{A_0}{z}\left[\frac{jk}{2z^2}\,(x^2+y^2)\right]\exp\left[\frac{-jk\,(x^2+y^2)}{2z}\right]$$
$$= \frac{-A}{z} + \frac{jk}{2z^2}\,(x^2+y^2)\,A. \tag{3}$$

Substituting (2) and (3) into the paraxial Helmholtz equation, we see that $\nabla_T^2 A - j2k\dfrac{\partial A}{\partial z} = 0$, so that (1) does indeed satisfy this equation.

Replacing z by $q(z) = z + jz_0$ in (1) does not alter the validity of the paraxial Helmholtz equation since jz_0 is a constant and therefore $[\partial/\partial_q](\cdot) = [\partial/\partial_z](\cdot)$.

At $z = 0$, we have $q = jz_0$, whereupon (1) gives: $A(\mathbf{r}) = \dfrac{A_0}{jz_0}\exp\left[\dfrac{-k\,(x^2+y^2)}{2\,z_0}\right]$, whence the intensity is written as $|A(\mathbf{r})|^2 = \left(\dfrac{A_0}{z_0}\right)^2 \exp\left[\dfrac{-k\,(x^2+y^2)}{z_0}\right]$.

This is a Gaussian function of x and y that has its peak at $x = y = 0$ and that decreases as the radial coordinate $\rho = \sqrt{x^2+y^2}$ increases. It reaches $1/e^2$ of its peak value at $\rho = \sqrt{\lambda z_0/\pi}$ [see (3.1-11)].

2.4 SIMPLE OPTICAL COMPONENTS

EXERCISE 2.4-1

Transmission Through a Prism

Substituting $d(x,y) \approx \alpha x$ into (2.4-5) leads to the desired result.

EXERCISE 2.4-2

Double-Convex Lens

$\mathrm{t}(x,y) = \mathrm{t}_1(x,y)\,\mathrm{t}_2(x,y) = h_{01}\exp\left[\dfrac{jk_o\left(x^2+y^2\right)}{2f_1}\right]\, h_{02}\exp\left[\dfrac{jk_o\left(x^2+y^2\right)}{2f_2}\right]$ where $f_1 = \dfrac{R_1}{n-1}$ and $f_2 = \dfrac{-R_2}{n-1}$ and h_{01} and h_{02} are constants.

Thus $\mathrm{t}(x,y) = h_0\exp\left[\dfrac{jk_o\left(x^2+y^2\right)}{2f}\right]$, where $\dfrac{1}{f} = \dfrac{1}{f_1} + \dfrac{1}{f_2} =$ $(n-1)(1/R_1 - 1/R_2)$ and $h_0 = h_{01}\,h_{02}$ is a constant. Note that R_2 is negative.

EXERCISE 2.4-3

Focusing of a Plane Wave by a Thin Lens

$U_1(x,y) = \exp\left(-jkz\right)$, and $\mathrm{t}(x,y) = h_0\exp\left[jk\left(x^2+y^2\right)/2f\right]$.
Therefore, $U_2(x,y) = U_1(x,y)\,\mathrm{t}(x,y) = h_0\exp\left\{-jk\left[z - \left(x^2+y^2\right)/2f\right]\right\}$.

The wavefronts of this wave are paraboloids of revolution, defined by $z - \left(x^2+y^2\right)/2f =$ constant, with radius of curvature $-f$, i.e., they approximate a spherical wave focused at a point a distance f to the right of the lens.

If the incident wave is a plane wave at a small angle θ, $U_1(x,y) \approx \exp\left[-jk(z+\theta x)\right]$, then

$$\begin{aligned} U_2(x,y) = U_1(x,y)\,\mathrm{t}(x,y) &\approx h_0\exp\left\{-jk\left[z+\theta x - \left(x^2+y^2\right)/2f\right]\right\}. \\ &= h_0\exp\left\{-jk\left[z - \left(x^2 - 2f\theta x + y^2\right)/2f\right]\right\}. \\ &= h_0\exp\left\{-jk\left[z - \left((x-f\theta)^2 + y^2\right)/2f\right]\right\}. \end{aligned}$$

This is a paraboloidal wave centered about the point $(f\theta, 0, f)$, as illustrated below.

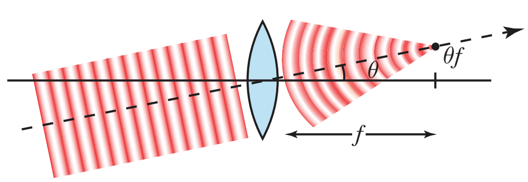

EXERCISE 2.4-4

Imaging Property of a Lens

Choose a coordinate system with $z = 0$ at the lens. The incident wave is a spherical wave centered at $z = -z_1$, i.e., $U_1(x, y) \approx \exp\left[-jk\left(x^2 + y^2\right)/2z_1\right]$ so that

$$U_2(x, y) \approx \exp\left[-jk\left(x^2 + y^2\right)/2z_1\right] \exp\left[jk\left(x^2 + y^2\right)/2f\right]$$
$$\approx \exp\left[jk\left(x^2 + y^2\right)/2z_2\right],$$

where $\frac{1}{z_2} = \frac{1}{f} - \frac{1}{z_1}$ or $\frac{1}{z_1} + \frac{1}{z_2} = \frac{1}{f}$.

The transmitted wave is, therefore, a spherical wave centered at the point $z = z_2$.

EXERCISE 2.4-5

Transmission Through a Diffraction Grating

a) $d(x) = \frac{d_0}{2}\left[1 + \cos\frac{2\pi x}{\Lambda}\right]$

$\mathrm{t}(x) = \exp\left(-jk_o d_0\right)\exp\left[-j\left(n-1\right)k_o d(x)\right]$
$= h_0 \exp\left[-j\left(n-1\right)\left(k_o d_0/2\right)\cos\left(2\pi x/\Lambda\right)\right]$, where
$h_0 = \exp\left[-j\left(n+1\right)\left(k_o d_0/2\right)\right]$.

b) Since $\mathrm{t}(x)$ is a periodic function of x with period Λ, it can be expanded in a Fourier series: $\mathrm{t}(x) = \sum_q C_q \exp\left(-jq2\pi x/\Lambda\right)$, where C_q are the Fourier coefficients. If the incident wave is a plane wave at a small angle θ_i, i.e., $U_1(x) = \exp\left[-jk_o\left(z + \theta_i\, x\right)\right]$, the transmitted wave has amplitude:

$U_2(x) = \mathrm{t}(x)U(x)$
$= \exp\left[-j\left(k_o z + k_o\theta_i\, x + q2\pi x/\Lambda\right)\right] = \exp\left[-jk_o\left(z + \theta_q\, x\right)\right]$,
where $\theta_q = \theta_i + q2\pi/k_o\Lambda = \theta_i + q\lambda/\Lambda$. Thus the transmitted wave is composed of plane waves at angles θ_q.

EXERCISE 2.4-6

Graded-Index Lens

Substituting $n = n_0\left[1 - \alpha^2\left(x^2 + y^2\right)/2\right]$ into (2.4-14), we obtain

$\mathrm{t} = \exp\left(-jnk_o d_0\right) = h_0 \exp\left[jn_0\alpha^2 k_o d_0\left(x^2 + y^2\right)/2\right]$, with $h_0 = \exp\left(-jn_0 k_o d_0\right)$.
Thus, $\mathrm{t} = h_0 \exp\left[jk_o\left(x^2 + y^2\right)/2f\right]$, where $1/2f = n_0\alpha^2 d_0/2$ so that $f = 1/n_0\alpha^2 d_0$.

This is the amplitude transmittance of a lens of focal length f.

2.5 INTERFERENCE

EXERCISE 2.5-1

Interference of a Plane Wave and a Spherical Wave

$I = I_1 + I_2 + 2\sqrt{I_1 I_2}\cos\varphi$, where $I_1 = |A_1|^2$, $I_2 = |A_2|^2$, and

$\varphi = k\left(x^2+y^2\right)/2z = \pi\left(x^2+y^2\right)/\lambda d$.

Therefore $I(x,y,d) = I_1 + I_2 + 2\sqrt{I_1 I_2}\cos\left[\pi\left(x^2+y^2\right)/\lambda d\right]$.

This locus of constant I are circles (x^2+y^2) = constant. The function $\cos\left(\pi x^2\right)$ is plotted in Table A.1-1. It is a sinusoidal function, called the chirp function, whose frequency increases as x increases. This is why the rings in the interference pattern become closer and closer as x^2+y^2 increases.

EXERCISE 2.5-2

Interference of Two Spherical Waves

$U_1 = \dfrac{A}{z}\exp\{-jkz\}\exp\left\{-jk\left[(x-a)^2+y^2\right]/2z\right\}$ and
$U_2 = \dfrac{A}{z}\exp\{-jkz\}\exp\left\{-jk\left[(x+a)^2+y^2\right]/2z\right\}$.

At $z = d$, $I = 2I_0 + 2I_0\cos\varphi$, where $I_0 = |A/d|^2$ and

$$\begin{aligned}\varphi &= (k/2d)\left\{\left[(x+a)^2+y^2\right]-\left[(x-a)^2+y^2\right]\right\}\\ &= (\pi/\lambda d)(4ax) = 4\pi ax/\lambda d.\end{aligned}$$

Therefore, $I = 2I_0\left[1+\cos\left(2\pi x\theta/\lambda\right)\right]$, where $\theta = 2a/d$.

EXERCISE 2.5-3

Bragg Reflection

The phase difference between two reflections is $\varphi = k\left(\Lambda_2 - \Lambda_1\right)$.
But $\Lambda_2 = \Lambda/\sin\theta$ and $\Lambda_1 = \Lambda_2\cos 2\theta = \Lambda\cos 2\theta/\sin\theta$.

Therefore, $\varphi = k\left(\Lambda/\sin\theta\right)(1-\cos 2\theta) = k\left(\Lambda/\sin\theta\right)2\sin^2\theta = k\left(2\Lambda\sin\theta\right)$.

For $\varphi = 2\pi$, we have $k\Lambda\sin\theta = \pi$ so that $2\Lambda\sin\theta/\lambda = 1$, or equivalently,

$\sin\theta = \lambda/2\Lambda$.

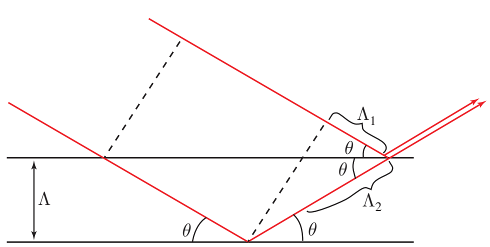

2.6 POLYCHROMATIC AND PULSED LIGHT

EXERCISE 2.6-1

Optical Doppler Radar

a) The two waves have a phase shift $\varphi = 2\pi\nu_1 t - 2\pi\nu_2 t = 2\pi(\nu_1 - \nu_2)t = 2\pi(2\mathsf{v}/c)\nu t$. The intensity of their superposition is $I = I_1 + I_2 + 2\sqrt{I_1 I_2}\cos[2\pi(2\mathsf{v}/c)\nu t]$. This is a sinusoidal function of time with frequency $2(\mathsf{v}/c)\nu$. The velocity v can be observed by monitoring I as a function of time.

b) $\varphi = k(z_2 - z_1) = k(2\mathsf{v}t) = (2\pi\nu/c)2\mathsf{v}t = 2\pi\left(2\frac{\mathsf{v}}{c}\nu\right)t$, so that the beat frequency is $\pm 2\frac{\mathsf{v}}{c}\nu$.

CHAPTER
3

BEAM OPTICS

3.1 THE GAUSSIAN BEAM

EXERCISE 3.1-1

Parameters of a Gaussian Laser Beam

Given: $\lambda = 633$ nm $= 633 \times 10^{-9}$ m; $P = 10^{-3}$ W; $W_0 = 0.05 \times 10^{-3}$ m

a) $\theta_0 = \lambda / (\pi W_0) = 4.03 \times 10^{-3}$ rad $= 4.03$ mrad.
$z_0 = W_0/\theta_0 = 0.012$.
Depth of focus $= 2z_0 = 0.025$ m $= 2.5$ cm.
At $z = 3.5 \times 10^5$ km $= 3.5 \times 10^8$ m, $W(z) = W_0\sqrt{1 + (z/z_0)^2} = 1.41 \times 10^6$ m.
Diameter $= 2821$ km.

b) At $z = 0, R = \infty$.
At $z = z_0, R = 2z_0 = 2.5$ cm.
At $z = 2z_0, R = z\left[1 + (z_0/z)^2\right] = 0.031$ m $= 3.1$ cm.

c) At beam center, $I = I_0 = 2P/\pi W_0^2 = 2.546 \times 10^5$ W/m^2 $= 25.46$ W/cm^2.
On beam axis at $z = z_0, I = I_0\left[W_0/W(z_0)\right]^2 = I_0/2 = 12.73$ W/cm^2.
A spherical wave of power $P = 100$ W at $z = z_0 = 2.5$ cm has intensity $I = P/(4\pi z^2) = 5.169 \times 10^4 = 5.169$ W/cm^2.

EXERCISE 3.1-2

Validity of the Paraxial Approximation for a Gaussian Beam

The condition (2.2-21) is $\partial A/\partial z \ll kA$.
In accordance with (3.1-4), $A = \dfrac{A_1}{q}\exp\dfrac{-jk\rho^2}{2q}$ where $q = z + jz_0$. Therefore,

$$\frac{\partial A}{\partial z} = -\left(\frac{A_1}{q^2}\right)q'\exp\left[\frac{-jk\rho^2}{2q}\right] + \left(\frac{A_1}{q}\right)\left[\frac{jk\rho^2q'}{2q^2}\right]\exp\left[\frac{-jk\rho^2}{2q}\right]$$
$$= -\frac{q'A}{q} + A\left[\frac{jk\rho^2q'}{2q^2}\right]$$

where $q' = \dfrac{\partial q}{\partial z} = 1.$

The condition $\partial A/\partial z \ll kA$ is therefore equivalent to
$-A/q + [jk\rho^2/2q^2]\,A \ll kA$, or $-1/kq + [j\rho^2/2q^2] \ll 1$.
Substituting $1/q = 1/R - j2/kW^2$, we then have
$(1/kR)\,[1 + 2\rho^2/W^2] + j\,[-(2/k^2W^2)\,(1 + \rho^2/W^2) + (\rho^2/W^2)\,/\,(2R^2/W^2)] \ll 1.$

Assuming that ρ is not much greater than W, i.e., for points not far outside the beam width, this condition is satisfied if
a) $kR \gg 1$;
b) $kW \gg 1$; and
c) $R \gg W$.

Condition a) signifies that the radius of curvature $R \gg \lambda$. Because the minimum radius of curvature is z_0, condition a) is satisfied if $z_0 \gg \lambda$. Similarly, condition b) is satisfied if $W_0 \gg \lambda$, or $\theta_0 = \lambda/\pi W_0 \ll 1$. However, condition c) is also satisfied if $\theta_0 \ll 1$: for small z, $R \gg W_0$; for $z = z_0$, $R = z_0 \gg W = \sqrt{2}W_0$ because $\theta_0 = W_0/z_0 \ll 1$; for large z, $R \approx z$ and $W = \theta_0 z$ so that $R/W = 1/\theta_0 \gg 1$.

In summary, the conditions $z_0 \gg \lambda$, $W_0 \gg \lambda$, and $\theta_0 \ll 1$ guarantee that $\partial A/\partial z \ll kA$ and, therefore, that the paraxial approximation is satisfied.

EXERCISE 3.1-3

Determination of a Beam with Given Width and Curvature

Use

$$W^2 = W_0^2 \left[1 + (z/z_0)^2\right] \quad (1)$$

$$R = z\left[1 + (z_0/z)^2\right] \quad (2)$$

to obtain $W^2/R = (z/z_0)\, W_0^2/z_0 = (z/z_0)\,(\lambda/\pi)$, from which

$$(z/z_0) = (\pi/\lambda)\, W^2/R. \quad (3)$$

Substituting (3) into (1) and (2) we obtain (3.1-26) and (3.1-25).

EXERCISE 3.1-4

Determination of the Width and Curvature at One Point Given the Width and Curvature at Another Point

Given: $\lambda = 10^{-6}$ m; At position 1, $R_1 = 1$ m and $W_1 = 10^{-3}$ m.
Find: R_2 and W_2 at position 2, $z_2 = z_1 + d$, $d = 0.1$ m.

We use the relations:

$$q_2 = q_1 + d$$

$$1/q_1 = 1/R_1 - j\lambda/\pi W_1^2$$

$$1/q_2 = 1/R_2 - j\lambda/\pi W_2^2.$$

Thus, $1/q_1 = 1 - j0.32$ and $q_1 = 0.91 + j0.29.$

Therefore $q_2 = 1.01 + j0.29$ and $1/q_2 = 0.92 - j0.26$, so that $R_2 = 1/0.92 = 1.09$ m and $\lambda/\pi W_2^2 = 0.26$, from which $W_2 = 1.11 \times 10^{-3}$ m $= 1.11$ mm.

EXERCISE 3.1-5

Identification of a Beam with Known Curvatures at Two Points

Using (3.1-9) and $z_2 = z_1 + d$, we obtain $R_1 = z_1\left[1 + (z_0/z_1)^2\right]$,
from which $z_1^2 - R_1 z_1 + z_0^2 = 0.$ (1)

We also obtain $R_2 = (z_1 + d)\left\{1 + \left[z_0/(z_1 + d)\right]^2\right\}$,
from which $(z_1 + d)^2 - R_2\,(z_1 + d)^2 + z_0^2 = 0.$ (2)

Equations (1) and (2) form a pair of equations in two unknowns: z_0 and z_1, that can be manipulated algebraically to obtain (3.1-27) and (3.1-28).

3.2 TRANSMISSION THROUGH OPTICAL COMPONENTS

EXERCISE 3.2-1

Beam Relaying

Considering a lens and substituting $z = z' = d/2$ in (3.2-6) we obtain $M = 1$.
From (3.2-9a), $r = z_0/(d/2 - f)$ and $M_r = |f/(d/2 - f)|$.

Inserting $M = 1$ into (3.2-9) we obtain $M_r^2 = 1 + r^2$, so that
$f^2/(d/2 - f)^2 = 1 + [z_0/(d/2 - f)]^2$,

from which $f^2 = (d/2 - f)^2 + z_0^2$, or $z_0^2 = f^2 - (d/2 - f)^2 = fd - (d/2)^2$
i.e., $z_0^2 = d(f - d/4)$.

Since z_0 is real, this last equation requires that $f \geq d/4$ or $d \leq 4f$.

EXERCISE 3.2-2

Beam Collimation

a) Substituting (3.2-9) and (3.2-9a) into (3.2-6), we obtain

$$(z' - f) = \frac{(z - f)[f/(z - f)]^2}{\left[1 + z_0^2/(z - f)^2\right]} = \frac{(z - f)f^2}{\left[(z - f)^2 + z_0^2\right]},$$

from which $\dfrac{z'}{f} - 1 = \dfrac{z/f - 1}{(z/f - 1)^2 + (z_0/f)^2}$ follows. (1)

b) Let $a = z_0/f$, $x = z/f - 1$, and $y = z'/f - 1$.
Then (1) becomes $y = x/[x^2 + a^2]$.

For a fixed value of a and allowing x to vary, y achieves its maximum value if
$\dfrac{dy}{dx} = \dfrac{1}{[x^2 + a^2]} - \dfrac{2x^2}{[x^2 + a^2]^2} = 0.$
This occurs at $[x^2 + a^2] = 2x^2$ or $x = a$,
i.e., if $z/f - 1 = z_0/f$ or $z = f + z_0$.

c) $z_0 = 1$ cm, $f = 50$ cm, $a = z_0/f = 0.02$.

Optimum $z = f + z_0 = 51$ cm,

Distance z' :

$$x = z/f - 1 = 51/50 - 1 = 0.02 = a.$$
$$y = x/[x^2 + a^2] = 1/2x = 25.$$
But $y = z'/f - 1$.
Therefore, $z' = f(1 + y) = 50 \times 26 = 1300$ cm.

Magnification: $M_r = f/(z - f) = 1/x = 50.$

$r = z_0/(z - f) = a/x = 1.$

$M = M_r/\sqrt{1 + r^2} = M_r/\sqrt{2} = 50/\sqrt{2} = 35.4.$

Width: $W_0' = MW_0 = 35.4W_0.$
$W_0 = \sqrt{\lambda z_0/\pi} \approx 56$ μm, $W_0' \approx 2$ mm.

EXERCISE 3.2-3

Beam Expansion

Imaging at the first lens:
Since $z \gg f_1$ and $z - f_1 \gg z_0$, applying (3.2-11) and (3.2-12) we obtain:

$$M_1 = f_1/\left(z - f_1\right) \approx f_1/z,$$

$$W_0'' = \left[f_1/\left(z - f_1\right)\right] W_0 \approx \left(f_1/z\right) W_0,$$

$$z_0'' = M_1^2 z_0 \approx \left(f_1/z\right)^2 z_0,$$

$$z_1 \approx f_1.$$

Imaging at the second lens:
Based on the results of Exercise 3.2-2, the optimal distance is
$z_2 = z_0'' + f_2$, so that $d = z_1 + z_2 = z_1 + z_0'' + f_2 \approx f_1 + \left(f_1/z\right)^2 z_0 + f_2$.

Also the magnification at this optimal distance is
$M_2 = \left[f_2/\left(z_2 - f_2\right)\right]/\sqrt{2} = f_2/z_0''\sqrt{2} = f_2/M_1^2 z_0\sqrt{2}$.

The overall magnification of the system is
$M = M_2 M_1 = f_2/M_1 z_0\sqrt{2} = \left(f_2/f_1\right)\left(z/\sqrt{2}z_0\right)$.

This is a large magnification since $f_2 \gg f_1$ and $z \gg z_0$.

EXERCISE 3.2-4

Variable-Reflectance Mirrors

The complex amplitude reflectance of this mirror is $\exp\left(-jk\rho^2/R\right)\exp\left(-\rho^2/W_m^2\right)$. Therefore, upon reflection, the phase of a Gaussian beam increases by $-k\rho^2/R$, so that the radius of curvature becomes R_2 where $1/R_2 = 1/R_1 + 2/R$.

In addition, the amplitude of the beam is multiplied by the factor $\exp\left(-\rho^2/W_m^2\right)$ and becomes $\exp\left(-\rho^2/W_2^2\right)$, where $1/W_2 = 1/W_1 + 1/W_m$.

The reflected beam remains Gaussian and has width W_2 and radius of curvature R_2, as provided by the above equations.

EXERCISE 3.2-5

Transmission of a Gaussian Beam Through a Transparent Plate

From (1.4-11), the elements of the *ABCD* matrix of the plate are: $A = 1$, $B = d/n$, $C = 0$, $D = 1$. Therefore, $q_2 = \left(Aq_1 + B\right)/\left(Cq_1 + D\right) = q_1 + d/n$, from which $z_2 + jz_{02} = z_1 + jz_{01} + d/n$ so that $z_{02} = z_{01}$ and $z_2 = z_1 + d/n$. It follows that the transmitted beam has the same depth of focus and its center is displaced by a distance d/n, as illustrated in the figure.

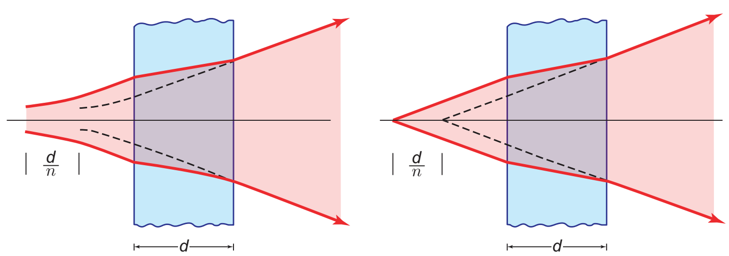

3.4 LAGUERRE–GAUSSIAN BEAMS

EXERCISE 3.4-1

Laguerre–Gaussian Beam as a Superposition of Hermite–Gaussian Beams

The Laguerre–Gaussian beam LG_{10} is identical to the superposed Hermite–Gaussian beams $\frac{1}{\sqrt{2}}(\text{HG}_{01} + j\text{HG}_{10})$, as is ascertained from the absolute square of (3.4-1) [see also the illustration in Fig. 3.4-1(a)].

At the beam waist, the Hermite–Gaussian beams may be expressed as

$$I_{1,0} = |A_{1,0}|^2\, \mathbb{G}_1^2\left(\sqrt{2}x/W_0\right) \mathbb{G}_0^2\left(\sqrt{2}y/W_0\right)$$

$$I_{0,1} = |A_{0,1}|^2\, \mathbb{G}_0^2\left(\sqrt{2}x/W_0\right) \mathbb{G}_1^2\left(\sqrt{2}y/W_0\right),$$

where $\mathbb{G}_0^2(u) = \exp(-u^2)$ and $\mathbb{G}_1^2(u) = 4u^2 \exp(-u^2)$.

In the absence of interference, and if $|A_{1,0}|^2 = |A_{0,1}|^2 = I_0$, the total intensity is the sum of the intensities:

$$I = 8I_0\left[\left(x^2+y^2\right)/W_0^2\right]\exp\left[-2\left(x^2+y^2\right)/W_0^2\right] = 8I_0\left[\rho^2/W_0^2\right]\exp\left[-2\rho^2/W_0^2\right],$$

where $\rho^2 = x^2 + y^2$.

The peak intensity occurs at the value of ρ for which $dI/d\rho = 0$, i.e., at $\rho = W_0/\sqrt{2}$ or $\rho\, W_0 \approx 0.707$. The intensity is 0 at $\rho = 0$, as shown in the figure below, and the $1/e^2$ points occur at $\rho \approx \left(0.23/\sqrt{2}\right) W_0$ and at $\rho \approx \left(2.12/\sqrt{2}\right) W_0$. Since the beam is circularly symmetric, it takes the form of a “donut” and hence is often colloquially referred to as the “donut beam.”

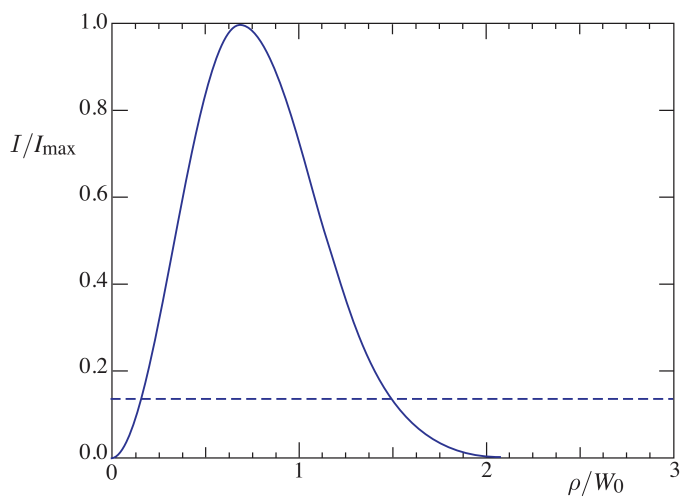

CHAPTER
4

FOURIER OPTICS

4.1 PROPAGATION OF LIGHT IN FREE SPACE

EXERCISE 4.1-1

Binary-Plate Cylindrical Lens

Near the position x, $\cos(\pi x^2/\lambda f)$ is approximately a harmonic function with local frequency $\nu_x = (1/2\pi)(\partial/\partial x)(\pi x^2/\lambda f) = x/\lambda f$. Its rectified version, $f(x) = \mathcal{U}[\cos(\pi x^2/\lambda f)]$, is approximately a periodic function with local frequency $\lambda f/x$ near the position x. The periodic function $f(x)$ can be analyzed as a sum of harmonic functions with spatial frequencies $\nu_x = qx/\lambda f$, where $q = 0, \pm 1, \pm 3, \pm 5 \ldots$. This structure therefore acts as a diffraction grating that bends the light by the approximate angles $\lambda \nu_x = \lambda(qx/\lambda f) = x/(f/q)$. All rays deflected by the approximate angle $x/(f/q)$ meet at the position f/q. Thus, the transparency acts as a cylindrical lens with focal lengths $\infty, \pm f, \pm f/3, \pm f/5, \ldots$.

EXERCISE 4.1-2

Gaussian Beams Revisited

Given: $U(x,y,0) = f(x,y) = A\exp[-(x^2+y^2)/W_0^2]$ at the input $(z=0)$ plane,
Find: $U(x,y,z) = g(x,y)$ at the distance z.

We shall use the Fourier-domain method.
The Fourier transform of $f(x,y)$ is obtained by using the fact that the Fourier transform of $\exp(-\pi t^2)$ is $\exp(-\pi\nu^2)$ (see Table A.1-1) and the scaling property of the Fourier transform (see Appendix A). Thus:

$$F(\nu_x,\nu_y) = A\pi W_0^2 \exp\left[-\pi^2 W_0^2\left(\nu_x^2+\nu_y^2\right)\right].$$

$$G(\nu_x,\nu_y) = F(\nu_x,\nu_y)H(\nu_x,\nu_y)$$

where $H(\nu_x,\nu_y) = H_0\exp\left[j\pi\lambda z\left(\nu_x^2+\nu_y^2\right)\right], \quad H_0 = \exp(-jkz)$

$$G(\nu_x,\nu_y) = A\pi W_0^2 \exp\left[-\pi^2 W_0^2\left(\nu_x^2+\nu_y^2\right)\right]\cdot\exp(-jkz)\cdot\exp\left[j\pi\lambda z\left(\nu_x^2+\nu_y^2\right)\right]$$

$$= B\exp\left[-\pi^2 Q^2\left(\nu_x^2+\nu_y^2\right)\right],$$

$B = A\pi W_0^2\exp(-jkz)$, where $\pi^2 Q^2 = \pi^2 W_0^2 - j\pi\lambda z$.

The inverse Fourier transform is $g(x,y) = (B/\pi Q^2)\exp[-(x^2+y^2)/Q^2]$.

Defining $1/Q^2 = jk/2q = j\pi/\lambda q$, we write

$$g(x,y) = B(j/\lambda q)\exp\left[-jk\left(x^2+y^2\right)/2q\right]$$

$$= A\left(j\pi W_0^2/\lambda q\right)\exp(-jkz)\exp\left[-jk\left(x^2+y^2\right)/2q\right].$$

The parameter $q = (j\pi/\lambda)Q^2 = (j/\pi\lambda)(\pi^2 W_0^2 - j\pi\lambda z) =$
$j\pi W_0^2/\lambda + z = z + jz_0$ where $z_0 = \pi W_0^2/\lambda$. Substituting, we obtain
$g(x,y) = A(jz_0/q)\exp(-jkz)\exp[-jk(x^2+y^2)/2q]$, where $q = z + jz_0$.

This is the equation of the Gaussian beam.

4.2 OPTICAL FOURIER TRANSFORM

EXERCISE 4.2-1

Conditions of Validity of the Fresnel and Fraunhofer Approximations: A Comparison

Givens: $\lambda = 0.5\ \mu$m $= 0.5 \times 10^{-6}$ m, , $a = 2 \times 10^{-2}$ m, $b = 10^{-2}$ m .
As shown in (4.1-13), the validity condition for the Fresnel approximation is $\frac{N_F \theta_m^2}{4} \ll 1$, where $N_F = a^2/\lambda d$ and $\theta_m = a/d$, so that $a^4/4\lambda d^3 \ll 1$ or $d \gg (a^4/4\lambda)^{1/3} = 0.43$ m.

As shown in (4.2-2), the validity conditions for the Fraunhofer approximation are $N_F \ll 1$ or $a^2/\lambda d \ll 1$ or $d \gg a^2/\lambda = 800$ m; AND $N'_F \ll 1$ or $b^2/\lambda d \ll 1$ or $d \gg b^2/\lambda = 200$ m.

Thus, the Fresnel approximation is applicable for distances much greater than 43 cm; and the Fraunhofer approximation is applicable for distances much greater than 800 m.

EXERCISE 4.2-2

The Inverse Fourier Transform

By examining (A.3-1) and (A.3-2) of Appendix A, we see that if $F(\nu_x, \nu_y)$ is the Fourier transform of $f(x, y)$, then $F(-\nu_x, -\nu_y)$ is the inverse Fourier transform of $f(x, y)$. Thus reversal of the coordinate system replaces the Fourier transform with the inverse Fourier transform.

4.3 DIFFRACTION OF LIGHT

EXERCISE 4.3-1

Fraunhofer Diffraction from a Rectangular Aperture

Using Table A.1-1 and the scaling property of the Fourier transform, the Fourier transform of the aperture function $p(x, y) = \mathrm{rect}\,(x/D_x)\,\mathrm{rect}\,(y/D_y)$ is $P(\nu_x, \nu_y) = D_x D_y\,\mathrm{sinc}(D_x \nu_x)\,\mathrm{sinc}(D_y y)$. Substituting into (4.3-5) we obtain (4.3-6). The first zero of the function $\mathrm{sinc}(\cdot)$ occur when its argument is ± 1, i.e., at $x = \pm \lambda d/D_x$ and $y = \pm \lambda d/D_y$.

EXERCISE 4.3-2

Fraunhofer Diffraction from a Circular Aperture

Using (A.3-5), the Fourier transform of an aperture function in the form of a circle of radius 1 is $P(\nu_x, \nu_y) = J_1\,(2\pi\nu_\rho)\,/\nu_\rho$.

For a radius $\frac{D}{2}$, $P\,(\nu_x, \nu_y) = \left(\frac{D}{2}\right)^2 \frac{J_1\,(2\pi\nu_\rho D/2)}{\nu_\rho D/2} = \left(\frac{D}{2}\right) \frac{J_1\,(\pi\nu_\rho D)}{\nu_\rho}$.

Substituting into (4.3-5) we obtain (4.3-8).

EXERCISE 4.3-3

Spot Size of a Focused Optical Beam

Equation (4.3-10) can be obtained by using the Fourier transform property of the lens, given in (4.2-7). Because (4.2-7) is identical to (4.3-5) with $d = f$, the focused beam has intensity given by (4.3-8) with $d = f$.

In accordance with (3.1-12) and (3.2-15) the focused Gaussian beam has intensity distribution $I(x, y) = I_0 \exp\left(-2\pi^2 W_0^2 \rho^2/\lambda^2 f^2\right)$, where W_0 is the waist radius of the incident beam. To compare this distribution with that in (4.3-10), we take $2W_0 = D$, assume that $\pi D/\lambda f = 1$, and plot the two functions $\exp\left(-\rho^2/2\right)$ and $\left[2J_1(\rho)/\rho\right]^2$:

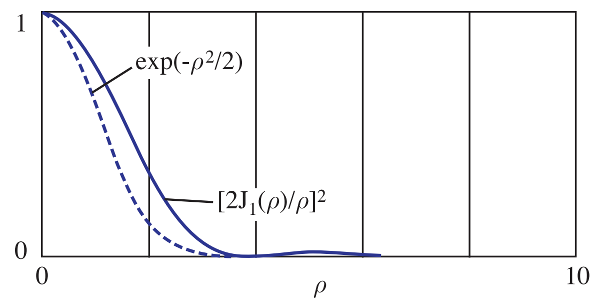

CHAPTER 5

ELECTROMAGNETIC OPTICS

5.5 ABSORPTION AND DISPERSION

EXERCISE 5.5-1

Dilute Absorbing Medium

Let χ_0 be the susceptibility of the host medium so that $n_0^2 = 1+\chi_0$. When impurities are present, the susceptibility of the host medium together with its suspension of impurities is characterized by $\chi = \chi_0 + \chi' + j\chi''$, with $\chi' \ll 1$ and $\chi'' \ll 1$. The overall refractive index and absorption coefficient are thus given by [see (5.5-5)]:

$$n - \frac{j\alpha}{2k_o} = \sqrt{1+\chi_0+\chi'+j\chi''} = \left[(1+\chi_0)\left(1+\frac{\chi'+j\chi''}{1+\chi_0}\right)\right]^{1/2}$$

$$\approx n_0\left[1+\frac{\chi'+j\chi''}{2\,(1+\chi_0)}\right] = n_0\left[1+\frac{\chi'+j\chi''}{2n_0^2}\right]$$

so that $n = n_0 + \dfrac{\chi'}{2n_0}$ and $\alpha = \dfrac{-k_o\chi''}{n_0}$.

CHAPTER 6

POLARIZATION OPTICS

6.1 POLARIZATION OF LIGHT

EXERCISE 6.1-1

Measurement of the Stokes Parameters

The expressions for S_0 and S_1 follow directly from the definition. The expression for S_2 is verified by substituting for A_{45} and A_{135} from (6.1-12). Similarly, the expression for S_3 is verified by substituting for A_R and A_L from (6.1-13).
The Stokes parameters can be measured if the absolute values (or the intensities) of components of the Jones vector are measured in three bases: the linearly polarized basis in the (x, y) directions, the linearly polarized basis in the $(45°, 135°)$ directions, and the circularly polarized basis (R, L). All six measurements are intensity measurements.

EXERCISE 6.1-2

Cascaded Wave Retarders

a) Parallel fast axes

$$\mathbf{T} = \begin{bmatrix} 1 & 0 \\ 0 & e^{-j\pi/2} \end{bmatrix} \begin{bmatrix} 1 & 0 \\ 0 & e^{-j\pi/2} \end{bmatrix} = \begin{bmatrix} 1 & 0 \\ 0 & e^{-j\pi} \end{bmatrix} = \text{A half-wave retarder}$$

b) Orthogonal fast axes

$$\mathbf{T} = \begin{bmatrix} 1 & 0 \\ 0 & e^{-j\pi/2} \end{bmatrix} \begin{bmatrix} e^{-j\pi/2} & 0 \\ 0 & 1 \end{bmatrix} = e^{-j\pi/2} \begin{bmatrix} 1 & 0 \\ 0 & 1 \end{bmatrix} = \text{A phase shifter}$$

EXERCISE 6.1-3

Jones Matrix of a Rotated Half-Wave Retarder

The Jones matrix of a half-wave retarder at angle 0 is $\mathbf{T} = \begin{bmatrix} 1 & 0 \\ 0 & -1 \end{bmatrix}$. The Jones matrix of a half-wave retarder at angle θ is

$$\mathbf{T} = \begin{bmatrix} \cos\theta & -\sin\theta \\ \sin\theta & \cos\theta \end{bmatrix} \begin{bmatrix} 1 & 0 \\ 0 & -1 \end{bmatrix} \begin{bmatrix} \cos\theta & \sin\theta \\ -\sin\theta & \cos\theta \end{bmatrix}, \tag{6.1-1}$$

which gives rise to

$$\mathbf{T} = \begin{bmatrix} \cos\theta & \sin\theta \\ -\sin\theta & \cos\theta \end{bmatrix}, \tag{6.1-2}$$

from which

$$\mathbf{T} = \begin{bmatrix} \cos 2\theta & \sin 2\theta \\ \sin 2\theta & -\cos 2\theta \end{bmatrix}. \tag{6.1-3}$$

If $\theta = 22.5°$, then $\mathbf{T}$ can be written as

$$\mathbf{T} = \begin{bmatrix} 1 & 1 \\ 1 & -1 \end{bmatrix}, \tag{6.1-4}$$

so that the output waves are proportional to the sum and difference of the input waves.

EXERCISE 6.1-4

Normal Modes of Simple Polarization Systems

a) $\mathbf{T} = \begin{bmatrix} 1 & 0 \\ 0 & 0 \end{bmatrix}$. Eigenvectors are $\begin{bmatrix} 1 \\ 0 \end{bmatrix}$ and $\begin{bmatrix} 0 \\ 1 \end{bmatrix}$;

Eigenvalues are 1 and 0.

b) $\mathbf{T} = \begin{bmatrix} 1 & 0 \\ 0 & e^{-j\Gamma} \end{bmatrix}$. Eigenvectors are $\begin{bmatrix} 1 \\ 0 \end{bmatrix}$ and $\begin{bmatrix} 0 \\ 1 \end{bmatrix}$;

Eigenvalues are 1 and $e^{-j\Gamma}$.

c) $\mathbf{T} = \begin{bmatrix} \cos\theta & -\sin\theta \\ \sin\theta & \cos\theta \end{bmatrix}$. Eigenvectors are $\begin{bmatrix} 1 \\ j \end{bmatrix}$ and $\begin{bmatrix} 0 \\ -j \end{bmatrix}$;

Eigenvalues are $e^{-j\theta}$ and $e^{j\theta}$.

6.2 REFLECTION AND REFRACTION

EXERCISE 6.2-1

Brewster Windows

Reflection does not occur at the first surface when θ_1 is the Brewster angle, $\theta_1 = \tan^{-1} n$. Snell's law provides $\sin\theta_2 = (1/n)\sin\theta_1 = (1/n)\left[n/\sqrt{1+n^2}\right] = 1/\sqrt{1+n^2}$, so that $\tan\theta_2 = 1/n$, i.e., θ_2 is also a Brewster angle for the second surface.
For $n = 1.5$, we have $\theta_1 = \tan^{-1} n = 56.3°$.

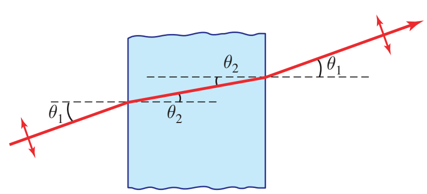

6.4 OPTICAL ACTIVITY AND MAGNETO-OPTICS

EXERCISE 6.4-1

Rotatory Power of an Optically Active Medium

If $G \ll n_0$, $n_\pm = \sqrt{n_0^2 \pm G} = n_0\sqrt{1 \pm G/n_0^2} \approx n_0 \pm G/2n_0$.

Therefore, $\rho = \pi\,(n_- - n_+)\,/\lambda_o = -\pi G/\lambda_o n_0$.

CHAPTER

7

PHOTONIC-CRYSTAL OPTICS

7.1 OPTICS OF DIELECTRIC LAYERED MEDIA

EXERCISE 7.1-1

Quarter-Wave Film as an Anti-Reflection Coating

The **M** matrix for the problem at hand is readily obtained by cascading the **M** matrix for a single dielectric boundary (see Example 7.1-2) and the **M** matrix for propagation followed by a boundary, in reverse order as usual. The result is:

$$\mathbf{M} = \frac{1}{2n_3}\begin{bmatrix}(n_3+n_2)\,e^{-j\varphi} & (n_3-n_2)\,e^{j\varphi}\\ (n_3-n_2)\,e^{-j\varphi} & (n_3+n_2)\,e^{j\varphi}\end{bmatrix}\frac{1}{2n_2}\begin{bmatrix}n_2+n_1 & n_2-n_1\\ n_2-n_1 & n_2+n_1\end{bmatrix},$$

with $\varphi = n_2 k_o d = 2\pi d/\lambda$ and $\lambda = \lambda_o/n_2$.

The B element of this matrix is

$$B = \frac{1}{4n_2n_3}\left[(n_3+n_2)(n_2-n_1)\,e^{-j\varphi} + (n_3-n_2)(n_2+n_1)\,e^{j\varphi}\right].$$

The reflection coefficient can be made to vanish if $B = 0$, i.e., if

$$(n_3+n_2)(n_2-n_1) + (n_3-n_2)(n_2+n_1)\,e^{j2\varphi} = 0.$$

This requires that $e^{j2\varphi}$ be real, i.e., that 2φ be an integer multiple of π.

The value $2\varphi = 4\pi d/\lambda = \pi$ leads to $d = \lambda/4$ and

$$(n_3+n_2)(n_2-n_1) - (n_3-n_2)(n_2+n_1) = 0,$$

whereupon we obtain $n_2^2 = n_1n_3$ or $n_2 = \sqrt{n_1n_3}$.

The choice $2\varphi = 2\pi$, or any even multiple of π, leads to

$$(n_3+n_2)(n_2-n_1) + (n_3-n_2)(n_2+n_1) = 0,$$

which gives the trivial solution $n_1 = n_3$.

CHAPTER
9

GUIDED-WAVE OPTICS

9.1 PLANAR-MIRROR WAVEGUIDES

EXERCISE 9.1-1

Optical Power

In accordance with (5.3-10), the power flow is determined by the Poynting vector $\mathbf{S} = \frac{1}{2}\mathbf{E} \times \mathbf{H}^*$. For the TE mode, we have $E_y = E_z = H_x = 0$. The component of $\mathbf{S}$ in the z direction is therefore $S_z = \frac{1}{2}E_x H_y^*$. Also, from Maxwell's equation (5.3-13), $\nabla \times \mathbf{E} = -j\omega\mu_o\mathbf{H}$, we have $-j\omega\mu_o H_y = \partial E_x/\partial z$, so that $S_z = (1/2j\omega\mu_o)\, E_x\, \partial E_x^*/\partial z$.

Substituting $E_x = \mathfrak{a}_m u_m(y)\exp(-j\beta_m z)$, we obtain $S_z = (\beta_m/2\omega\mu_o)|\mathfrak{a}_m|^2|u_m(y)|^2$.

The total power flow in the z direction is the integral of S_z with respect to y. Since the integral of $|u_m(y)|^2$ is unity, the power flow is $(\beta_m/2\omega\mu_o)|\mathfrak{a}_m|^2$. Furthermore, because $\beta_m = k\cos\theta_m = (\omega/c)\cos\theta_m$, we can write the power flow as $(1/2\mu_o c)|\mathfrak{a}_m|^2\cos\theta_m = (1/2\eta)|\mathfrak{a}_m|^2\cos\theta_m$.

EXERCISE 9.1-2

Optical Power in a Multimode Field

In accordance with Exercise 9.1-1, the power flow in the z direction is the integral of $S_z = (1/2j\omega\mu_o)\, E_x\, \partial E_x^*/\partial z$ with respect to y. Making use of the substitution $E_x = \sum_m \mathfrak{a}_m u_m(y)\exp(-j\beta_m z)$, we obtain

$$S_z = (\beta_m/2\omega\mu_o)\sum_m \mathfrak{a}_m u_m(y)\exp(-j\beta_m z)\sum_n \mathfrak{a}_n^* u_n^*(y)\exp(j\beta_n z).$$

Because the integral of $u_m(y)u_n^*(y)$ with respect to y is unity for $n = m$ and zero otherwise, the total power is
$\sum_m (\beta_m/2\omega\mu_o)\,|\mathfrak{a}_m|^2 = \sum_m (1/2\eta)\,|\mathfrak{a}_m|^2\cos\theta_m$.

9.2 PLANAR DIELECTRIC WAVEGUIDES

EXERCISE 9.2-1

Confinement Factor

Since the waveguide is symmetric we consider confinement only for $y > 0$.

For $y < d/2,\ u_m(y) = A_m\cos(k\sin\theta_m y),\ \ m$ even (1a)

$= A_m\sin(k\sin\theta_m y),\ \ m$ odd.

For $y > d/2,\ u_m(y) = B_m\exp(-\gamma_m y)$, (1b)

where $\gamma_m = n_2 k_o\sqrt{(n_1/n_2)^2\cos^2\theta_m - 1}\,.$ (2)

Because $u_m(y)$ must be continuous at $y = d/2$,

$A_m \cos(k \sin\theta_m d/2) = B_m \exp(-\gamma_m d/2), \quad m$ even (3a)

$A_m \sin(k \sin\theta_m d/2) = B_m \exp(-\gamma_m d/2), \quad m$ odd. (3b)

The power in the region $y < d/2$ is $P_1 = \int_0^{d/2} u_m^2(y)dy$.
Substituting from (1a) and integrating, we have

$P_1 = A_m^2(d/4)\left[1 + (-1)^m \sin(kd\sin\theta_m)/kd\sin\theta_m\right]$. (4)

Similarly, the power in the region $y > d/2$ is:

$P_2 = B_m^2(1/2\gamma_m)\exp(-\gamma_m d)$. (5)

The confinement ratio $\Gamma_m = \dfrac{P_1}{P_1 + P_2} = \dfrac{1}{1 + P_2/P_1}$ (6)

can be obtained by substituting from (4) and (5) and using (3) to substitute for B_m/A_m:

$$\frac{P_2}{P_1} = \frac{(1/\gamma_m d)\left[1 + (-1)^m \cos(kd\sin\theta_m)\right]}{1 + (-1)^m \sin(kd\sin\theta_m)/kd\sin\theta_m}\ . \tag{7}$$

It is convenient to write the result in terms of the variable $M = \dfrac{\sin\overline{\theta}_c}{\lambda/2d}$ (8)

by writing $kd = 2\pi d/\lambda = \pi M/\sin\overline{\theta}_c$, (9)

$$\begin{aligned}\gamma_m d &= kd\,(n_2/n_1)\sqrt{(n_1/n_2)^2\cos^2\theta_m + 1}\\ &= kd\sqrt{\cos^2\theta_m - \cos^2\overline{\theta}_c} = kd\sqrt{\sin^2\overline{\theta}_c - \sin^2\theta_m}\\ &= \pi M\sqrt{1 - \sin^2\theta_m/\sin^2\overline{\theta}_c}\,.\end{aligned} \tag{10}$$

It is also convenient to define the ratio: $s_m = \sin\theta_m/\sin\overline{\theta}_c$
and write $\gamma_m d = \pi M\sqrt{1 - s_m}$. (11)

Using (10) and (11) in (7) then leads to

$$\frac{P_2}{P_1} = \frac{s_m}{\sqrt{1 - s_m^2}}\ \frac{1 + (-1)^m\cos(\pi M s_m)}{\pi M s_m + (-1)^m \sin(\pi M s_m)}\,. \tag{12}$$

This provides an expression for the confinement ratio $\Gamma_m = 1/(1 + P_2/P_1)$ as a function of the parameter M, which represents the number of modes, and the parameter $s_m = \sin\theta_m/\sin\overline{\theta}_c$, which is determined by the normalized angles of the modes.

As an example, consider the case $M = 8$. The parameters s_m are determined from the characteristic equation (9.2-4), which can be written in terms of M and s_m as:

$$\tan(M s_m \pi/2 - m\pi/2) = \sqrt{1/s_m^2 - 1}\,.$$

Solutions of this equation are displayed in Fig. 9.2-2 for $M = 8$. For $m = 0$, the first intersection point occurs at $\sin\theta_0 = 0.933(\lambda/2d)$, or $s_0 \approx 0.933/M$. Similarly, $s_1 \approx 1.86/M$; $s_2 \approx 2.778/M$; and so on.

Substituting these values into (12) and (6) leads to the following confinement ratios: $\Gamma_0 \approx 0.999$; $\Gamma_1 \approx 0.996$; and $\Gamma_2 \approx 0.990$. The lowest-order mode therefore has the highest power confinement factor, as promised.

EXERCISE 9.2-2

The Asymmetric Planar Waveguide

Let the complements of the critical angles for reflection from the substrate and the cover be $\overline{\theta}_{c2} = \cos^{-1}(n_2/n_1)$ and $\overline{\theta}_{c3} = \cos^{-1}(n_3/n_1)$, respectively. Since $n_2 > n_3$, $\overline{\theta}_{c2} < \overline{\theta}_{c3}$. Therefore, a guided ray must be inclined at an angle θ smaller than the smaller of θ_{c2} and θ_{c3}, i.e., $\theta < \theta_{c2}$.

a) Since the numerical aperture is governed by θ_{c2}, $\mathrm{NA} = \sqrt{n_1^2 - n_2^2}\,$.

b) The self-consistency condition in the symmetric waveguide (9.2-1) is thus modified to:

$$\frac{2\pi}{\lambda}\,2d\,\sin\theta - \varphi_{r2} - \varphi_{r3} = 2\pi m\,, \qquad m = 0, 1, 2, \ldots\,,$$

where φ_{r2} and φ_{r3} are, respectively, the phase shifts introduced by total internal reflection at the substrate and cover boundaries. These phases are given by the general formula in (9.2-3), making use of the appropriate critical angles θ_{c2} and θ_{c3}.

c) The number of modes is governed by the critical angle of reflection at the substrate. It is therefore given by $M \doteq (2d/\lambda_o)\,\mathrm{NA}$, where $\mathrm{NA} = \sqrt{n_1^2 - n_2^2}\,$.

CHAPTER
10

FIBER OPTICS

10.3 ATTENUATION AND DISPERSION

EXERCISE 10.3-1

Optimal Grade Profile Parameter

The group velocities are $v_q = (d\beta_q/d\omega)^{-1}$, where $\beta_q = n_1 k_o \left[1 - (q/M)^s \Delta\right]$; $M = s n_1^2 k_o^2 a^2 \Delta$; $s = p/(p+2)$; and $k_o = \omega/c_o$.

To simplify the process of taking the derivative we write

$$\beta_q = (n_1\omega/c_o)\left[1 - x_q\right] \text{ where } x_q = (q/M)^s \Delta.$$

$$\begin{aligned} d\beta_q/d\omega &= (1/c_o)\left[d\left(n_1\omega\right)/d\omega\right](1 - x_q) - n_1\left(\omega/c_o\right)dx_q/d\omega \\ &= (N_1/c_o)\left(1 - x_q\right) n_1 \left(\omega/c_o\right)\, dx_q/d\omega \\ &= (N_1/c_o)\left[1 + x_q\phi\right], \end{aligned}$$

where $N_1 = d\left(n_1\omega\right)/d\omega$ is the group refractive index and
$\phi = -1 - (n_1/N_1)\left(\omega/x_q\right)\, dx_q/d\omega.$ (1)

If ϕx_q is small, the group velocity is
$v_q = \left(d\beta_q/d\omega\right)^{-1} = (c_o/N_1)\left[1 + x_q\phi\right]^{-1} \approx (c_o/N_1)\left[1 - x_q\phi\right].$ (2)

We now proceed to determine ϕ:

$$\begin{aligned} dx_q/d\omega &= s(q/M)^{s-1} q\left[\left(-1/M^2\right) dM/d\omega\right]\Delta + (q/M)^s d\Delta/d\omega \\ &= -s x_q (1/M) dM/d\omega + x_q (1/\Delta) d\Delta/d\omega\,; \end{aligned} \quad (3)$$

$$\begin{aligned} dM/d\omega &= 2 s n_1 k_o \left[d\left(n_1 k_o\right)/d\omega\right] a^2 \Delta + s\left(n_1 k_o\right)^2 a^2 d\Delta/d\omega \\ &= 2M\left(1/n_1 k_o\right) d\left(n_1 k_o\right)/d\omega + M(1/\Delta)\, d\Delta/d\omega \\ &= M\left[\left(2/n_1 k_o\right) N_1/c_o + (1/\Delta)\, d\Delta/d\omega\right]. \end{aligned} \quad (4)$$

Substituting into (3), we have:

$$\begin{aligned} (1/x_q)\, dx_q/d\omega &= -s\left[\left(2/n_1 k_o\right) N_1/c_o + (1/\Delta) d\Delta/d\omega\right] + (1/\Delta) d\Delta/d\omega \\ &= -2sN_1/n_1\omega + (1-s)(1/\Delta)d\Delta/d\omega. \end{aligned}$$

We now use (1) to obtain $\phi = -1 + 2s - (1-s)p_s/2$ with $p_s = 2\left(n_1/N_1\right)\left(\omega/\Delta\right) d\Delta/d\omega$.

Thus $\phi = -1 + 2p/(p+2) - p_s/(p+2) = (p - 2 - p_s)/(p+2)$, which, when substituted into (2), gives (10.3-10).

EXERCISE 10.3-2

Differential Group Delay in a Two-Segment Fiber

a) If $L = 500$ m is the length of a segment, then the group delays of the x and y components at the end of the first segment are:
$T_x = LN_x/c = 2.4367\ \mu$s and $T_y = LN_y/c = 2.4383\ \mu$s.

Each of these components can be analyzed into two components of equal magnitudes along the principal axes x' and y' of the second segment. These components travel to the end of the second segment with group delays $T_{x'}$ and $T_{y'}$. The overall delay may therefore take four values: $T_x + T_{x'}$, $T_y + T_{y'}$, $T_x + T_{y'}$, and $T_y + T_{x'}$. Since $T_x = T_{x'}$ and $T_y = T_{y'}$, we actually have three possible delays: $2T_x = 4.8733\ \mu$s, $2T_y = 4.8767\ \mu$s, and $T_x + T_y = 4.873\ \mu$s. Since the pulse with the delay $T_x + T_y$ results from two possibilities, its amplitude depends on the phase shifts encountered, which are sensitive to the phase velocities and the exact lengths of the fiber segments, and is sensitive to any slight disturbance in the system. This middle pulse will therefore have random polarization.

The differential delays between the fastest pulse and the slowest pulse is $2T_y - 2T_x = 3.4$ ns. To determine whether this differential delay will be visible, we examine the pulse broadening due to GVD. For a single segment, the GVD broadening is $D\sigma_\lambda L = 20 \times 50 \times 0.5 = 500$ ps, so that the width of each pulse is broadened from an initial value of 100 ps to a value of 1 ns. The shape of the received pulses will therefore appear as shown below:

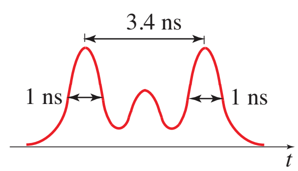

b) The two fiber segments are equivalent to two cascaded identical retarders with their principal axes rotated by $45°$. The Jones matrix of this system is the product of the matrices

$$\mathbf{T} = \begin{bmatrix}\cos\theta & -\sin\theta\\ \sin\theta & \cos\theta\end{bmatrix}\begin{bmatrix}1 & 0\\ 0 & e^{-j\varphi}\end{bmatrix}\begin{bmatrix}\cos\theta & \sin\theta\\ -\sin\theta & \cos\theta\end{bmatrix}\begin{bmatrix}1 & 0\\ 0 & e^{-j\varphi}\end{bmatrix},$$

where $\varphi = (N_x - N_y)2\pi L/\lambda$ is the retardation introduced by a segment and θ is the angle of rotation. Since $\theta = 45°$,

$$\mathbf{T} = \frac{1}{\sqrt{2}}\begin{bmatrix}1 & -1\\ 1 & 1\end{bmatrix}\begin{bmatrix}1 & 0\\ 0 & e^{-j\varphi}\end{bmatrix}\frac{1}{\sqrt{2}}\begin{bmatrix}1 & 1\\ -1 & 1\end{bmatrix}\begin{bmatrix}1 & 0\\ 0 & e^{-j\varphi}\end{bmatrix}$$

and therefore

$$\mathbf{T} = \frac{1}{2}\begin{bmatrix}1 + e^{-j\varphi} & e^{-j\varphi}(1 - e^{-j\varphi})\\ 1 - e^{-j\varphi} & e^{-j\varphi}(1 + e^{-j\varphi})\end{bmatrix}.$$

The eigenvalues and eigenvectors of this matrix may be determined for any value of φ. Since the matrix is unitary, the eigenvalues will always be phase factors. For example, if $\varphi = \pi$ then the eigenvalues are $\pm j$ and the eigenvectors are $\begin{bmatrix}1\\ \mp j\end{bmatrix}$, representing circularly polarized modes. In any case, a pulse in one of the polarization modes travels with a single group velocity so that it arrives as a single pulse instead of two.

CHAPTER 11

RESONATOR OPTICS

11.1 PLANAR-MIRROR RESONATORS

EXERCISE 11.1-1

Resonance Frequencies of a Traveling-Wave Resonator

a) *Three-mirror ring resonator*: At resonance, the round trip phase shift, $3kd + 3\pi$, is equal to a multiple of 2π. Thus, $3kd + \pi = q2\pi$, where q is an integer, so that $3kd = (2q-1)\pi$ or $3(2\pi\nu/c)d = (2q-1)\pi$. Consequently $\nu_q = (2q-1)(c/6d)$ so that the allowed frequencies are odd multiples of $c/6d$. Two consecutive resonances are therefore separated by a frequency $\nu_F = 2(c/6d) = c/3d$.

b) *Four-mirror bow-tie resonator*: At resonance, the round trip phase shift, $(4 + 2\sqrt{5})kd + 4\pi$, is equal to a multiple of 2π, i.e., $(4+2\sqrt{5})kd + 4\pi = q2\pi$, where q is an integer. Thus, $(4+2\sqrt{5})kd = q2\pi$, or $(4+2\sqrt{5})(2\pi\nu/c)d = q2\pi$, from which $\nu_q = q[c/(4+2\sqrt{5})d\,]$. Two consecutive resonances are therefore separated by a frequency $\nu_F = [c/(4+2\sqrt{5})d\,]$.

EXERCISE 11.1-2

Resonator Modes and Spectral Width

Given: $\mathcal{R}_1 = 0.98$, $\mathcal{R}_2 = 0.99$, $d = 1$ m, $n = 1$, $c = c_o/n = c_o = 3\times10^8$ m/s.
Frequency spacing between modes is $\nu_F = c/2d = 1.5\times10^8$ Hz $= 150$ MHz.
Loss coefficient $\alpha_r = (1/2d)\ln(1/\mathcal{R}_1\mathcal{R}_2) = 0.015$.
Using (11.1-28), the Finesse $\mathcal{F} \approx \pi/\alpha_r d = 207.7$.
The spectral linewidth is $\delta\nu = \nu_F/\mathcal{F} = 7.22\times10^5$ Hz $= 722$ kHz.
This approximation is appropriate since $\alpha_r d = 0.015 \ll 1$.

11.2 SPHERICAL-MIRROR RESONATORS

EXERCISE 11.2-1

Maximum Resonator Length for Confined Rays

The confinement condition is $0 \le (1 + d/R_1)(1 + d/R_2) \le 1$. Substituting $R_1 = -0.5$ m and $R_2 = -1$ m, we obtain $0 \le (1-2d)(1-d) \le 1$. Letting $x = (1-2d)(1-d)$, the confinement condition becomes $0 \le x \le 1$. The figure below shows a plot of x versus d. Based on this figure, the maximum value of d for which the resonator is stable is $d = 1.5$ m.

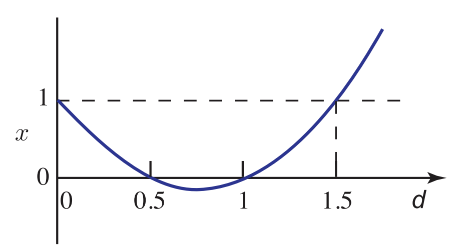

EXERCISE 11.2-2

A Plano-Concave Resonator

For a plano-concave resonator, $R_1 = \infty$ and $R_2 = -|R|$. Substituting $z_1 = 0$ and $z_2 = d$ into (11.2-13) we have $|R| = d + z_0^2/d$, from which $z_0^2 = d(|R| - d)$. For confinement, $z_0^2 > 0$ so that $|R| > d$.

From (11.2-10), we have

$$W_0^2 = \lambda z_0/\pi = (\lambda/\pi)\,[d(|R| - d)]^{1/2} \quad \text{and}$$

$$W_1 = W_0 = (\lambda d/\pi)^{1/2}\,(|R|/d - 1)^{1/4}. \quad \text{Using (11.2-16), this leads to}$$

$$W_2^2 = W_0^2(1 + d^2/z_0^2) = W_0^2\,[1 + d/(|R| - d)] = W_0^2|R|/(|R| - d),$$

from which

$$W_2 = \frac{(\lambda d/\pi)^{1/2}\,(|R|/d - 1)^{1/4}\,(|R|/d)^{1/2}}{(|R|/d - 1)^{1/2}} = (\lambda d/\pi)^{1/2}\left[\frac{(|R|/d)^2}{(|R|/d - 1)}\right]^{1/4}.$$

The quantities W_1 and W_2 are plotted versus $d/|R|$ below:

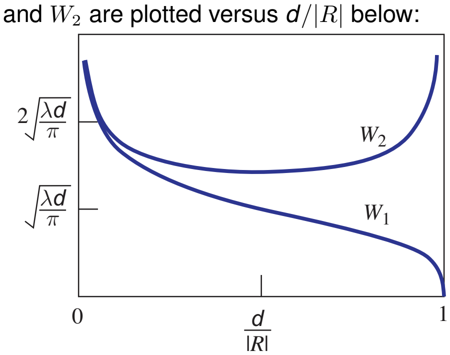

EXERCISE 11.2-3

Resonance Frequencies of a Confocal Resonator

Given: $d = 30$ cm $= 0.3$ m; $c = c_o/n = c_o$.
$z_1 = -z_0$ and $z_2 = z_0$.
$\nu_F = c/2d = 5 \times 10^8\ \text{Hz} = 500$ MHz.

$$\begin{aligned}\Delta\zeta &= \tan^{-1}(z_2/z_0) - \tan^{-1}(z_1/z_0)\\ &= \tan^{-1}(1) - \tan^{-1}(-1)\\ &= \pi/4 - (-\pi/4)\\ &= \pi/2.\end{aligned}$$

$(\Delta\zeta/\pi)\nu_F = \Delta\nu_F/2 = 250$ MHz.
$\nu_q = q\nu_F + \nu_F/2 = (q + 1/2)\nu_F$.

At the central frequency $q \approx \nu/\nu_F = (5 \times 10^{14})/(5 \times 10^8) = 10^6$, for

$q = 10^6$: $\nu_q = 5 \times 10^{14} + 2.5 \times 10^8$ Hz
$q = 10^6 + 1$: $\nu_q = 5 \times 10^{14} + 7.5 \times 10^8$ Hz
$q = 10^6 + 2$: $\nu_q = 5 \times 10^{14} + 12.5 \times 10^8$ Hz
$q = 10^6 + 3$: $\nu_q = 5 \times 10^{14} + 17.5 \times 10^8$ Hz

$q = 10^6 - 1$: $\nu_q = 5 \times 10^{14} - 2.5 \times 10^8$ Hz
$q = 10^6 - 2$: $\nu_q = 5 \times 10^{14} - 7.5 \times 10^8$ Hz
$q = 10^6 - 3$: $\nu_q = 5 \times 10^{14} - 12.5 \times 10^8$ Hz
$q = 10^6 - 4$: $\nu_q = 5 \times 10^{14} - 17.5 \times 10^8$ Hz

Thus, there are 8 modes within the band $5 \times 10^{14} \pm 2 \times 10^9$ Hz.

EXERCISE 11.2-4

Resonance Frequencies of the Symmetrical Confocal Resonator

For confocal symmetric resonators, we have $(\Delta\zeta/\pi)\nu_F = \nu_F/2$.
From (11.2-33), we see that $\nu_{l,\,m,\,q} = [q + (l+m+1)/2]\,\nu_F$.

The set of modes for which $l+m+1$ is even are spaced at frequency intervals ν_F. Modes for which $l+m+1$ is odd are also spaced at frequency intervals ν_F, but are displaced from the even modes by frequency $\nu_F/2$.

11.3 TWO- AND THREE-DIMENSIONAL RESONATORS

EXERCISE 11.3-1

Density of Modes in a Two-Dimensional Resonator

a) The number of modes with frequency between 0 and ν is the same as the number of modes with wavenumber between 0 and $k = 2\pi\nu/c$.

In accordance with Fig. 11.3-2, this number is approximated by the area of a quadrant in k space $(\pi k^2/4)$ divided by the area per mode $(\pi/d)^2$, and then multiplied by a factor of two to account for the two polarizations per mode. This number is thus $2\,(\pi k^2/4)\,/\,(\pi/d)^2 \;=\; k^2 d^2/2\pi \;=\; (2\pi\nu/c)^2\, d^2/2\pi \;=\; 2\pi\nu^2 d^2/c^2$. Consequently, the number of modes per unit area, in the frequency band 0 to ν, is $N_\nu = 2\pi\nu^2/c^2$.

b) The density of modes per unit area per unit frequency interval is therefore $M(\nu) = dN_\nu/d\nu = 4\pi\nu/c^2$.

CHAPTER

12

STATISTICAL OPTICS

12.1 STATISTICAL PROPERTIES OF RANDOM LIGHT

EXERCISE 12.1-1

Coherence Time

a) Coherence time $= \int_{-\infty}^{\infty} |g(\tau)|^2 d\tau = \int_{-\infty}^{\infty} \exp\left(\dfrac{-2|\tau|}{\tau_c}\right) d\tau = 2\int_0^{\infty} \exp\left(\dfrac{-2\tau}{\tau_c}\right) d\tau = \tau_c$.
$|g(\tau)|$ decreases by a factor $1/e = 0.368$ at $\tau = \tau_c$.

b) Coherence time $= \int_{-\infty}^{\infty} |g(\tau)|^2 d\tau = \int_{-\infty}^{\infty} \exp\left(\dfrac{-\pi\tau^2}{\tau_c^2}\right) d\tau = \tau_c$.
$|g(\tau)|$ decreases by a factor of $\exp(-\pi) = 0.043$ at $\tau = \tau_c$.

EXERCISE 12.1-2

Relation Between Spectral Width and Coherence Time

Since $S(\nu)$ is the Fourier transform of $G(\tau)$, we have
$\int_0^{\infty} S(\nu) d\nu = G(0)$. (1)

From Parseval's theorem, we write
$\int_0^{\infty} S^2(\nu) d\nu = \int_{-\infty}^{\infty} |G(\tau)|^2 d\tau$. (2)

Squaring both sides of (1) and dividing by the two sides of (2), while making use of the definitions of $\Delta\nu_c$, τ_c, and $g(\tau)$, we obtain
$\Delta\nu_c = |G(0)|^2 / \int |G(\tau)|^2 d\tau = 1/\int |g(\tau)|^2 d\tau = 1/\tau_c$.

EXERCISE 12.1-3

Differential Equations Governing the Mutual Coherence Function

$G = \langle U^*(r_1,t) U(r_2,t+\tau)\rangle$.
Therefore, $\nabla_1^2 G = \langle [\nabla_1^2 U^*(r_1,t)]\, U(r_2,t+\tau)\rangle$.

Since U obeys the wave equation, $\nabla^2 U = (1/c^2)\partial^2 U/\partial t^2$, and
$\nabla_1^2 G = (1/c^2)\langle [(\partial^2/\partial t^2)\, U^*(r_1,t)]\, U(r_2,t+\tau)\rangle$. (1)

We now proceed to prove that $\langle [(\partial^2/\partial t^2)\, U^*(r_1,t)]\, U(r_2,t+\tau)\rangle = (\partial^2/\partial\tau^2)\, G$,
so that $\nabla_1^2 G = (\partial^2/\partial\tau^2)\, G$:

Proof: $\langle [(\partial/\partial t) U^*(r_1,t)]\, U(r_2,t+\tau)\rangle$

$$= \langle \lim_{\Delta t\to 0} (1/\Delta t)\, [U^*(r_1,t+\Delta t) - U^*(r_1,t)]\, U(r_2,t+\tau)\rangle$$

$$= \lim_{\Delta t\to 0} (1/\Delta t)\, [G(r_1,r_2,\tau-\Delta t) - G(r_1,r_2,\tau)]$$

$$= -(\partial/\partial\tau) G(r_1,r_2,\tau)$$

Similarly, $\langle [(\partial^2/\partial t^2) U^*(r_1,t)]\, U(r_2,t+\tau)\rangle = (\partial^2/\partial\tau^2)\, G$.

12.4 PARTIAL POLARIZATION

EXERCISE 12.4-1

Partially Polarized Light

The coherency matrix for the superposition of unpolarized light whose intensity is given by $(I_x + I_y)(1 - \mathbb{P})$, and linearly polarized light of intensity $(I_x + I_y)\mathbb{P}$ at angle θ, is

$$G = (1 - \mathbb{P}) \left[\frac{I_x + I_y}{2}\right] \begin{bmatrix}1 & 0\\ 0 & 1\end{bmatrix} + \mathbb{P}\,(I_x + I_y) \begin{bmatrix}\cos^2\theta & \cos\theta\sin\theta\\ \cos\theta\sin\theta & \sin^2\theta\end{bmatrix}.$$

The four elements of this matrix are

$$G_{xx} = (I_x + I_y)\,(1 - \mathbb{P})/2 + (I_x + I_y)\,\mathbb{P}\cos^2\theta, \tag{1}$$

$$G_{yy} = (I_x + I_y)\,(1 - \mathbb{P})/2 + (I_x + I_y)\,\mathbb{P}\sin^2\theta, \tag{2}$$

$$G_{xy} = G_{yx} = (I_x + I_y)\,\mathbb{P}\sin\theta\cos\theta. \tag{3}$$

We wish to show that for some θ,

$$G_{xx} = I_x, \tag{4}$$

$$G_{yy} = I_y, \tag{5}$$

$$G_{xy} = G_{yx} = (I_x I_y)\,|g_{xy}|^2. \tag{6}$$

From (4) and (1) we have

$$\cos^2\theta = \frac{I_x - (I_x + I_y)\,(1 - \mathbb{P})/2}{(I_x + I_y)\mathbb{P}}, \tag{7}$$

while from (5) and (2) we have

$$\sin^2\theta = \frac{I_y - (I_x + I_y)\,(1 - \mathbb{P})/2}{(I_x + I_y)\mathbb{P}}. \tag{8}$$

Adding (7) and (8) we obtain $\cos^2\theta + \sin^2\theta = 1$, so that if (7) is satisfied, (8) is automatically satisfied.

Let us now verify (6). From (3), we find

$$G_{xy}^2 = (I_x + I_y)^2\,\mathbb{P}^2 \sin^2\theta\cos^2\theta. \tag{9}$$

Substituting (7) and (8) into (9) yields

$$\begin{aligned}
G_{xy}^2 &= [I_x - (I_x + I_y)(1 - \mathbb{P})/2]\,[I_y - (I_x + I_y)(1 - \mathbb{P})/2]\\
&= I_x I_y + \tfrac{1}{4}(I_x + I_y)^2(1 - \mathbb{P})^2 - \tfrac{1}{2}(I_x + I_y)^2(1 - \mathbb{P})\\
&= I_x I_y + \tfrac{1}{4}(I_x + I_y)^2(1 - \mathbb{P})[(1 - \mathbb{P}) - 2]\\
&= I_x I_y - \tfrac{1}{4}(I_x + I_y)^2(1 - \mathbb{P}^2).
\end{aligned} \tag{10}$$

From the definition of $\mathbb{P}$ provided in (12.4-13), we find

$1 - \mathbb{P}^2 = \dfrac{4\,(1 - |g_{xy}|^2)\,I_x I_y}{(I_x + I_y)^2}$, so that (10) gives

$G_{xy}^2 = I_x I_y - I_x I_y (1 - |g_{xy}|^2) = I_x I_y |g_{xy}|^2$, indicating that (6) is also satisfied.

CHAPTER
13

PHOTON OPTICS

13.1 THE PHOTON

EXERCISE 13.1-1

Photon in a Gaussian Beam

a) In accordance with (3.1-12), the intensity of a Gaussian beam at $z = 0$ is $I(\rho, 0) \propto \exp(-2\rho^2/W_0^2)$. The probability p of detecting the photon within a circle of radius W_0 is thus given by the ratio

$$p = \frac{\int_0^{W_0} I(\rho,0) 2\pi\rho \, d\rho}{\int_0^{\infty} I(\rho,0) 2\pi\rho \, d\rho}.$$

Transforming the integration variable to $x = \dfrac{\rho^2}{W_0^2}$, so that $dx = \dfrac{2\rho \, d\rho}{W_0^2}$, we have

$$p = \frac{\int_0^1 \exp(-2x) dx}{\int_0^{\infty} \exp(-2x) dx} = \frac{(1 - e^{-2})}{(1-0)} = 0.86.$$

Indeed, recall from the discussion following (3.1-17) that the power contained within a circle of radius W_0 is 86% of the total power in the beam.

b) The average number of photons is $p\,n = 0.86\,n$.

EXERCISE 13.1-2

Photon-Momentum Recoil

Photon momentum $= \hbar k = \hbar\omega/c = E/c$. The recoil momentum $p = Mv$, where M is the mass of the ^{198}Hg atom and v is its velocity, so that $v = E/Mc$.
Substituting $E = 4.88$ eV $= 4.88 \times 1.6 \times 10^{-19}$ J; $M = 198 \times 1.66 \times 10^{-27}$ kg; and $c = 3 \times 10^8$ m/s, we obtain $v = 7.9 \times 10^{-3}$ m/s.

The RMS thermal velocity of the atom is $v_{\text{thermal}} = \sqrt{3kT/M}$.
At $T = 300°\text{K}$, $kT = 1.38 \times 10^{-23} \times 300$, so that $v_{\text{thermal}} = 194$ m/s, which is much larger than the recoil velocity.

EXERCISE 13.1-3

Single Photon in a Mach–Zehnder Interferometer

Using the interference formula for the Mach–Zehnder interferometer (2.5-6), the intensity in the detector branch is
$I \propto I_0 [1 + \cos(2\pi d/\lambda)] \propto I_0 \cos^2(\pi d/\lambda)$, where $2I_0$ is the total incident intensity. If the wave contains a single photon, the probability of its detection by the detector is $1 + \cos(2\pi d/\lambda) \propto \cos^2(\pi d/\lambda)$, as shown in the figure. The probability of finding the photon in the other output branch of the interferometer is $1 - \cos(2\pi d/\lambda) \propto \sin^2(\pi d/\lambda)$, which is also shown in the figure. The probability of finding the photon in either of the two branches is the sum $\cos^2(\pi d/\lambda) + \sin^2(\pi d/\lambda) = 1$, as expected.

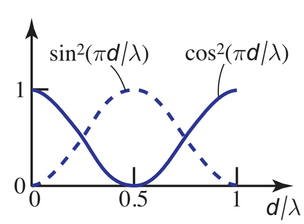

EXERCISE 13.1-4

Single Photon in a Gaussian Wavepacket

a) The Gaussian function $f(t) = |\mathfrak{a}(t)|^2 = \exp(-t^2/2\tau^2)$ has an RMS width, as defined by Equation (A.2-1), that is $\sigma_t = \tau$. Since $z = ct$, the time uncertainty of the function $\mathfrak{a}(t - z/c)$ is σ_t and the positional uncertainty is $\sigma_z = c\sigma_t$.

b) The Fourier transform of $\mathfrak{a}(t)$ is also Gaussian, $A(\nu) = (1/2\sqrt{\pi}\sigma_\nu)\exp(-\nu^2/4\sigma_\nu^2)$, where $\sigma_\nu = 1/4\pi\sigma_t$. The RMS width of $|A(\nu)|^2$ is σ_ν. Since the energy $E = h\nu$, the energy uncertainty is $\sigma_E = h\sigma_\nu = h/4\pi\sigma_t = \hbar/2\sigma_t$, from which (13.1-20) follows. Because the momentum $p = h/\lambda = (h/c)\nu$, the momentum uncertainty is $\sigma_p = (h/c)\sigma_\nu = h/4c\pi\sigma_t = \hbar/2c\sigma_t$. Therefore, $\sigma_z\sigma_p = (c\sigma_t)(\hbar/2c\sigma_t) = \hbar/2$, from which (13.1-21) follows.

13.2 PHOTON STREAMS

EXERCISE 13.2-1

Average Energy of a Resonator Mode in Thermal Equilibrium

The average number of photons $\overline{n}$ for a single mode of thermal light is given by (13.2-21). The average energy $\overline{E} = h\nu\overline{n}$ so that $\overline{E} = h\nu/[\exp(h\nu/kT) - 1]$. A plot of $\overline{E}$ versus $h\nu$ for two values of kT is shown below. In the limit $h\nu/kT \ll 1$, i.e., when the photon energy is much smaller than the unit of thermal energy, $\exp(h\nu/kT) \approx 1 + (h\nu/kT)$ so that $\overline{E} \approx kT$. In this limit, the average energy is what would be obtained if the light were not quantized.

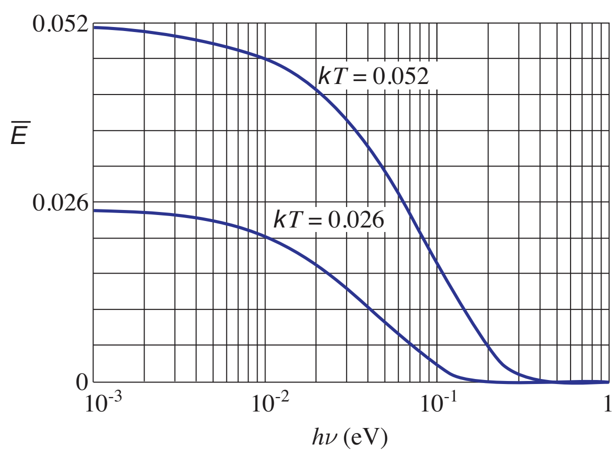

CHAPTER

14

LIGHT AND MATTER

14.3 INTERACTIONS OF PHOTONS WITH ATOMS

EXERCISE 14.3-1

Frequency of Spontaneously Emitted Photons

In accordance with (14.3-1) the probability density of spontaneous emission into a single prescribed mode is $p_{\rm sp} = (c/V)\,\sigma(\nu)$. The probability density of spontaneous emission into any of the modes in the band ν to $\nu + d\nu$ is therefore $P_{\rm sp}\,d\nu = (c/V)\,\sigma(\nu)\,M(\nu)\,V\,d\nu$, where $M(\nu) = 8\pi\nu^2/c^3$ is the density of modes per unit volume.

Using $M(\nu) = 8\pi\nu^2/c^3$, $\sigma(\nu) = Sg(\nu)$, and $S = \lambda^2/8\pi t_{\rm sp}$, we thus obtain $P_{\rm sp}\,d\nu = (1/t_{\rm sp})\,g(\nu)\,d\nu$. The probability that the emitted photon has a frequency between ν and $\nu + d\nu$ is therefore proportional to $g(\nu)d\nu$. Hence, when many photons are emitted the distribution of their frequencies is proportional to $g(\nu)$.

EXERCISE 14.3-2

Doppler-Broadened Lineshape Function

a) The average lineshape function is $\overline{g}(\nu) = \int_{-\infty}^{\infty} g(\nu - v\nu_0/c)\,p(v)\,dv$. It is convenient to transform the integration variable from v to $x = (\nu_0/c)v$, which gives rise to
$\overline{g}(\nu) = \int_{-\infty}^{\infty} g(\nu - x)\,p_x(x)\,dx,$ (1)
where $p_x(x) = (c/\nu_0)\,p(cv/\nu_0)$. This result follows because transforming a random variable v to another random variable av, where a is a constant, modifies the probability density function to $(1/a)\,p(v/a)$. Since $p(v)$ is a Gaussian function of width σ_v, $p_x(x)$ is a Gaussian function of width $\sigma_x = (\nu_0/c)\sigma_v$. Note that x has units of frequency. Equation (1) is the convolution of a Lorentzian function $g(\nu)$ of width $\Delta\nu$ with a Gaussian function of width σ_x.

b) If $\Delta\nu \ll \nu_0\sigma_v/c$, then $\Delta\nu \ll \sigma_x$, i.e., the Lorentzian function $g(\nu)$ in the convolution integral (1) is much narrower than the Gaussian function. Since $g(\nu)$ is a narrow function of unit area, it can be treated for the purposes of integration as a delta function $\delta(\nu)$. Thus (1) gives: $\overline{g}(\nu) \approx \int_{-\infty}^{\infty} \delta(\nu - x)\,p_x(x)\,dx = p(\nu)$, i.e., $\overline{g}(\nu)$ is approximately Gaussian with width $\sigma_D = \sigma_x = (\nu_0/c)\sigma_v = \sigma_v/\lambda = \sqrt{kT/M}\,/\,\lambda$.

c) At $T = 300^\circ$ K, for the Ne transition we substitute the following into (14.3-43) and (14.3-44): $\lambda \approx \lambda_o = 632.8 \times 10^{-9}$ m, $M \approx 20\,m_{\rm p} = 20(1.67 \times 10^{-27}$ kg) so that $\Delta\nu_D = 2.35\,\sigma_D = 1.3 \times 10^9$ Hz $= 1.3$ GHz. For the CO_2 transition, $\lambda \approx \lambda_o = 10.6 \times 10^{-6}$ m, $M \approx 44\,m_{\rm p} = 44(1.67 \times 10^{-27}$ kg), so that $\Delta\nu_D = 5.3 \times 10^7$ Hz $= 53$ MHz.

d) The maximum value of $\overline{\sigma}(\nu)$ is

$$\overline{\sigma}_0 = \overline{\sigma}(\nu_0) = (\lambda^2/8\pi t_{\rm sp})\,\overline{g}(\nu_0) = (\lambda^2/8\pi t_{\rm sp})\left[1/\sqrt{2\pi}\sigma_D\right]$$

$$= (\lambda^2/8\pi t_{\rm sp})\left[2.35/\sqrt{2\pi}\Delta\nu_D\right] \approx \frac{0.94(\lambda^2/8\pi)}{t_{\rm sp}\Delta\nu_D}.$$

For the Lorentzian lineshape $\overline{\sigma}_0 = \dfrac{(2/\pi)(\lambda^2/8\pi)}{t_{\rm sp}\,\Delta\nu} = \dfrac{0.64(\lambda^2/8\pi)}{t_{\rm sp}\,\Delta\nu}$, which is similar to the Gaussian result. Note, however, that $\Delta\nu_D$ is typically much greater than $\Delta\nu$ so that $\overline{\sigma}_0$ is much smaller in the Doppler-broadened-Gaussian case.

14.4 THERMAL LIGHT

EXERCISE 14.4-1

Frequency of Maximum Blackbody Energy Density

Defining $x = h\nu/kT$, (14.4-9) gives $\varrho(\nu) = \dfrac{[8\pi(kT)^3/c^3h^2]x^3}{[e^x - 1]}$.

The frequency at which $\varrho(\nu)$ is maximum is obtained by equating $d\varrho/dx$ to zero.

This yields $3x^2[e^x - 1] - x^3[e^x] = 0$, or $3(e^x - 1) = xe^x$, from which $x = 3(1 - e^{-x})$. Numerical solution of this nonlinear equation provides $x \approx 2.821$. For $T = 300^\circ$ K, we thus have $\nu = \nu_\mathrm{p} = xkT/h = 1.76 \times 10^{13} = 17.6$ THz, which is consistent with the plot presented in Fig. 14.4-4.

CHAPTER
15

LASER AMPLIFIERS

15.1 THEORY OF LASER AMPLIFICATION

EXERCISE 15.1-1

Attenuation and Gain in a Ruby Laser Amplifier

Parameters: $\lambda_o = 694.3 \times 10^{-9}$ m; $n = 1.76$; $\lambda = \lambda_o/n$; $T = 300°$ K; $\Delta\nu = 330 \times 10^9$ Hz; $t_{\text{sp}} = 3 \times 10^{-3}$s; $N_a = N_1 + N_2 = 10^{28}$ m^{-3}; $h = 6.62 \times 10^{-34}$ J-s; $k = 1.38 \times 10^{-23}$ J/°K.

a) In thermal equilibrium
$N_2/N_1 = \exp[-(E_2 - E_1)/kT] = \exp(-h\nu/kT) = \exp(-hc_o/\lambda_o kT) \approx 10^{-30}$.
Therefore $N_2 \ll N_1$ so that $N_1 \approx N_a$, i.e., almost all the atoms are in the lower-level energy state. The attenuation coefficient at the central frequency $= \alpha(\nu_0) = -\gamma(\nu_0) = -N(\lambda^2/8\pi t_{\text{sp}})\, g(\nu_0) = -N(\lambda^2/8\pi t_{\text{sp}})\,(2/\pi\Delta\nu)$, where $N = N_2 - N_1 \approx -N_a$. Therefore, $\alpha(\nu_0) = N_a(\lambda^2/8\pi t_{\text{sp}})\,(2/\pi\Delta\nu) = 3.98 \times 10^4$ m$^{-1} = 398$ cm^{-1}.

b) For $\gamma(\nu_0) = N(\lambda^2/8\pi t_{\text{sp}})\,(2/\pi\Delta\nu) = 50$ m^{-1}, the population becomes inverted for $N = N_2 - N_1 = (50)(4)\pi^2 t_{\text{sp}}\Delta\nu/\lambda^2 = 1.254 \times 10^{25}$ m$^{-3} = 1.254 \times 10^{19}$ cm^{-3}.

c) To attain a gain $G = \exp[\gamma(\nu_0)d] = 4$, we require $d = \ln(4)/\gamma(\nu_0) = 2.77$ cm.

15.2 AMPLIFIER PUMPING

EXERCISE 15.2-1

Optical Pumping

The populations of the three energy levels (2, 1, and the ground state) are N_2, N_1, and N_g, respectively. The total population is $N_1 + N_2 + N_g = N_a$. Since level 1 is short lived, $N_1 \approx 0$, so that $N_2 + N_g \approx N_a$ and

$$N_g \approx N_a - N_2. \qquad (1)$$

The system is pumped by transitions between the ground state and level 2, so that $R_2 = (N_g - N_2)W$. Using (1), we therefore obtain $R_2 = (N_a - 2N_2)W$. In this case, it is apparent that the rate R_2 is dependent on N_2. Now, from (15.2-7) the population difference $N_0 \approx R_2 t_{\text{sp}} = (N_a - 2N_2)Wt_{\text{sp}}$. But $N_0 = N_2 - N_1 \approx N_2$. Thus $N_0 = (N_a - 2N_0)Wt_{\text{sp}}$. Solving for N_0 we have $N_0 = N_a t_{\text{sp}} W/(1 + 2t_{\text{sp}}W)$. In the limit where $W \ll 1/2t_{\text{sp}}$, we obtain $N_0 \approx N_a t_{\text{sp}} W$, which is proportional to W. However for larger W, in the domain where it is not negligible in comparison with $1/2t_{\text{sp}}$, saturation sets in and N_0 loses its proportionality to W.

EXERCISE 15.2-2

Saturation Time Constant

If $t_{\text{sp}} \ll \tau_{\text{nr}}$ (i.e., nonradiative transitions are slow), and

$t_{\text{sp}} \ll \tau_{20}$ (i.e., decay to levels other than level 1 is slow), and

$t_{\text{sp}} \gg \tau_1$ (i.e., decay from level 1 is fast, i.e., level 1 is short-lived),

then $1/\tau_2 = 1/\tau_{20} + 1/t_{\text{sp}} + 1/\tau_{\text{nr}} \approx 1/t_{\text{sp}}$, so that $\tau_2 \approx t_{\text{sp}}$; furthermore $1/\tau_{21} = 1/t_{\text{sp}} + 1/\tau_{\text{nr}} \approx 1/t_{\text{sp}}$, so that $\tau_{21} \approx t_{\text{sp}}$. Under these conditions, it follows that the saturation time constant provided in (15.2-11) can be approximated as $\tau_s = \tau_2 + \tau_1(1 - \tau_2/\tau_{21}) \approx t_{\text{sp}} + \tau_1(1 - t_{\text{sp}}/t_{\text{sp}}) \approx t_{\text{sp}}$, thereby demonstrating that $\tau_s \approx t_{\text{sp}}$.

EXERCISE 15.2-3

Pumping Power in Three- and Four-Level Systems

3-level laser amplifier:
For a three-level scheme, in accordance with (15.2-30), when $N_0 = 0$ we have $t_{\rm sp} W = 1$ so that $W = 1/t_{\rm sp}$. Now, when the pumping transition probability is twice as large, as assumed in the problem for the three-level scheme, namely $W = 2/t_{\rm sp}$, (15.2-30) yields $N_0 = \frac{1}{3} N_a$. The pumping power is then $P = h\nu_{31} R$, where $R = (N_1 - N_3) W$. Since $N_3 \approx 0$, we obtain $R \approx N_1 W$. Because $N_2 + N_1 = N_a$ and $N_2 - N_1 = N_0$, by subtraction we obtain $2N_1 = N_a - N_0 = N_a - \frac{1}{3}N_a = \frac{2}{3}N_a$, so that $N_1 = \frac{1}{3}N_a$. It follows that $R = \frac{1}{3}N_a W = \frac{1}{3}N_a(2/t_{\rm sp}) = \frac{2}{3}N_a/t_{\rm sp}$, which leads to $P = \frac{2}{3}h\nu_{31} N_a/t_{\rm sp}$.

4-level laser amplifier:
For a four-level scheme, in accordance with (15.2-20), when $N_0 = 0$ we have $W = 0$. Now, when the pumping transition probability is $W = 1/2t_{\rm sp}$, as assumed in the problem for the four-level scheme, (15.2-20) yields $N_0 = \frac{1}{3}N_a$. The pumping power is then $P = h\nu_{30} R$, where $R = (N_g - N_3)W \approx N_g W$. But since $N_g = N_a - N_0 = N_a - \frac{1}{3}N_a = \frac{2}{3}N_a$, we have $R = \frac{2}{3}N_a(1/2t_{\rm sp}) = \frac{1}{3}N_a/t_{\rm sp}$, from which $P = \frac{1}{3}h\nu_{30}N_a/t_{\rm sp}$.

Comparison:
Under these special conditions, and assuming that the two systems have the same values of N_a and $t_{\rm sp}$, the ratio of the 4-level to 3-level pumping powers required to achieve this population difference is $\nu_{30}/2\nu_{31}$.

15.4 AMPLIFIER NONLINEARITY

EXERCISE 15.4-1

Saturation Photon-Flux Density for Ruby

Parameters: $\lambda_o = 694.3 \times 10^{-9}$ m; $n = 1.76$; $\tau_s = 2t_{\rm sp}$; $\Delta\nu = 3.3 \times 10^{11}$ Hz; $c_o = 3 \times 10^8$ m/s; $h = 6.63 \times 10^{-34}$ J-s.
From (15.4-2), we have $1/\phi_s(\nu_0) = (\lambda^2/8\pi)\,(\tau_s/t_{\rm sp})\,g(\nu_0) = (\lambda^2/8\pi)(2)(2/\pi\Delta\nu) = (\lambda_o/n)^2/2\pi^2\Delta\nu$, where we have made use of (15.1-8) for $g(\nu_0)$. Inserting the numerical parameter values leads to $\phi_s(\nu_0) = 4.186 \times 10^{25}$ m^{-2}s^{-1}. This corresponds to a saturation intensity $I_s = h\nu_0\,\phi_s(\nu_0) = (c_o h/\lambda_o)\,\phi_s(\nu_0) = 1.2\times 10^7$ W/m^2 $= 1200$ W/cm^2.

EXERCISE 15.4-2

Spectral Broadening of a Saturated Amplifier

Making use of (15.4-2), (15.4-3), (15.4-4), and (15.1-8), we have:

$$\gamma(\nu) = \gamma_0(\nu)/[1+\phi/\phi_s], \text{ where } \gamma_0(\nu) = ag(\nu), \quad a = N_0\lambda^2/8\pi t_{\rm sp},$$

$$\text{and } 1/\phi_s = bg(\nu), \quad b = (\lambda^2/8\pi)(\tau_s/t_{\rm sp}),$$

$$\text{and } g(\nu) = (\Delta\nu/2\pi)/[(\nu-\nu_0)^2 + (\Delta\nu/2)^2].$$

Therefore,

$$\gamma(\nu) = \frac{ag(\nu)}{1 + b\phi\,g(\nu)}$$

$$= \frac{a\,(\Delta\nu/2\pi)}{(\nu-\nu_0)^2 + (\Delta\nu/2)^2 + b\phi\,\Delta\nu/2\pi} = \frac{a\,(\Delta\nu/2\pi)}{(\nu-\nu_0)^2 + (\Delta\nu_s/2)^2}\,,$$

where

$$\begin{aligned}(\Delta\nu_s/2)^2 &= (\Delta\nu/2)^2 + b\phi\,\Delta\nu/2\pi \\ &= (\Delta\nu/2)^2[1 + b\phi\,(2/\pi\Delta\nu)] \\ &= (\Delta\nu/2)^2[1 + b\phi\,g(\nu_0)] \\ &= (\Delta\nu/2)^2[1 + \phi/\phi_s(\nu_0)].\end{aligned}$$

Taking the square-root of both sides of this equation yields the desired result: $\Delta\nu_s = \Delta\nu\sqrt{1+\phi/\phi_s(\nu_0)}$.

15.5 AMPLIFIER NOISE

EXERCISE 15.5-1

Amplified Spontaneous Emission (ASE)

a) In the unsaturated case $\gamma(\nu) \approx \gamma_0(\nu)$, whereupon the differential equation (15.5-3) becomes $d\phi/dz = \gamma_0(\nu)\phi + \xi_{\rm sp}(\nu)$. To solve this differential equation, we use a trial solution of the form $\phi(z) = A\exp[\gamma_0(\nu)z] + B$. Substitution yields $\gamma_0(\nu)A\exp[\gamma_0(\nu)z] = \gamma_0(\nu)A\exp[\gamma_0(\nu)z] + \gamma_0(\nu)B + \xi_{\rm sp}(\nu)$, from which it is clear that $B = -\xi_{\rm sp}(\nu)/\gamma_0(\nu)$. The initial condition $\phi(0) = 0$ is satisfied if $A + B = 0$, or $A = -B = \xi_{\rm sp}(\nu)/\gamma_0(\nu)$. It follows that the solution is $\phi(z) = \phi_{\rm sp}\{\exp[\gamma_0(\nu)z] - 1\}$, where $\phi_{\rm sp}(\nu) = \xi_{\rm sp}(\nu)/\gamma_0(\nu)$. At $z = d$, we therefore find $\phi(d) = \phi_{\rm sp}\{\exp[\gamma_0(\nu)d] - 1\}$.

b) Following (15.1-9) for spontaneous emission with a Lorentzian profile, the unsaturated gain coefficient is

$$\gamma_0(\nu) = \frac{\gamma_0(\nu_0)(\Delta\nu/2)^2}{(\nu-\nu_0)^2 + (\Delta\nu/2)^2}\,.$$

The frequency dependence of this gain coefficient, normalized to *unity height*, is then

$$g_1(\nu) = \frac{\gamma_0(\nu)}{\gamma_0(\nu_0)} = \frac{(\Delta\nu/2)^2}{[(\nu-\nu_0)^2 + (\Delta\nu/2)^2]}\,.$$

This quantity differs from the Lorentzian lineshape function provided in (15.1-8), which is normalized to *unit area*. The function $g_1(\nu)$ is plotted in the figure below for $\Delta\nu = \nu_0/100$.

In the same figure, we present the frequency dependence of the equivalent function applicable for ASE, also normalized to *unit height*:

$$g_2(\nu) = \frac{\{\exp[\gamma_0(\nu)d] - 1\}}{\{\exp[\gamma_0(\nu_0)d] - 1\}} = \frac{\{\exp[a g_1(\nu)] - 1\}}{\{\exp(a) - 1\}},$$

with $a = \gamma_0(\nu_0)d = 5$.

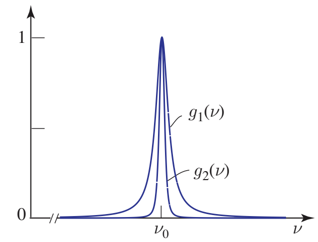

It is clear that $g_2(\nu)$ is narrower than $g_1(\nu)$, indicating that the amplification of spontaneous emission is accompanied by spectral narrowing.

C H A P T E R

16

LASERS

16.1 THEORY OF LASER OSCILLATION

EXERCISE 16.1-1

Threshold of a Ruby Laser

Parameters: $\lambda_o = 694.3 \times 10^{-9}$ m; $n = 1.76$; $\lambda = \lambda_o/n$; $\Delta\nu = 330 \times 10^9$ Hz;
$N_a = N_1 + N_2 = 1.58 \times 10^{19}$ cm^{-3}; $h = 6.62 \times 10^{-34}$J-s; $k = 1.38 \times 10^{-23}$ J/°K;
$c_o = 3 \times 10^8$ m/s; $c = c_o/n$; $\alpha(\nu_0) = -\gamma_0(\nu_0) \approx 0.2$ cm^{-1}; $d = 10$ cm; $A = 1$ cm^2.

a) $\gamma_0(\nu) = N_0\,\sigma(\nu)$, where $N_0 = N_2 - N_1$.
At thermal equilibrium at $T = 300°$ K, $N_2/N_1 = \exp(-h\nu/kT) = \exp(-hc_o/\lambda_o kT) \approx 10^{-30}$ (see Exercise 15.1-1). Therefore $N_2 \ll N_1$ and $N_1 \approx N_a$, i.e., almost all of the atoms are in the lower energy state. In this case $N_0 = N_2 - N_1 \approx -N_a$. The gain coefficient, $\gamma_0(\nu_0) = N_0\sigma(\nu_0) \approx -N_a\sigma(\nu_0)$, is then negative and corresponds to an absorption coefficient $\alpha(\nu_0) \approx N_a\sigma(\nu_0)$. Since $\alpha(\nu_0) \approx 0.2$ cm^{-1}, $\sigma(\nu_0) \approx \alpha(\nu_0)/N_a = 1.27 \times 10^{-20}$ cm^2.

b) The resonator has parameters $d = 0.1$ m, $\mathcal{R}_1 = \mathcal{R}_2 = 0.8$, and $\alpha_s = 0$. Its loss coefficient is $\alpha_r = \alpha_s + (1/2d)\ln(1/\mathcal{R}_1\mathcal{R}_2) = 2.231$ m$^{-1} = 0.0223$ cm^{-1}. The photon lifetime is thus $\tau_p = (\alpha_r c)^{-1} = 1.49 \times 10^{-9} = 1.49$ ns.

c) The threshold population difference is $N_t = \alpha_r/\sigma(\nu_0) = (0.0223\text{ cm}^{-1})/(1.27 \times 10^{-20}\text{ cm}^2) = 1.76 \times 10^{18}$ cm^{-3}.

16.2 CHARACTERISTICS OF THE LASER OUTPUT

EXERCISE 16.2-1

Number of Modes in a Gas Laser

a) The gain coefficient is given by $\gamma_0(\nu) = \gamma_0(\nu_0)\exp[-(\nu-\nu_0)^2/2\sigma_D^2]$ with $\Delta\nu_D = \sqrt{8\ln 2}\,\sigma_D$. The allowed oscillation band is obtained from equating the gain coefficient $\gamma_0(\nu)$ to the loss coefficient α_r:

$\gamma_0(\nu_0)\exp[-(\nu-\nu_0)^2/2\sigma_D^2] = \alpha_r$ or $(\nu-\nu_0)^2/2\sigma_D^2 = \ln[\gamma_0(\nu_0)/\alpha_r]$, so that
$(\nu-\nu_0)^2 = 2\sigma_D^2\ln[\gamma_0(\nu_0)/\alpha_r]$ or $(\nu-\nu_0) = \pm\sigma_D\sqrt{2\ln[\gamma_0(\nu_0)/\alpha_r]}$.

Thus $B = 2\sigma_D\sqrt{2\ln[\gamma_0(\nu_0)/\alpha_r]}$, from which we obtain
$$B = 2\Delta\nu_D(8\ln 2)^{-1/2}\,[2\ln(\gamma_0(\nu_0)/\alpha_r)]^{1/2}. \quad (1)$$

b) $\Delta\nu_D = 1.5 \times 10^9$ Hz; $\gamma_0(\nu_0) = 2 \times 10^{-3}$ cm^{-1}; $d = 100$ cm; $\mathcal{R}_1 = 1$; $\mathcal{R}_2 = 0.97$; and $\alpha_s = 0$, so that $\alpha_r = \alpha_s + (1/2d)\ln(1/\mathcal{R}_1\mathcal{R}_2) = 1.52 \times 10^{-4}$ cm^{-1}.

Bandwidth: From (1) above, we have $B = 2.89 \times 10^9$ Hz $= 2.89$ GHz.
Modal spacing: $\nu_F = c/2d = (c_o/n)/2d$. Using $n = 1$, $d = 100$ cm, and $c_o = 3 \times 10^{10}$ cm/s, we obtain $\nu_F = 1.5 \times 10^8$ Hz $= 0.15$ GHz.
Number of modes: $M = B/\nu_F = 19.3$, corresponding to a maximum of 19 modes.

16.4 PULSED LASERS

EXERCISE 16.4-1

Population-Difference Rate Equation for a Four-Level System

Since $\tau_1 \ll \tau_{\rm sp}$, level 1 is short lived and we may therefore assume that $N_1 \approx 0$ so that $N = N_2 - N_1 \approx N_2$. Substituting $N_1 = 0$ and $N_2 = N$ into (15.2-8), and assuming that $\tau_2 \approx t_{\rm sp}$, we obtain

$$dN/dt = R_2 - N/t_{\rm sp} - NW_i. \qquad (1)$$

Under steady-state conditions ($dN/dt = 0$), with $W_i = 0$, (1) yields $R_2 - N/t_{\rm sp} = 0$ so that the steady-state population difference in the absence of amplifier radiation is $N_0 = R_2 t_{\rm sp}$. Substituting $R_2 = N_0/t_{\rm sp}$ into (1), we obtain

$$dN/dt = N_0/t_{\rm sp} - N/t_{\rm sp} - W_i N. \qquad (2)$$

Equation (2) is identical to (16.4-5) except for the factor of two in the W_i term. This can be understood as follows: In the 3-level laser system, a photon emitted from level 2 decreases N_2 by unity and simultaneously increases N_1 by unity, so that the population difference $N = N_2 - N_1$ decreases by two.

In the 4-level system, on the other hand, level 1 is short-lived and cannot maintain any additions to its population. Thus, a photon emitted from level 2 decreases N_2 by unity but entails no change in N_1, which is 0 at all times. The result is a decrease of N by unity and the absence of the factor of two.

EXERCISE 16.4-2

Pulsed Ruby Laser

Given: $\lambda_o = 694.3 \times 10^{-9}$ m; $n = 1.76$; $\sigma(\nu_0) = 1.27 \times 10^{-24}$ m^2; $h = 6.62 \times 10^{-34}$ J-s; $c_o = 3 \times 10^8$ m/s; and $N_i/N_{\rm t} = 6$.

Resonator: The resonator has parameters $d = 0.1$ m; $A = 1$ cm^2; $\mathcal{R}_1 = \mathcal{R}_2 = 0.8$; and $\alpha_s = 0$. Its loss coefficient is $\alpha_r = \alpha_s + (1/2d)\ln(1/\mathcal{R}_1\mathcal{R}_2) = 2.231\ \mathrm{m}^{-1} = 0.0223\ \mathrm{cm}^{-1}$. The photon lifetime is thus $\tau_p = (\alpha_r c)^{-1} = 1.49 \times 10^{-9} = 1.49$ ns.

Threshold population difference: $N_{\rm t} = \alpha_r/\sigma(\nu_0) = 1.76 \times 10^{24}$ m^{-3}.

Peak Pulse Power: Using (16.4-14), together with $N_{\rm t}/N_i = \frac{1}{6}$, we have $\mathfrak{n}_p = \frac{1}{2} \cdot 6N_{\rm t}[1 + \frac{1}{6}\ln\frac{1}{6} - \frac{1}{6}] = 3 \times 1.76 \times 10^{24} \times [1 + \frac{1}{6}\ln\frac{1}{6} - \frac{1}{6}] = 2.82 \times 10^{24}$ m^{-3}. Furthermore, $\mathfrak{n}_p/N_{\rm t} = 3[1 + \frac{1}{6}\ln\frac{1}{6} - \frac{1}{6}] = 1.604$, which is consistent with the curve labeled $N_i/N_{\rm t} = 6$ in Fig. 16.4-8. From (16.4-15), the peak power is $P_p = h\nu\,\mathcal{T}\,(c/2d)\,V\mathfrak{n}_p$. Substituting $c = c_o/n$, $\nu = c_o/\lambda_o$, $\mathcal{T} = 1 - \mathcal{R}_1$, and taking the resonator cross-sectional area to be $A = 1$ cm^2 so that the resonator volume is $V = 10^{-4}d = 10^{-5}$ m^3, we obtain $P_p = 1.38 \times 10^9$ W $= 1.38$ GW.

Pulse Energy: The energy of the pulse is determined from (16.4-23), which in turn requires knowledge of the final population difference N_f. To determine N_f, (16.4-22) can be rewritten in the form $Y\exp(-Y) = X\exp(-X)$ where $X = N_i/N_{\rm t}$ and $Y = N_f/N_{\rm t}$. Given that $X = N_i/N_{\rm t} = 6$, we have $X\exp(-X) = 6\exp(-6) = 0.015$. It follows that $Y\exp(-Y) = 0.015$, which has the solution $Y = 0.015$, so that $N_f = 0.015 N_{\rm t}$. Using (16.4-23), we obtain $E = \frac{1}{2}h\nu\,\mathcal{T}\,(c/2d)\,V\tau_p\,(N_i - N_f) = 3.83$ J.

Duration and Shape of Laser Pulse: The shape of the laser pulse is provided by the curve labeled $N_i/N_{\rm t} = 6$ in Fig. 16.4-8. From this figure the pulse width at half maximum value is roughly estimated to be $1.5\,\tau_p$. An approximate calculation for the duration of the pulse can be obtained by dividing the energy [3.83 J as obtained from (16.4-23)] by the peak pulse power [1.38 GW as obtained from (16.4-15)]. This leads to $\tau_{\rm pulse} \approx E/P_p = 2.78 \times 10^{-9}$ s $= 2.78$ ns. This calculation, which yields $\tau_{\rm pulse} \approx 1.87\tau_p$, assumes that the pulse is square and thus provides only a rough approximation for $\tau_{\rm pulse}$.

EXERCISE 16.4-3

Demonstration of Pulsing by Mode Locking

a) When the magnitudes and phases are equal, the intensity can be obtained from (16.4-31), with the substitutions $A = 1$ and $M = 11$:

$$I(t) = |\mathcal{A}(t)|^2 = |A|^2 \left[\frac{\sin(M\pi t/T_F)}{\sin(\pi t/T_F)}\right]^2 = \left[\frac{\sin(11\pi t/T_F)}{\sin(\pi t/T_F)}\right]^2.$$

This function is plotted as a function of t/T_F in Fig. (a) below. It is a periodic set of narrow pulses of height $M^2 = 121$.

b) When the magnitudes are $\exp(-q^2/50)$ and the phases are equal (say 0), the total complex amplitude, from (16.4-28), is:
$\mathcal{A}(t) = \sum_{q=-5}^{5} \exp(-q^2/50)\exp(jq2\pi t/T_F)$
$= 1 + \sum_{q=1}^{5} 2\exp(-q^2/50)\cos(q2\pi t/T_F)$.
The function $I(t) = |\mathcal{A}(t)|^2$ is plotted as a function of t/T_F in Fig. (b) below. Again, this is a periodic set of narrow pulses. Note the reduction of the side lobes in comparison with Fig. (a).

c) Here, the magnitudes are equal and the phases are random so that $\mathcal{A}(t) = \sum_{q=-5}^{5} \exp(jq2\pi t/T_F + j\varphi_q)$, where the φ_q are random variables chosen from a uniformly distributed probability density function between 0 and 2π. A MATLAB program was written to compute $I(t) = |\mathcal{A}(t)|^2$. The random phases φ_q were generated using the random-number generator in MATLAB. The result, plotted as a function of t/T_F in Fig. (c) below, is a random periodic function whose values typically lie between 0 and 50.

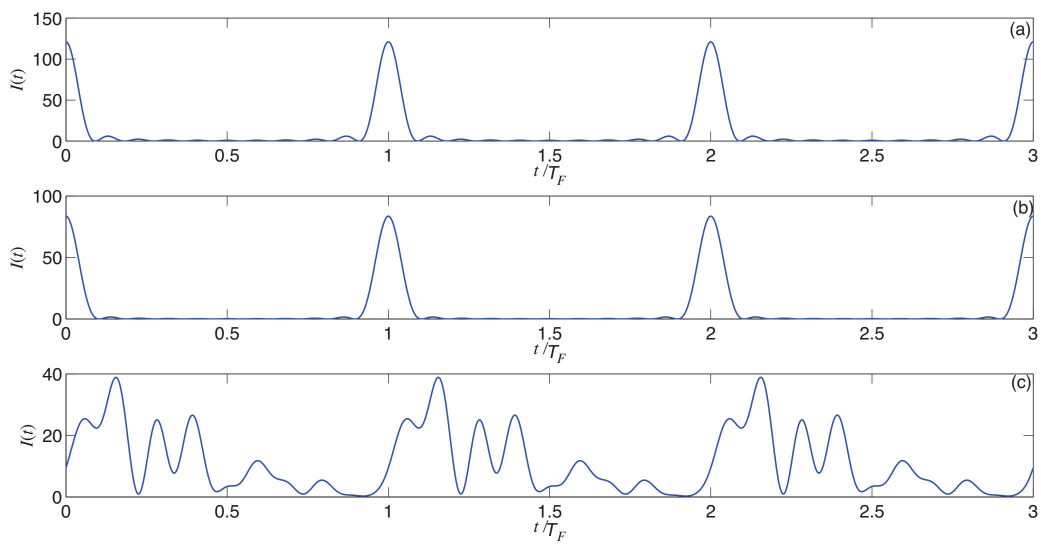

CHAPTER 17

SEMICONDUCTOR OPTICS

17.1 SEMICONDUCTORS

EXERCISE 17.1-1

Energy–Momentum Relation for a Free Electron

a) The one-dimensional time-independent Schrödinger equation for a particle of mass m_0 in a potential $V = 0$ (which is appropriate for a free particle) is

$$\frac{-\hbar^2}{2m_0}\,\frac{\partial^2\psi(x)}{\partial x^2} = E\,\psi(x)\,.$$

Substituting a plane-wave trial solution of the form $\psi(x) = A\,\exp(-jkx)$, where A is a constant, leads to

$$\frac{-\hbar^2}{2m_0}\,(-jk)^2\,e^{-jkx} = E\,e^{-jkx},$$

so that $E = \dfrac{\hbar^2 k^2}{2m_0}$.

b) The relativistic energy–momentum relation for a free particle of mass m_0 is

$$E^2 = p^2c^2 + m_0^2c^4. \tag{1}$$

For a free electron of mass m_0, the rest energy m_0c^2 has a value 0.511 MeV. For a nonrelativistic electron, it is thus convenient to carry out a Taylor-series expansion for the energy E, retaining the first term. Recalling that $\sqrt{1+x} \approx 1 + x/2$ for $x \ll 1$, we have

$$\begin{aligned} E &= \sqrt{p^2c^2 + m_0^2c^4} = \left[m_0^2c^4\left(1 + \frac{p^2c^2}{m_0^2c^4}\right)\right]^{1/2} \\ &\approx m_0c^2\left(1 + \frac{p^2c^2}{2m_0^2c^4}\right) \\ &= m_0c^2 + \frac{p^2}{2m_0}\,. \end{aligned}$$

Since m_0c^2 is the rest energy of the particle, the kinetic energy of a free nonrelativistic electron of mass m_0 is $E = p^2/2m_0$. With $p = \hbar k$, this becomes $E = \hbar^2k^2/2m_0$, which varies *quadratically* with k, in accordance with (17.1-1).

A free photon, on the other hand, is massless so that $m_0 = 0$, whereupon (1) becomes $E = pc$. Substituting $p = \hbar k$, this becomes $E = c\hbar k$, which varies *linearly* with k, in accordance with (17.1-2).

The distinction results in different behavior for the dispersion diagrams of electrons in semiconductors (Fig. 17.1-5) and photons in photonic crystals (Fig. 7.2-5).

EXERCISE 17.1-2

Exponential Approximation of the Fermi Function

For $E - E_f \gg kT$, (17.1-9) becomes the exponential function
$f(E) \approx \exp[-(E - E_f)/kT]$. (1)

Substituting (1) into (17.1-11), and making use of (17.1-7) and (17.1-10), we obtain:
$\mathrm{n} = \int_{E_c}^{\infty} A(E - E_c)^{1/2} \exp[-(E - E_f)/kT]\, dE$, (2)
where $A = (2m_c)^{3/2}/2\pi^2\hbar^3$ is a constant. To perform the integral in (2) we use the transformation $u = (E - E_c)/kT$, with $du = dE/kT$, whereupon $\exp[-(E - E_f)/kT] = \exp(-u)\exp[-(E_c - E_f)/kT]$, and the integral becomes:

$$\begin{aligned}\mathrm{n} &= A(kT)^{3/2} \exp\left[-\frac{E_c - E_f}{kT}\right] \int_0^{\infty} u^{1/2} \exp(-u)\, du \\ &= \frac{4\pi(2m_c kT)^{3/2}}{h^3} \sqrt{\frac{\pi}{4}}\, \exp\left[-\frac{E_c - E_f}{kT}\right],\end{aligned}$$

from which (17.1-12) follows. A similar analysis leads to (17.1-13), and (17.1-14) follows by multiplication.

If $m_v = m_c$, then $N_c = N_v$, whereupon (17.1-12) and (17.1-13) provide
$\mathrm{n}/\mathrm{p} = \exp[+(E_f - E_v)/kT - (E_c - E_f)/kT]$. Thus, if $(E_c - E_f) < (E_f - E_v)$, the argument of the exponent is positive and therefore so is n/p, i.e., if E_f is closer to the conduction band than to the valence band, then $\mathrm{n} > \mathrm{p}$, and *vice versa*.

EXERCISE 17.1-3

Determination of the Quasi-Fermi Levels Given the Electron and Hole Concentrations

a) At $T = 0^\circ$ K, the Fermi function $f_c(E) = 1$ for $E < E_{fc}$ and 0 otherwise. When this is used together with (17.1-7) and (17.1-10) to evaluate the integral in (17.1-11), we obtain:
$\mathrm{n} = \int_{E_c}^{E_{fc}} A(E - E_c)^{1/2}\, dE = \frac{2}{3}A(E_{fc} - E_c)^{3/2}$, where $A = (2m_c)^{3/2}/2\pi^2\hbar^3$ is a constant. It follows that $E_{fc} - E_c = (3\mathrm{n}/2A)^{2/3}$ from which (17.1-18a) follows. Equation (17.1-18b) can be similarly obtained.

b) The concentration n is the area under the function $\varrho_c(E)f_c(E)$. When $T > 0^\circ$ K, $f_c(E)$ no longer assumes the values 1 and 0 with a transition at E_{fc} (see middle panel of figure below). However, if the quasi-Fermi level lies deep within the conduction band, for $T > 0^\circ$ K the product function $\varrho_c(E)f_c(E)$ will be a smooth curve with an area close to that for the $T = 0^\circ$ K case, as is evident in the right panel of the figure below. In that case the expression in (17.1-18a) will be approximately applicable. A parallel argument for the valence band leads to the approximate validity of (17.1-18b).

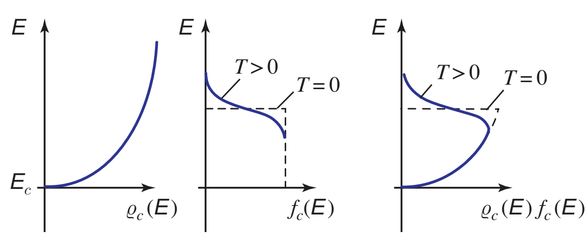

EXERCISE 17.1-4

Electron–Hole Pair Injection in GaAs

Parameters for GaAs: $E_g = 1.42$ eV; $m_c = 0.07m_0$; $m_v = 0.5m_0$; $m_0 = 9.11 \times 10^{-31}$ kg, $\mathrm{r} = 10^{-11}$ cm^3/s; $T = 300^\circ$ K.

a) Using the value of $\mathrm{n_i} = 1.8 \times 10^6$ cm^{-3} from Table 17.1-3, together with $\mathrm{n_0} = 10^{16}$ cm^{-3}, we obtain $\mathrm{p_0} = \mathrm{n_i^2/n_0} = 3.24 \times 10^{-4}$ cm^{-3}. In this case $\mathrm{n_0} \gg \mathrm{p_0}$.

b) With injection at a rate $R = 10^{23}$ cm^{-3}s^{-1}, the steady-state concentrations can be determined from (17.1-22), which provides: $R = \mathrm{r(np - n_0p_0) = r\Delta n(n_0 + p_0 + \Delta n) \approx r\Delta n(n_0 + \Delta n)}$, so that $\Delta\mathrm{n}^2 + \mathrm{n_0}\Delta\mathrm{n} - R/\mathrm{r} = 0$. Solving this quadratic equation for $\Delta\mathrm{n}$ yields: $\Delta\mathrm{n} = \frac{1}{2}\left[-\mathrm{n_0} + (\mathrm{n_0^2} + 4R/\mathrm{r})^{1/2}\right] = 9.5 \times 10^{16}$ cm^{-3}. Thus, $\Delta\mathrm{n}$ is about 9.5 times greater than $\mathrm{n_0}$.

c) Since $\Delta\mathrm{n} = 9.5 \times 10^{16}$ cm^{-3} $\gg \mathrm{n_0}$, we use (17.1-24) to obtain $\tau \approx 952$ ns.

d) The separation between the quasi-Fermi levels at $T = 0^\circ$ K may be determined by subtracting (17.1-18b) from (17.1-18a):
$E_{fc} - E_{fv} = E_g + (3\pi^2)^{2/3}(\hbar^2/2)\left[\mathrm{n}^{2/3}/m_c + \mathrm{p}^{2/3}/m_v\right]$.
Converting the values for $\mathrm{n = n_0 + \Delta n}$ and $\mathrm{p = p_0 + \Delta n \approx \Delta n}$ obtained above from units of cm^{-3} to m^{-3} by multiplying by them by 10^6, and dividing by the electronic charge e to convert from J to eV, substitution yields the following:

$$
\begin{aligned}
E_{fc} - E_{fv} &= E_g + \frac{(3\pi^2)^{2/3}}{2}\,\frac{\hbar^2}{m_0 e}\left[\frac{(\mathrm{n} \times 10^6)^{2/3}}{0.07} + \frac{(\mathrm{p} \times 10^6)^{2/3}}{0.5}\right] \\
&= E_g + \frac{(3\pi^2)^{2/3}}{2}\,\frac{\hbar^2}{m_0 e}\left[\frac{(10 \times 10^{21} + 95 \times 10^{21})^{2/3}}{0.07} + \frac{(95 \times 10^{21})^{2/3}}{0.5}\right] \\
&= E_g + \frac{(3\pi^2)^{2/3}}{2}\,\frac{\hbar^2}{m_0 e}\left[\frac{22.3 \times 10^{14}}{0.07} + \frac{20.8 \times 10^{14}}{0.5}\right] \\
&= E_g + 4.785 \cdot \frac{43.8 \times 10^{-68}}{5.74 \times 10^{-48}}\left[\frac{22.3 \times 10^{14}}{0.07} + \frac{20.8 \times 10^{14}}{0.5}\right] \\
&= E_g + 0.013\ \text{eV}\,.
\end{aligned}
$$

Thus, $E_{fc} - E_{fv}$ is 0.013 eV greater than the bandgap energy E_g so that $E_{fc} - E_{fv} = 1.433$ eV. Using (17.1-18a) and (17.1-18b) separately, we find $E_{fc} - E_c \approx 0.011$ eV and $E_v - E_{fv} \approx 0.002$ eV, so that the quasi-Fermi levels lie within, but very near the edges of, the conduction and valence bands.

However, neither $E_{fc} - E_c$ nor $E_v - E_{fv}$ are $\gg kT = 0.026$ eV at $T = 300^\circ$ K, so that (17.1-18a) and (17.1-18b) should not be used for this carrier concentration at $T = 300^\circ$ K (see Exercise 17.1-3); hence $T = 0^\circ$ K was expressly specified for this part of the problem.

EXERCISE 17.1-5

Energy Levels of a Quantum Well

Inside the well ($0 < x < d$), $V = 0$ and the one-dimensional time-independent Schrödinger equation is $(-\hbar^2/2m)\,d^2\psi/dx^2 = E\psi$ or $d^2\psi/dx^2 + k^2\psi = 0$, where $k^2 = 2mE/\hbar^2$. This equation has the general solution $\psi(x) = A\sin(kx) + B\cos(kx)$.

At the boundaries of the infinite well ($x = 0$ and $x = d$), we require $\psi(x) = 0$. Therefore, $B = 0$ and $\sin(kd) = 0$. This is possible if $kd = q\pi$, $q = 1, 2, 3, ...$, so that k must have one of the values $k_q = q\pi/d$, just as for the standing waves in a Fabry–Perot resonator [see (11.1-2) and (11.1-3)]. The corresponding energy $E = (\hbar^2/2m)k^2$

is thus quantized to the values $E_q = (\hbar^2/2m)(q\pi/d)^2$. The first three energy levels $(q = 1, 2, 3)$ are therefore: $E_1 = 4.9\hbar^2/md^2$, $E_2 = 19.7\hbar^2/md^2$, and $E_3 = 44.4\hbar^2/md^2$.

By comparison, a quantum well of finite depth $V_0 = 32\hbar^2/md^2$ has energies: $E_1 = 3.2\hbar^2/md^2$, $E_2 = 11.9\hbar^2/md^2$, and $E_3 = 25.9\hbar^2/md^2$, as illustrated in Fig. 17.1-26(b). Finiteness of the well depth is seen to compress the energy-level spacings and to yield a continuum of energy levels above V_0.

17.2 INTERACTIONS OF PHOTONS WITH CHARGE CARRIERS

EXERCISE 17.2-1

Requirement for the Photon Emission Rate to Exceed the Absorption Rate

a) In thermal equilibrium $E_{fc} = E_{fv} = E_f$ and, in accordance with (17.1-9), $f(E) = 1/\{\exp[(E - E_f)/kT + 1]\}$. The difference between the emission and absorption conditions, given by (17.2-10) and (17.2-11), respectively, is $f_e(\nu) - f_a(\nu) = f_c(E_2) - f_v(E_1)$. Since $f_c(E) = f_v(E) = f(E)$ in thermal equilibrium, we have $f_e(\nu) - f_a(\nu) = f(E_2) - f(E_1)$. Because $f(E)$ is a monotonically decreasing function of E, we obtain $f(E_2) < f(E_1)$ so that $f_e(\nu) - f_a(\nu) < 0$. Thus, $f_e(\nu) < f_a(\nu)$, which indicates that the rate of emission is smaller than the rate of absorption.

b) In quasi-equilibrium, we have $f_e(\nu) - f_a(\nu) = f_c(E_2) - f_v(E_1) = (1/\{1 + \exp[(E_2 - E_{fc})/kT]\}) - (1/\{1 + \exp[(E_1 - E_{fv})/kT]\})$. This is a positive quantity if $\exp[(E_2 - E_{fc})/kT] < \exp[(E_1 - E_{fv})/kT]$, or equivalently if $(E_2 - E_{fc}) < (E_1 - E_{fv})$, or if $E_2 - E_1 < E_{fc} - E_{fv}$. Since $E_2 - E_1 = h\nu$, the emission rate is greater than the absorption rate if $h\nu < E_{fc} - E_{fv}$, or equivalently if $E_{fc} - E_{fv} > h\nu$. This implies that the separation between the two Fermi levels is greater than the bandgap energy, namely, that E_{fc} and E_{fv} must lie within the conduction and valence bands, respectively.

EXERCISE 17.2-2

Wavelength of Maximum Interband Absorption

In accordance with (17.2-29), $\alpha(\nu)$ is proportional to $(h\nu - E_g)^{1/2}\,(h\nu)^{-2}$. This function has its maximum value, $\nu_{\rm p}$, when its derivative with respect to ν is 0. This occurs when $-2(h\nu_{\rm p} - E_g)^{1/2} + \frac{1}{2}\,h\nu_{\rm p}(h\nu_{\rm p} - E_g)^{-1/2} = 0$ or $\frac{1}{4}h\nu_{\rm p} = (h\nu_{\rm p} - E_g)$ so that $h\nu_{\rm p} = \frac{4}{3}E_g$.

To find the maximum value of the wavelength, $\lambda_{\rm p}$, however, we need to write $\alpha(\nu)$ as $\alpha(\lambda_o)$ instead, and then take the derivative with respect to λ_o. Since $\nu = c_o/\lambda_o$, we have $\alpha(\lambda_o) \propto (hc_o/\lambda_o - hc_o/\lambda_g)^{1/2}\,(\lambda_o/hc_o)^2 \propto (1/\lambda_o - 1/\lambda_g)^{1/2}\,(\lambda_o)^2$. Setting the derivative of $\alpha(\lambda_o)$ equal to zero yields $2\,(1/\lambda_{\rm p} - 1/\lambda_g)^{1/2}\,\lambda_{\rm p} - \frac{1}{2}\,(1/\lambda_{\rm p} - 1/\lambda_g)^{-1/2}\,(\lambda_{\rm p}^2/\lambda_{\rm p}^2) = 0$ so that $4\,(1/\lambda_{\rm p} - 1/\lambda_g)\,\lambda_{\rm p} = 1$, which leads to $\lambda_{\rm p} = \frac{3}{4}\lambda_g$ or $\lambda_{\rm p}\,(\mu\text{m}) = \frac{3}{4}\cdot 1.24/E_g$ (eV).

For GaAs, $E_g = 1.42$ eV so that $\lambda_{\rm p} = \frac{3}{4}\cdot 1.24/1.42 = 0.65$ μm, which lies in the red.

In view of the results obtained in Prob. 14.4-5, we know that $\lambda_{\rm p}$ cannot necessarily be evaluated as $c_o/\nu_{\rm p}$. In this case, however it turns out that evaluating $\lambda_{\rm p}$ in terms of $c_o/\nu_{\rm p}$ also leads to $\frac{3}{4}c_o h/E_g$, so that both approaches yield the same result.

CHAPTER
18

LEDS AND LASER DIODES

18.1 LIGHT-EMITTING DIODES

EXERCISE 18.1-1

Quasi-Fermi Levels of a Pumped Semiconductor

a) At $T = 0^\circ$ K, the Fermi function $f_c(E) = 1$ for $E < E_{fc}$, and 0 otherwise. This expression may be used together with (17.1-7) and (17.1-10) to evaluate the integral in (17.1-11). Using the substitution $x = (E - E_c)$ to evaluate the integral, we obtain

$$\Delta \mathrm{n} = \int_{E_c}^{E_{fc}} A(E - E_c)^{1/2} dE = \tfrac{2}{3} A(E_{fc} - E_c)^{3/2},$$

where $A = (2m_c)^{3/2}/2\pi^2\hbar^3$ is a constant. Thus, $E_{fc} - E_c = (3/2A)^{2/3}\,\Delta \mathrm{n}^{2/3}$, from which (18.1-12a) follows. Equation (18.1-12b) is similarly obtained, and (18.1-12c) follows from simple subtraction, where $1/m_r = 1/m_c + 1/m_v$ [see (17.2-5)]. The calculation is the same as that provided in Exercise 17.1-3.

b) From (18.1-5)–(18.1-7), we have $f_e(\nu) = f_c(E_2)[1 - f_v(E_1)]$, where $E_2 = E_c + (m_r/m_c)(h\nu - E_g)$ and $E_1 = E_2 - h\nu$. At $T = 0^\circ$ K, the Fermi function $f_c(E_2)$ is unity as long as $E_2 < E_{fc}$ and is 0 otherwise. Similarly, the Fermi function $f_v(E_1)$ is unity for $E_1 < E_{fv}$ and is 0 otherwise. For $h\nu > E_g$, as $h\nu$ increases, we see that E_2 increases and E_1 decreases. But as long as these two values lie below E_{fc} and above E_{fv}, respectively, $f_c(E_2) = 1$ and $1 - f_v(E_1) = 1$, so that $f_e(\nu) = 1$. When $h\nu$ exceeds the value $E_{fc} - E_{fv}$, we see that E_2 exceeds E_{fc} and E_1 lies below E_{fv}, so that $f_c(E_2) = 0$ and $1 - f_v(E_1) = 0$, indicating that $f_e(\nu) = 0$. The function $f_e(\nu)$ is therefore a rectangular function with value 1 for $E_g < h\nu < E_{fc} - E_{fv}$, and value 0 otherwise, as shown in Fig. (*a*) below.

According to (18.1-3), the rate of spontaneous emission r_{sp} is proportional to $\varrho(\nu) f_e(\nu)$, where $\varrho(\nu) \propto (h\nu - E_g)^{1/2}$. Therefore, the dependence of r_{sp} on ν is as illustrated in Fig. (*a*) below for $T = 0^\circ$ K. The effect of increasing the temperature ($T > 0^\circ$ K) is to smooth the Fermi function so that the functions $f_e(\nu)$ and $r_{\mathrm{sp}}(\nu)$ take the forms shown in Fig. (*b*) below.

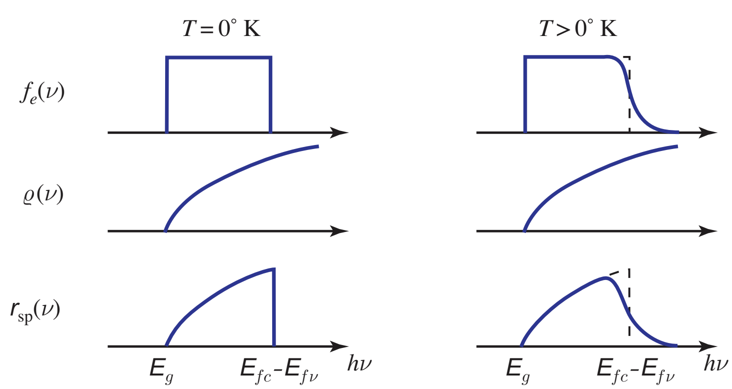

(*a*) (*b*)

EXERCISE 18.1-2

Spectral Intensity of Injection Electroluminescence under Weak Injection

From (18.1-3)–(18.1-5), we have $r_{\rm sp}(\nu) = \tau_{\rm r}^{-1}\varrho(\nu)f_e(\nu)$, where
$\varrho(\nu) = [(2m_r)^{3/2}/\pi\hbar^2](h\nu - E_g)^{1/2}$ and $f_e(\nu) = f_c(E_2)[1 - f_v(E_1)]$.

When the Fermi distributions are approximated by their tails, we have

$f_c(E_2) \approx \exp[-(E_2 - E_{fc})/kT]$ and $1 - f_v(E_1) \approx \exp[-(E_{fv} - E_1)/kT]$

whereupon $f_e(\nu) \approx \exp[(E_{fc} - E_{fv})/kT] \cdot \exp[-(E_2 - E_1)/kT]$
$= \exp[(E_{fc} - E_{fv})/kT] \cdot \exp(-h\nu/kT)$.

Substituting this approximate expression for $f_e(\nu)$ into the above expression for $r_{\rm sp}(\nu)$ leads to (18.1-13a) and (18.1-13b).

EXERCISE 18.1-3

Electroluminescence Spectral Linewidth

a) Equation (18.1-13a) may be written in the form $r_{\rm sp}(\nu) = D(kT)^{1/2}u^{1/2}\exp(-u)$, where $u = (h\nu - E_g)/kT$. The function $u^{1/2}\exp(-u)$ has its peak value when its derivative with respect to u vanishes, i.e., when $-u^{1/2}\exp(-u) + \frac{1}{2}u^{-1/2}\exp(-u) = 0$, from which we obtain $u = \frac{1}{2}$, i.e., $(h\nu - E_g)/kT = \frac{1}{2}$ or $h\nu = E_g + \frac{1}{2}kT$.

b) The peak of the function $u^{1/2}e^{-u}$ occurs at $u = \frac{1}{2}$, where the function has the value $(\frac{1}{2})^{1/2}e^{-1/2}$. The function reaches half its peak value where $u^{1/2}e^{-u} = \frac{1}{2} \times (\frac{1}{2})^{1/2}e^{-1/2}$, i.e., where $u^{1/2}e^{-u} = (\frac{1}{2})^{3/2}e^{-1/2}$. Squaring both sides of this equation leads to $ue^{-2u} = (\frac{1}{2})^3e^{-1} = 0.046$. Computation shows that the roots of this equation are approximately $u_1 = 0.051$ and $u_2 = 1.84$. The difference between these values, $u_2 - u_1 = 1.79 \approx 1.8$, corresponds to $[(h\nu_2 - E_g)/kT - (h\nu_1 - E_g)/kT] \approx 1.8$ so that $h(\nu_2 - \nu_1) \approx 1.8\,kT$. The FWHM spectral width is, therefore, $\Delta\nu \approx 1.8\,kT/h$, confirming (18.1-15). Note that $\Delta\nu$ is independent of ν.

c) Since $\nu = c/\lambda$, we have $\Delta\nu = -(c/\lambda^2)\Delta\lambda$. The magnitude of the wavelength spectral width $\Delta\lambda$ that corresponds to the frequency spectral width $\Delta\nu \approx 1.8\,kT/h$ is therefore $\Delta\lambda \approx (\lambda_{\rm p}^2/c)\Delta\nu = (\lambda_{\rm p}^2/c)(1.8\,kT/h) = 1.8\,(\lambda_{\rm p}^2/hc)\,kT$. If we express λ in μm, and kT in eV, the foregoing equation becomes
$\Delta\lambda\,(\text{in }\mu\text{m}) \times 10^{-6} \approx 1.8 \cdot [\lambda_{\rm p}^2\,(\text{in }\mu\text{m}^2) \times 10^{-12}/hc] \cdot [kT\,(\text{in eV}) \cdot e]$ or
$\Delta\lambda\,(\text{in }\mu\text{m}) \approx [1.8/(10^6 \times hc/e)] \cdot [\lambda_{\rm p}^2\,(\text{in }\mu\text{m}^2)] \cdot [kT\,(\text{in eV})]$.
Now, since $(10^6 \times hc/e) = 1.24$ and $1.8/1.24 \approx 1.45$, we obtain the final result
$\Delta\lambda\,(\text{in }\mu\text{m}) \approx 1.45 \cdot [\lambda_{\rm p}^2\,(\text{in }\mu\text{m}^2)] \cdot [kT\,(\text{in eV})]$, in agreement with (18.1-16).

In contrast with the frequency spectral width $\Delta\nu$, which is independent of ν, the wavelength spectral width $\Delta\lambda$ increases as $\lambda_{\rm p}^2$.

d) At $T = 300^\circ$ K, we have $kT = 0.026$ eV. The frequency spectral width is given by $\Delta\nu = 1.8\,kT/h = 1.8 \cdot 0.026 \cdot 1.6 \times 10^{-19}/6.6 \times 10^{-34} = 11.3 \times 10^{12}$ Hz $= 11.3$ THz. It is independent of the wavelength $\lambda_{\rm p}$.

The wavelength spectral width is $\Delta\lambda\,(\text{in }\mu\text{m}) \approx 1.45 \cdot [\lambda_{\rm p}^2\,(\text{in }\mu\text{m}^2)] \cdot [kT\,(\text{in eV})]$. For $\lambda_{\rm p} = 0.8\ \mu$m, we have $\Delta\lambda \approx 1.45 \cdot [0.8^2] \cdot [0.026] \approx 0.024\ \mu$m = 24 nm. For $\lambda_{\rm p} = 1.6\ \mu$m, on the other hand, we have $\Delta\lambda \approx 1.45 \cdot [1.6^2] \cdot [0.026] \approx 0.096\ \mu$m = 96 nm, confirming that $\Delta\lambda$ increases as $\lambda_{\rm p}^2$ (doubling the wavelength, from 0.8 to 1.6 μm, results in quadrupling of the wavelength spectral width, from 24 to 96 nm).

EXERCISE 18.1-4

Extraction of Light from a Planar-Surface LED

a) We begin with $\eta_3 = \frac{1}{2}(1-\cos\theta_c)$ and make use of Snell's law for the critical angle:

$$\sin\theta_c = 1/n \quad \text{and therefore} \quad \cos\theta_c = \sqrt{1-\sin^2\theta_c}$$

$$\text{so that} \quad \eta_3 = \tfrac{1}{2}\left(1-\sqrt{1-1/n^2}\right).$$

$$\text{Since} \quad \left(1-\frac{1}{n^2}\right)^{1/2} \approx 1-\frac{1}{2n^2} \quad \text{for} \quad \frac{1}{n^2} \ll 1, \quad \text{we have}$$

$$\eta_3 \approx \tfrac{1}{2}\left(\frac{1}{2n^2}\right) = \frac{1}{4n^2}\,.$$

b)

$$\theta_c = \sin^{-1}(1/n) \quad \text{and} \quad \eta_3 \approx 1/4n^2 \quad \text{so}$$

$$\theta_c(\text{GaAs}) = \sin^{-1}(1/3.6) = 16.1^\circ \quad \text{and} \quad \eta_3(\text{GaAs}) = 0.019$$

$$\theta_c(\text{GaN}) = \sin^{-1}(1/2.5) = 23.6^\circ \quad \text{and} \quad \eta_3(\text{GaN}) = 0.040$$

$$\theta_c(\text{polymer}) = \sin^{-1}(1/1.5) = 41.8^\circ \quad \text{and} \quad \eta_3(\text{polymer}) = 0.111.$$

c) From GaAs ($n_1 = 3.6$) to polymer ($n_2 = 1.5$), the critical angle θ_{c1} is obtained from $n_1 \sin\theta_{c1} = n_2$ so that $\theta_{c1} = \sin^{-1}(1.5/3.6) = 24.6^\circ$. Thus, $\eta_3 = \frac{1}{2}[1-\cos(24.6^\circ)] = 0.045$. As shown in part *b*) above, light escaping from GaAs into air has $\eta_3(\text{GaAs}) = 0.019$ so the enhancement in the fraction of extracted light is $0.045/0.019 \approx 2.4$.

d) From $n_1 = 3.6$ to $n_2 = 1.5$, using generalizations of (18.1-21) and (18.1-22) we have:

$$\eta_2\,\eta_3 = \left[1-\frac{(n_1-n_2)^2}{(n_1+n_2)^2}\right]\cdot\frac{1}{2}\left[1-\sqrt{1-\left(\frac{n_2}{n_1}\right)^2}\,\right]$$

$$\approx \frac{4n_1n_2}{(n_1+n_2)^2}\cdot\frac{1}{4}\,\frac{n_2^2}{n_1^2} = \frac{n_2^3}{n_1(n_1+n_2)^2}.$$

Similarly, from $n_2 = 1.5$ to $n_3 = 1$, we have:

$$\eta_2'\,\eta_3' \approx \frac{n_3^3}{n_2(n_2+n_3)^2}\,.$$

The product $\eta_2\,\eta_3\,\eta_2'\,\eta_3'$ is maximized for $\dfrac{\partial(\eta_2\,\eta_3\,\eta_2'\,\eta_3')}{\partial n_2} = 0$ or

$$\frac{\partial}{\partial n_2}\left(\frac{n_2^3}{n_1(n_1+n_2)^2}\cdot\frac{n_3^3}{n_2(n_2+n_3)^2}\right) = \frac{n_3^3}{n_1}\,\frac{\partial}{\partial n_2}\left(\frac{n_2^2}{(n_1+n_2)^2\,(n_2+n_3)^2}\right) = 0.$$

Thus, $(n_1+n_2)^2\,(n_2+n_3)^2\cdot 2n_2 - n_2^2[(n_1+n_2)^2\cdot 2(n_2+n_3)+(n_2+n_3)^2\cdot 2(n_1+n_2)] = 0$, which provides $n_2 = n_1$, indicating that the introduction of an intermediate layer of arbitrary thickness is not helpful in maximizing the fraction of light emitted from the LED into air if Fresnel reflection is accommodated.

The use of an intermediate-index material in the form of a quarter-wave film can be useful in this connection, however, as shown in Exercise 7.1-1.

CHAPTER
19

PHOTODETECTORS

19.6 NOISE IN PHOTODETECTORS

EXERCISE 19.6-1

Signal-to-Noise Ratio of a Resistance-Limited Receiver

Parameters: $\eta = 1$; $R_L = 50\Omega$; $T = 300^\circ$ K; $B = 100$ MHz $= 10^8$ Hz; $e = 1.6 \times 10^{-19}$ C; $\lambda = 1.55$ μm $= 1.55 \times 10^{-6}$ m; $h = 6.63 \times 10^{-34}$ J $\cdot$ s; $k = 1.38 \times 10^{-23}$ J/°K.

Resistor thermal-noise current variance: $\sigma_i^2 = 4kT/R_L$.
Photoelectron-noise current variance: $2e\bar{\imath}B = 2e^2\Phi B$.

When the two variances are equal, we have $4kT/R_L = 2e^2\Phi B$, so that the
Photon flux $\Phi = 2kT/e^2 R_L B = 6.5 \times 10^7$ photons/sec, and the
Optical power $P = h\nu\Phi = hc\Phi/\lambda = 8.3 \times 10^{-12}$ W $= 8.3$ pW.

EXERCISE 19.6-2

Sensitivity of an Analog APD Receiver

From (19.6-39), we have $\text{SNR}_0 = \overline{G}^2 \overline{m}_0^2 / (\overline{G}^2 F \overline{m}_0 + \sigma_q^2)$, from which we obtain
$\overline{m}_0^2 - \text{SNR}_0\, F\, \overline{m}_0 - \text{SNR}_0\, \sigma^2/\overline{G}^2 = 0$.

This is a quadratic equation in $\overline{m}_0$ whose positive solution is

$$\overline{m}_0 = \tfrac{1}{2}\left[F \cdot \text{SNR}_0 + \sqrt{F^2\,\text{SNR}_0^2 + 4\sigma_q^2\,\text{SNR}_0/\overline{G}^2}\,\right]$$

$$= F \cdot \text{SNR}_0 \left[\tfrac{1}{2} + \sqrt{\tfrac{1}{4} + \sigma_q^2/F^2\,\overline{G}^2\,\text{SNR}_0}\,\right].$$

In the limit as $\sigma_q^2 \to 0$, this reduces to $\overline{m}_0 = F \cdot \text{SNR}_0$ as promised.

EXERCISE 19.6-3

Effect of Quantum Efficiency and Background Noise on Receiver Sensitivity

a) **State 0:** Neither signal nor background photons are present. Hence, the probability is unity that zero photoelectrons are detected in this OOK system; there is thus no possibility for error and $p_0 = 0$.

State 1: An average of $\overline{n}$ photons is present in a receiver counting time T. This gives rise to an average of $\overline{m} = \eta\overline{n}$ photoelectrons, which follow the Poisson distribution $p(m) = \overline{m}^m \exp(-\overline{m})/m!$. An error (a "miss") occurs if zero photoelectrons are observed in the receiver counting time T; this occurs with probability $p_1 = p(0) = \exp(-\overline{m}) = \exp(-\eta\overline{n})$.

The bit error rate for this system is thus $\text{BER} = \frac{1}{2}(p_1 + p_0) = \frac{1}{2}\exp(-\eta\overline{n}) = \frac{1}{2}\exp(-2\eta\overline{n}_0)$ since $\eta\overline{n}_0 = \frac{1}{2}\eta\overline{n}$. For a $\text{BER} = 10^{-9}$, we thus have $\eta\overline{n}_0 = 10$, corresponding to $\overline{m}_0 = 10$ *photoelectrons per bit* and to $\overline{n}_0 = 10/\eta$ *photons per bit*.

b) **State 0:** The number of photons n is Poisson distributed with mean $\overline{n}_B$ associated with the background, and so too is the number of photoelectrons m since the quantum efficiency η is assumed to be unity.

State 1: The number of photons n is Poisson distributed with mean $\overline{n}_B + \overline{n}$, where $\overline{n}$ represents the mean number of signal photons.

Decision rule: Select a threshold $n_{\rm th}$; If $n > n_{\rm th}$, decide 1; otherwise decide 0.

Error probabilities:
$p_0 =$ probability that $n > n_{\rm th}$ if $p(n)$ is Poisson distributed with mean $\overline{n}_B$.
$p_1 =$ probability that $n \le n_{\rm th}$ if $p(n)$ is Poisson distributed with mean $\overline{n}_B + \overline{n}$.

$$\begin{aligned}
\mathrm{BER} &= \tfrac{1}{2}p_0 + \tfrac{1}{2}p_1 \\
&= \tfrac{1}{2}\sum_{n=n_{\rm th}}^{\infty} \overline{n}_B^{\,n} \exp[-\overline{n}_B]/n! + \tfrac{1}{2}\sum_{n=0}^{n_{\rm th}} (\overline{n}_B + \overline{n})^n \exp[-(\overline{n}_B + \overline{n})]/n!.
\end{aligned}$$

The expression for the BER is a function of $\overline{n}_B$, $\overline{n}$, and $n_{\rm th}$. The required plots can be generated numerically; for given values of $\overline{n}_B$ and $\overline{n}$, we can determine the value of $n_{\rm th}$ that minimizes the BER. The optimal threshold turns out to be $n_{\rm th} = \overline{n}/\ln(1 + \overline{n}/\overline{n}_B)$ as shown, for example, in B. E. A. Saleh, *Photoelectron Statistics*, Springer-Verlag, 1978, p. 315 (in this reference, BER is denoted P_e, $\overline{n}_B$ is denoted $\overline{n}_b$, and $\overline{n}$ is denoted $\overline{n}_s$).

CHAPTER
20

ACOUSTO-OPTICS

20.2 ACOUSTO-OPTIC DEVICES

EXERCISE 20.2-1

Parameters of Acousto-Optic Modulators

Modulator 1
$n = 1.46$; $v_s = 6\times10^3$ m/s; $f = 50$ MHz $= 5\times10^7$ Hz; $\lambda_o = 633\times10^{-9}$ m; $\delta\theta = 10^{-3}$ rad;
$\lambda = \lambda_o/n = 433 \times 10^{-9}$ m; $\Lambda = v_s/f = 1.2 \times 10^{-4}$ m.
Bragg Angle $\theta_{\mathcal{B}} = \sin^{-1}(\lambda/2\Lambda) = 1.8$ mrad.
Bandwidth $B = v_s/D = v_s/(\lambda/\delta\theta) = 13.9$ MHz.

Modulator 2
$n = 4.8$; $v_s = 2.2 \times 10^3$ m/s; $f = 100$ MHz $= 10^8$ Hz; $\lambda_o = 10.6 \times 10^{-6}$ m; $D = 10^{-3}$ m;
$\lambda = \lambda_o/n = 2.2 \times 10^{-6}$ m; $\Lambda = v_s/f = 22 \times 10^{-6}$ m.
Bragg Angle $\theta_{\mathcal{B}} = \sin^{-1}(\lambda/2\Lambda) = 50$ mrad.
Bandwidth $B = v_s/D = 2.2$ MHz.

EXERCISE 20.2-2

Parameters of an Acousto-Optic Scanner

Parameters: $v_s = 6 \times 10^3$ m/s; $n = 1.46$; $\lambda_o = 633 \times 10^{-9}$ m; $f_{\min} = 4 \times 10^7$ Hz; $f_{\max} = 6 \times 10^7$ Hz; $N = 100$.

Beam width D: From (20.2-8) we have $N = \mathcal{T}B = (D/v_s)B$, where $B = f_{\max} - f_{\min} = 2 \times 10^7$ Hz. Therefore, $D = Nv_s/B = 3$ cm.

Scan angle $\Delta\theta$: Since $N = \Delta\theta/\delta\theta$ and $\delta\theta = \lambda/D$, we have $\Delta\theta = N\lambda/D$. This is the angle within the medium. The corresponding angle outside the medium is $nN\lambda/D = N\lambda_o/D = 2.11$ mrad $= 0.12°$.

Slower sound: We have $N = (D/v_s)B$, which is inversely proportional to v_s. Thus, if v_s is reduced from 6 to 3.1 km/s, with all other parameters remaining the same, N increases from 100 to $100 \times 6/3.1 = 193.5$.

EXERCISE 20.2-3

Resolving Power of an Acousto-Optic Filter

Let $\overline{\theta}_{\mathcal{B}} = \sin^{-1}(\overline{\lambda}/2\Lambda)$ be the Bragg angle at wavelength $\overline{\lambda}$. Consider the consequences of fixing the angle θ at the value $\overline{\theta}_{\mathcal{B}}$ and altering the wavelength λ. The Bragg angle is then altered and since θ is no longer the Bragg angle, the reflection efficiency decreases. Considering small angles, it is evident from Fig. 20.1-3 that when θ differs from $\theta_{\mathcal{B}}$ by $\lambda/2L$, where L is the length of the cell, the reflection efficiency diminishes to zero. This occurs when $\lambda/2\Lambda - \overline{\lambda}/2\Lambda \approx \lambda/2L$. Defining $\Delta\lambda = \lambda - \overline{\lambda}$ as the minimum resolvable wavelength difference, we thus have $\Delta\lambda/2\Lambda \approx \lambda/2L$, so that $\Delta\lambda/\lambda \approx \Lambda/L = (1/f)(v_s/L) = 1/f\mathcal{T}$, where $\mathcal{T}$ is the transit time. It follows that the spectral resolving power of the acousto-optic filter is given by $\lambda/\Delta\lambda = f\mathcal{T}$.

20.3 ACOUSTO-OPTICS OF ANISOTROPIC MEDIA

EXERCISE 20.3-1

Transverse Acoustic Wave in a Cubic Crystal

As indicated in Example 20.3-2, all strain components of the transverse acoustic wave vanish except $s_{13} = s_{31} = S_0 \cos(\Omega t - qz)$. In accordance with Table 21.2-1 for contracted indices, this component is denoted s_5.

The photoelasticity matrix for the cubic crystal is provided in (20.3-4) so that the components of the impermeability tensor $\boldsymbol{\eta}$ are given by

$$\Delta \begin{bmatrix} \eta_{11} \\ \eta_{22} \\ \eta_{33} \\ \eta_{32} \\ \eta_{31} \\ \eta_{12} \end{bmatrix} = \begin{bmatrix} \mathrm{p}_{11} \mathrm{p}_{12} \mathrm{p}_{12} & 0 & 0 & 0 \\ \mathrm{p}_{12} \mathrm{p}_{11} \mathrm{p}_{12} & 0 & 0 & 0 \\ \mathrm{p}_{12} \mathrm{p}_{12} \mathrm{p}_{11} & 0 & 0 & 0 \\ 0 \;\; 0 \;\; 0 & \mathrm{p}_{44} & 0 & 0 \\ 0 \;\; 0 \;\; 0 & 0 & \mathrm{p}_{44} & 0 \\ 0 \;\; 0 \;\; 0 & 0 & 0 & \mathrm{p}_{44} \end{bmatrix} \begin{bmatrix} 0 \\ 0 \\ 0 \\ 0 \\ s_5 \\ 0 \end{bmatrix} .$$

The sole nonzero component is therefore $\Delta\eta_{31} = \Delta\eta_{13} = \mathrm{p}_{44} s_5$.
Moreover, since the crystal is cubic, $\eta_{11} = \eta_{22} = \eta_{33} = 1/n^2$.
The index ellipsoid, given by $\sum_{ij} \eta_{ij}\, x_i x_j = 1,\ i, j = 1, 2, 3$, may therefore be written in the form

$(x_1^2 + x_2^2 + x_3^2)/n^2 + 2\mathrm{p}_{44} s_5 x_1 x_3 = 0$, or

$x_2^2/n^2 + [(x_1^2 + x_3^2)/n^2 + 2\mathrm{p}_{44} s_5 x_1 x_3] = 0.$

The transformation $u_1 = (x_1 - x_3)/\sqrt{2}$; $u_3 = (x_1 + x_3)/\sqrt{2}$; $u_2 = x_2$ yields the ellipsoid $u_1^2/n_1^2 + u_2^2/n_2^2 + u_3^2/n_3^2 = 1$, with

$$1/n_1^2 = 1/n^2 + \mathrm{p}_{44} s_5 \tag{1}$$
$$n_2 = n \tag{2}$$
$$1/n_3^2 = 1/n^2 - \mathrm{p}_{44} s_5. \tag{3}$$

For $\mathrm{p}_{44} s_5 \ll 1$, Taylor-series expansions of (1) and (3) provide the desired results.

CHAPTER
21

ELECTRO-OPTICS

21.1 PRINCIPLES OF ELECTRO-OPTICS

EXERCISE 21.1-1

Coupling-Efficiency Spectral Response

According to (21.1-22), the switching voltage at wavelength $\overline{\lambda}_0$ is $V_0 = \sqrt{3}\,\mathcal{C}\,\overline{\lambda}_0\,d/\pi n^3 \mathrm{r}$. The coupling efficiency at $V = V_0$ for light at wavelength $\overline{\lambda}_0$ is 0. However, at a different wavelength, say λ_0, the coupling efficiency is given by (21.1-23):
$\mathcal{T} = (\pi/2)^2\,\mathrm{sinc}^2\left\{\frac{1}{2}[1+3(V/V_{01})^2]^{1/2}\right\}$, where $V_{01} = \sqrt{3}\,\mathcal{C}\,\lambda_0\,d/\pi n^3\mathrm{r}$ is the appropriate switching voltage at the wavelength λ_0. Fixing the applied voltage at $V = V_0$ and substituting $(V_0/V_{01}) = (\overline{\lambda}_0/\lambda_0)$ leads to $\mathcal{T} = (\pi/2)^2\,\mathrm{sinc}^2\left\{\frac{1}{2}[1+3(\overline{\lambda}_0/\lambda_0)^2]^{1/2}\right\}$.
The distance between λ_0 and $\overline{\lambda}_0$ is conveniently framed in terms of the relative deviation $u \equiv (\lambda_0 - \overline{\lambda}_0)/\overline{\lambda}_0$, so that $\overline{\lambda}_0/\lambda_0 = 1/(1+u)$. Expressing the coupling efficiency in terms of u provides $\mathcal{T} = (\pi/2)^2\,\mathrm{sinc}^2\left\{\frac{1}{2}[1+3/(1+u)^2]^{1/2}\right\}$, which is plotted below. For $u = 0$ the coupling efficiency is 0, as expected. As $|u|$ increases, representing increasing wavelength deviation, $\mathcal{T}$ increases so that light is coupled by the device. At $u = 0.1$, for example, we obtain $\mathcal{T} = 0.0127$, indicating that a 10% relative wavelength deviation away from $\overline{\lambda}_0$ results in a 1.27% coupling efficiency.

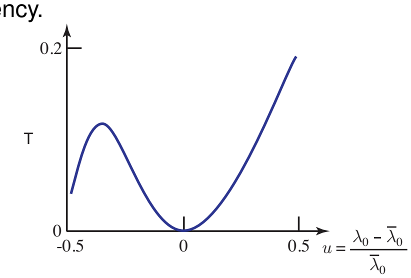

21.2 ELECTRO-OPTICS OF ANISOTROPIC MEDIA

EXERCISE 21.2-1

Intensity Modulation Using the Kerr Effect

When an electric field E is applied to an isotropic material exhibiting the Kerr electro-optic effect, the material becomes uniaxial with the optic axis along the direction of the electric field, and with refractive indices given by (21.2-23) and (21.2-24), respectively: $n_o(E) = n - \frac{1}{2}n^3\mathrm{s}_{12}E^2$ and $n_e(E) = n - \frac{1}{2}n^3\mathrm{s}_{11}E^2$. For a longitudinal electro-optic modulator, the light propagates along the direction of the electric field so the refractive index is $n_o(E)$. For a cell of length d with an applied voltage V, we have $E = V/d$.

Phase Shift:
$$\varphi = \left(\frac{2\pi}{\lambda_o}\right) n_o(E) d = \left(\frac{2\pi}{\lambda_o}\right) n d - \left(\frac{\pi}{\lambda_o}\right) n^3 \mathrm{s}_{12} \left(\frac{V}{d}\right)^2 d = \varphi_0 - \pi\left(\frac{V}{V_\pi}\right)^2,$$
where $\varphi_0 = (2\pi/\lambda_o)nd$ and $V_\pi = (\lambda_o d/n^3\mathrm{s}_{12})^{1/2}$.

Phase Retardation: Since the light is traveling along the optic axis there is no phase retardation ($V_\pi = \infty$).

CHAPTER
22

NONLINEAR OPTICS

22.1 NONLINEAR OPTICAL MEDIA

EXERCISE 22.1-1

Intensity of Light Required to Elicit Nonlinear Effects

a) The ratio of the second to first terms in (22.1-2) is $2\mathrm{d}\mathcal{E}/\epsilon_o\chi$, which is chosen to be 0.01 and therefore requires $\mathcal{E} = \epsilon_o\chi/200\mathrm{d} = \epsilon_o(n^2-1)/200\mathrm{d}$. Substituting $\epsilon_o = 8.85\times10^{-12}$ F/m, along with $n = 1.5$ and $\mathrm{d} = 6.8\times10^{-24}$ C/V^2 for ADP ($NH_4H_2PO_4$), we obtain $\mathcal{E} = 8.13\times10^9$ V/m. This corresponds to an intensity $I = \mathcal{E}^2/\eta$, where $\eta = \eta_o/n$ and $\eta_o = \sqrt{\mu_o/\epsilon_o} = 377\,\Omega$. This in turn gives $I = 2.63\times10^{17}$ W/m^2 $= 2.63\times10^{13}$ W/cm^2, which is very large.

b) The ratio of the third term to the first in (22.1-2), $4\chi^{(3)}\mathcal{E}^2/\epsilon_o\chi$, is also taken to be 0.01, which requires $\mathcal{E}^2 = \epsilon_o\chi/400\chi^{(3)} = \epsilon_o(n^2-1)/400\chi^{(3)}$. Substituting $\epsilon_o = 8.85\times10^{-12}$ F/m, along with $n = 1.6$ and $\chi^{(3)} = 4.4\times10^{-32}$ Cm/V^3 for CS_2, leads to $\mathcal{E} = 8.86\times10^8$ V/m. The corresponding intensity is $I = \mathcal{E}^2/\eta = n\mathcal{E}^2/\eta_o = 3.33\times10^{15}$ W/m^2 $= 3.33\times10^{11}$ W/cm^2.

22.2 SECOND-ORDER NONLINEAR OPTICS

EXERCISE 22.2-1

Non-Collinear Type-II Second-Harmonic Generation (SHG)

From (22.2-26) we have

$$n_o(\omega)\sin\theta_1 = n(\theta+\theta_2,\omega)\sin\theta_2 \qquad (1)$$

$$n_o(\omega)\cos\theta_1 + n(\theta+\theta_2,\omega)\cos\theta_2 = 2n(\theta,2\omega). \qquad (2)$$

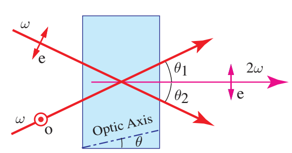

Therefore

$$n_o^2(\omega)\sin^2\theta_1 = n^2(\theta+\theta_2,\omega)\sin^2\theta_2 \qquad (3)$$

$$n_o^2(\omega)\cos^2\theta_1 = [2n(\theta,2\omega) - n(\theta+\theta_2,\omega)\cos\theta_2]^2. \qquad (4)$$

Adding (3) and (4), we obtain

$$n_o^2(\omega) = n^2(\theta+\theta_2,\omega) + 4n^2(\theta,2\omega) - 4n(\theta,2\omega)\,n(\theta+\theta_2,\omega)\cos\theta_2$$

so that

$$n_o^2(\omega) = \left[\frac{\cos^2(\theta+\theta_2)}{n_{o_1}^2} + \frac{\sin^2(\theta+\theta_2)}{n_{e_1}^2}\right]^{-1} + 4\left[\frac{\cos^2\theta}{n_{o_2}^2} + \frac{\sin^2\theta}{n_{e_2}^2}\right]^{-1}$$
$$- 4\cos\theta_2\left[\frac{\cos^2\theta}{n_{o_2}^2} + \frac{\sin^2\theta}{n_{e_2}^2}\right]^{-1/2}\left[\frac{\cos^2(\theta+\theta_2)}{n_{o_1}^2} + \frac{\sin^2(\theta+\theta_2)}{n_{e_1}^2}\right]^{-1/2}. \qquad (5)$$

For a KDP crystal, $\lambda_1 = 1.06\ \mu\text{m}$ and $\lambda_2 = \lambda_1/2$, and we have $n_{o_1} = 1.494$, $n_{e_1} = 1.4599$, $n_{o_2} = 1.5123$, $n_{e_2} = 1.4707$.

The procedure for solving (5) is as follows:

a) Substitute $n_{o_1}, n_{o_2}, n_{e_1}, n_{e_2}$ into (5).
b) Substitute θ from $0 \to 90°$.
c) Use a Matlab program to solve for the value of θ_2 that satisfies (5).
d) Use (1) to compute θ_1

A plot of the resultant values of θ_1 and θ_2 versus the angle between the optic axis θ and the direction of the SH wave is shown in the figure.

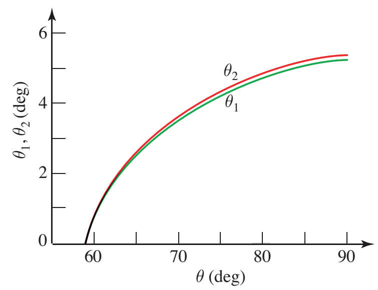

22.3 THIRD-ORDER NONLINEAR OPTICS

EXERCISE 22.3-1

Third-Order Nonlinear Optical Media Exhibit the Kerr Electro-Optic Effect

$\mathcal{P}_{\rm NL} = 4\chi^{(3)}\mathcal{E}^3 = 4\chi^{(3)}[E(0) + \frac{1}{2}E(\omega)e^{j\omega t} + \frac{1}{2}E(\omega)^* e^{-j\omega t}]^3$.

Carrying out the expansion shows that the term proportional to $e^{j\omega t}$ has amplitude $\frac{1}{2}P_{\rm NL}(\omega)$, where $P_{\rm NL}(\omega) = 4\chi^{(3)}[3E^2(0)E(\omega) + \frac{1}{2}|E(\omega)|^2 E(\omega)]$.

If $|E(\omega)| \ll E(0)$, the second term above is negligible and $P_{\rm NL}(\omega) \approx 12\chi^{(3)}E^2(0)E(\omega)$, which can be cast in the form $\epsilon_o\, \Delta\chi\, E(\omega)$ with $\Delta\chi \approx 12\chi^{(3)}E^2(0)/\epsilon_o$.

Since $\chi = n^2 - 1$, we have $\Delta\chi = 2n\Delta n$ and $\Delta n = \Delta\chi/2n$. Thus, $\Delta n \approx 6\chi^{(3)}E^2(0)/\epsilon_o n$, which is equivalent to a refractive-index change associated with the Kerr electro-optic effect given by $\Delta n = -\frac{1}{2}\mathrm{s}\, n^2\, E^2(0)$, provided that $\mathrm{s} = -12\chi^{(3)}/\epsilon_o\, n^4$.

EXERCISE 22.3-2

Optical Kerr Lens

The intensity $I \approx I_0[1 - (x^2 + y^2)/W^2]$ induces a nonlinear refractive index $n(I) = n + n_2 I = n + n_2 I_0[1 - (x^2 + y^2)/W^2]$ in a thin sheet of material that exhibits the optical Kerr effect. The result is a medium whose complex amplitude transmittance is given by $\exp[-jk_o\, \mathsf{d}\, n(I)] = \exp[-jk_o \mathsf{d}\,(n + n_2 I_0)] \cdot \exp[jk_o \mathsf{d}\, n_2\, I_0(x^2 + y^2)/W^2] = h_0 \exp[jk_o(x^2 + y^2)/2f]$, where $h_0 = \exp[-jk_o \mathsf{d}\,(n + n_2 I_0)]$ and $1/2f = n_2 I_0 \mathsf{d}/W^2$. Hence, $f = W^2/2n_2 I_0 \mathsf{d}$, revealing that the medium acts as a lens whose focal length f is inversely proportional to I_0.

EXERCISE 22.3-3

Optical Kerr Effect in the Presence of Three Waves

$$\begin{aligned}\mathcal{P}_{\rm NL} &= 4\chi^{(3)}\mathcal{E}^3\\ &= \tfrac{1}{2}\chi^{(3)}[E(\omega_1)\exp(j\omega_1 t) + E^*(\omega_1)\exp(-j\omega_1 t)\\ &\quad +E(\omega_2)\exp(j\omega_2 t) + E^*(\omega_2)\exp(-j\omega_2 t)\\ &\quad +E(\omega_3)\exp(j\omega_3 t) + E^*(\omega_3)\exp(-j\omega_3 t)]^3.\end{aligned}$$

The term that varies as $\exp(j\omega_1 t)$ has an amplitude $\frac{1}{2}P_{\rm NL}(\omega_1)$ where
$P_{\rm NL}(\omega_1) = \chi^{(3)}\,[3|E(\omega_1)|^2\,E(\omega_1) + 6|E(\omega_2)|^2\,E(\omega_1) + 6|E(\omega_3)|^2\,E(\omega_1)\,]$.

Substituting $I_1 = |E(\omega_1)|^2/2\eta$, $I_2 = |E(\omega_2)|^2/2\eta$, and $I_3 = |E(\omega_3)|^2/2\eta$, we obtain
$P_{\rm NL}(\omega_1) = 2\eta\chi^{(3)}[\,3I_1 + 6I_2 + 6I_3\,]\,E(\omega_1) = 2\epsilon_o n\,\Delta n\,E(\omega_1)$, where
$\Delta n = n_2 I,\ n_2 = 3\eta\chi^{(3)}/\epsilon_o n = 3\eta_o\chi^{(3)}/\epsilon_o n^2$, and $I = I_1 + 2I_2 + 2I_3$.

The wave travels with a velocity $c_o/(n+\Delta n) = c_o/(n+n_2 I)$ controlled by the intensities of the three waves.

22.4 SECOND-ORDER NONLINEAR OPTICS: COUPLED WAVES

EXERCISE 22.4-1

SHG as Degenerate Three-Wave Mixing

As in the non-degenerate 3-wave mixing case, we make use of (22.4-1), (22.4-2), and (22.4-3), but here we have only two waves at frequencies $\omega_1 = \omega$ and $\omega_3 = 2\omega$.
Substituting $E = \frac{1}{2}\{E_1\exp(j\omega t) + E_1^*\exp(-j\omega t) + E_3\exp(j2\omega t) + E_3^*\exp(-j2\omega t)\}$ into (22.4-3), we obtain
$\mathcal{P}_{\rm NL} = \frac{1}{2}\{P_1\exp(j\omega t) + P_1^*\exp(-j\omega t) + P_3\exp(j2\omega t) + P_3^*\exp(-j2\omega t)\}$, where
$P_1 = 2\mathrm{d}E_3E_1^*$ and $P_3 = \mathrm{d}E_1E_1$. Substituting this in turn into (22.4-2) then leads to
$\mathcal{S}_{\rm NL} = \frac{1}{2}\{S_1\exp(j\omega t) + S_1^*\exp(-j\omega t) + S_3\exp(j2\omega t) + S_3^*\exp(-j2\omega t)\}$, where
$S_1 = \mu_o\omega^2 P_1 = 2\mu_o\omega^2\mathrm{d}E_3E_1^*$ and $S_3 = \mu_o(2\omega)^2P_3 = \mu_o\omega_3^2\mathrm{d}E_1E_1^*$, from which (22.4-16) follow.

EXERCISE 22.4-2

Photon-Number Conservation: The Manley–Rowe Relations

These results follow directly from (2a), (2b), and (2c) in the solution to Exercise 22.4-3.

EXERCISE 22.4-3

Energy Conservation

Multiply (22.4-20a) by $\mathfrak{a}_1^*$:
$$\mathfrak{a}_1^* d\mathfrak{a}_1/dz = -j\mathfrak{g}\mathfrak{a}_1^*\mathfrak{a}_2^*\mathfrak{a}_3\exp(-j\Delta kz). \qquad (1)$$

Add (1) to its conjugate and note that $\mathfrak{a}_1^* d\mathfrak{a}_1/dz + \mathfrak{a}_1 d\mathfrak{a}_1^*/dz = (d/dz)|\mathfrak{a}_1|^2$, to obtain:
$$(d/dz)|\mathfrak{a}_1|^2 = -j\mathfrak{g}\mathfrak{a}_1^*\mathfrak{a}_2^*\mathfrak{a}_3\exp(-j\Delta kz) + \text{c.c.} \qquad (2a)$$
Similarly,
$$(d/dz)|\mathfrak{a}_2|^2 = -j\mathfrak{g}\mathfrak{a}_1^*\mathfrak{a}_2^*\mathfrak{a}_3\exp(-j\Delta kz) + \text{c.c.} \qquad (2b)$$
$$\begin{aligned}(d/dz)|\mathfrak{a}_3|^2 &= -j\mathfrak{g}\mathfrak{a}_1\mathfrak{a}_2\mathfrak{a}_3^*\exp(j\Delta kz) + \text{c.c.}\\ &= \ \ j\mathfrak{g}\mathfrak{a}_1^*\mathfrak{a}_2^*\mathfrak{a}_3\exp(-j\Delta kz) + \text{c.c.} \qquad (2c)\end{aligned}$$

Now multiply (2a) by $\hbar\omega_1$, (2b) by $\hbar\omega_2$, and (2c) by $\hbar\omega_3$ and add the three equations:

$(d/dz)[\,\hbar\omega_1|\mathfrak{a}_1|^2+\hbar\omega_2|\mathfrak{a}_2|^2+\hbar\omega_3|\mathfrak{a}_3|^2\,] = -j\mathfrak{g}\hbar(\omega_1+\omega_2-\omega_3)\mathfrak{a}_1^*\mathfrak{a}_2^*\mathfrak{a}_3\exp(-j\Delta kz)+$ c.c. (3)

Because $\omega_3=\omega_1+\omega_2$, the right-hand side of (3) vanishes and we obtain:
$(d/dz)[\,\hbar\omega_1|\mathfrak{a}_1|^2+\hbar\omega_2|\mathfrak{a}_2|^2+\hbar\omega_3|\mathfrak{a}_3|^2\,] = (d/dz)(I_1+I_2+I_3)=0.$ (4)

EXERCISE 22.4-4

Coupled-Wave Equations for SHG

Write E_1 and E_3 as $E_1=(2\eta\hbar\omega)^{1/2}\mathfrak{a}_1\exp(-jk_1z)$ and $E_3=(2\eta\hbar2\omega)^{1/2}\mathfrak{a}_3\exp(-jk_3z)$, respectively, and insert these formulas into (22.4-16a). Use of the slowly varying envelope approximation in (22.4-19) on the resulting equation then leads to

$$(2\eta\hbar\omega)^{1/2}(-j2k_1)(d\mathfrak{a}_1/dz)\exp(-jk_1z) = \\ -2\mu_o\omega^2\mathrm{d}(2\eta\hbar\omega)^{1/2}(4\eta\hbar\omega)^{1/2}\mathfrak{a}_3\exp(-jk_3z)\mathfrak{a}_1^*\exp(jk_1z),$$

whence $(d\mathfrak{a}_1/dz)=(\mu_o\omega^2\mathrm{d}/jk_1)(4\eta\hbar\omega)^{1/2}\mathfrak{a}_3\mathfrak{a}_1^*\exp(-j\Delta kz)=-j\mathfrak{g}\mathfrak{a}_3\mathfrak{a}_1^*\exp(-j\Delta kz)$, where $\Delta k=k_3-2k_1$ and $\mathfrak{g}=(\mu_o\omega^2\mathrm{d}/k_1)(4\eta\hbar\omega)^{1/2}$, or $\mathfrak{g}^2=(\mu_oc\omega\mathrm{d})^2(4\eta\hbar\omega)=(\eta\omega\mathrm{d})^2(4\eta\hbar\omega)=4\hbar\omega^3\eta^3\mathrm{d}^2$.

Equation (22.4-27b) can be similarly obtained.

EXERCISE 22.4-5

Infrared Up-Conversion

Parameters: $\mathrm{d}=1.5\times10^{-22}$ C/V^2; $n=2.6$; $\lambda_1=10.6\times10^{-6}$ m; $\lambda_2=1.06\times10^{-6}$ m; $P_2=1$ W; $A=10^{-8}$ m^2; $L=10^{-2}$ m.

Wavelengths: Since $\omega_3=\omega_1+\omega_2$, we have $1/\lambda_3=1/\lambda_1+1/\lambda_2$ or $\lambda_3=\lambda_1\lambda_2/(\lambda_1+\lambda_2)$. Hence, $\lambda_3=0.9636\times10^{-6}$ m $=963.6$ nm.

Up-conversion efficiency: As provided in (22.4-43), the up-conversion efficiency is expressed as $\eta_{\mathrm{OFC}}=2\eta_o^3\omega_3^2(\mathrm{d}^2/n^3)(L^2/A)P_2$. Substituting $\eta_o=377\,\Omega$; $\omega_3=2\pi c_o/\lambda_3=1.96\times10^{15}$ rad/s; $\mathrm{d}^2/n^3=1.3\times10^{-45}$ C^2/V^4; $L^2/A=10^4$; and $c_o=3\times10^8$ m/s, leads to $\eta_{\mathrm{OFC}}\approx5.4\times10^{-3}=0.54\%$.

EXERCISE 22.4-6

Gain of an OPA

Parameters: $\lambda_1=2.5\ \mu\mathrm{m}$; $\lambda_3=1.064\ \mu\mathrm{m}$; $L=2$ cm; $G=3$ dB;
For KTP: $n=1.75$ and $\mathrm{d}=2.3\times10^{-23}$ C/V^2.

a) Since $\omega_2=\omega_3-\omega_1$, we have $1/\lambda_2=1/\lambda_3-1/\lambda_1$ or $\lambda_2=\lambda_3\lambda_1/(\lambda_1-\lambda_3)$. Thus, $\lambda_2=1.85\ \mu\mathrm{m}$.

b) From (22.4-47), $C=\sqrt{2\omega_1\omega_2\,\eta_o^3\dfrac{\mathrm{d}^2}{n^3}}=2\pi c_o\mathrm{d}\sqrt{\dfrac{2}{\lambda_1\lambda_2}\left(\dfrac{\eta_o}{n}\right)^3}=9.0\times10^{-5}\ \ \mathrm{W}^{-1/2}$.

c) A gain of 3 dB signifies that $G=\cosh^2(\gamma L/2)=2$ so that $\sqrt{2}=\cosh(\gamma L/2)$ and $\gamma L/2=\cosh^{-1}\sqrt{2}=\ln(1+\sqrt{2})$. Thus,

$\gamma=(2/L)\ln(1+\sqrt{2})=88\ \mathrm{m}^{-1}$. Also, from (22.4-47) we have

$\gamma=2C\sqrt{P_3/A}$, so that

$$\frac{P_3}{A}=\left(\frac{\gamma}{2C}\right)^2=2.39\times10^{11}\ \mathrm{W/m^2}.$$

d) If the laser power is 2.39 W, then the beam cross-sectional area is $A=10\ \mu\mathrm{m}^2$.

22.5 THIRD-ORDER NONLINEAR OPTICS: COUPLED WAVES

EXERCISE 22.5-1

THG in the Undepleted-Pump Approximation

We begin with the Helmholtz equations (22.5-4) at the fundamental and third-harmonic frequencies,

$$(\nabla^2 + k_q^2)E_q = -S_q, \quad q = 1, 3,$$

where (22.5-23) provides

$$S_1 = \mu_o \omega_1^2 \chi^{(3)} \left[3E_3 E_1^{*2} + 3E_1 \left(|E_1|^2 + 2|E_3|^2\right)\right]$$
$$S_3 = \mu_o \omega_3^2 \chi^{(3)} \left[E_1^3 + 3E_3 \left(|E_3|^2 + 2|E_1|^2\right)\right].$$

Using the relations $E_q = A_q \exp(-jk_q z)$, $q = 1, 3$, and the slowly varying envelope approximation (22.4-19), $(\nabla^2 + k_q^2)[A_q \exp(-jk_q z)] \approx -j2k_q(dA_q/dz)\exp(-jk_q z)$, the Helmholtz equations become

$$\frac{dA_1}{dz} = -j\tfrac{3}{2}\eta\omega_1\chi^{(3)}\left[A_3 A_1^{*2}\exp(j\Delta k\, z) + A_1\left(|A_1|^2 + 2|A_3|^2\right)\right]$$
$$\frac{dA_3}{dz} = -j\tfrac{1}{2}\eta\omega_3\chi^{(3)}\left[A_1^3\exp(-j\Delta k\, z) + 3A_3\left(|A_3|^2 + 2|A_1|^2\right)\right],$$

where $\Delta k = 3k_1 - k_3$.

Under the undepleted pump approximation ($|A_3| \ll |A_1|$), the amplitude of the fundamental wave A_1 is assumed to be approximately constant (i.e., it does not vary with z), so the only equation of interest is

$$\frac{dA_3}{dz} = -j\tfrac{1}{2}\eta\omega_3\chi^{(3)}\left[A_1^3\exp(-j\Delta k\, z) + 3A_3\left(|A_3|^2 + 2|A_1|^2\right)\right].$$

The first term on the right-hand side of this equation represents third-harmonic generation while the second term represents the optical Kerr effect.

This equation may simplified since $|A_3| \ll |A_1|$. The term $|A_3|^2$ in the sum $|A_3|^2 + 2|A_1|^2$ may therefore be neglected. The term $6A_3|A_1|^2$, which is much smaller than A_1^3, may also be neglected. In any case, since A_1 is constant, the term $6A_3|A_1|^2$ represents a constant change of the refractive index due to the optical Kerr effect, and may be ignored in the context of third-harmonic generation.

Thus, the final outcome is

$$\frac{dA_3}{dz} \approx -j\tfrac{1}{2}\eta\omega_3\chi^{(3)}A_1^3\exp(-j\Delta k\, z).$$

With the substitution $A_q = \sqrt{2\eta\hbar\omega_q}\,\mathfrak{a}_q$, this result may be written as

$$\frac{d\mathfrak{a}_3}{dz} = -j\mathfrak{g}\mathfrak{a}_1^3\exp(-j\Delta k\, z) \quad \text{with} \quad \mathfrak{g} = \hbar\sqrt{\omega_1^3\omega_3}\,\eta^2\chi^{(3)}.$$

22.7 DISPERSIVE NONLINEAR MEDIA

EXERCISE 22.7-1

Polarization Density for an Anharmonic-Oscillator Medium

In accordance with Newton's law, $\mathcal{F} = ma$, we have
$e\mathcal{E} - (\kappa x + \kappa_2 x^2) - m\zeta\, dx/dt = m\, d^2x/dt^2$.

Dividing by m, reordering terms, and substituting $\kappa/m = \omega_0^2$,
we obtain $d^2x/dt^2 + \zeta\, dx/dt + \omega_0^2\, x + (\kappa_2/m)\, x^2 = (e/m)\, \mathcal{E}$. (1)

For a medium containing N atoms per unit volume, the polarization density is $\mathcal{P} = Nex$.
Substituting $x = \mathcal{P}/Ne$ into (1), we obtain
$d^2\mathcal{P}/dt^2 + \zeta\, d\mathcal{P}/dt + \omega_0^2\, \mathcal{P} + (\kappa_2/m)\, \mathcal{P}^2/Ne = (Ne^2/m)\, \mathcal{E}$. (2)

Defining two parameters, χ_0 and b, such that
$\omega_0^2 \epsilon_0 \chi_0 = Ne^2/m$ (3)
and
$\omega_0^2 \epsilon_0 \chi_0 b = \kappa_2/mNe$, (4)
respectively, leads to (22.7-8).

Equation (3) provides that $\chi_0 = Ne^2/m\omega_0^2\epsilon_0$ while (4) gives $b = \kappa_2/(mNe\omega_0^2\epsilon_0\chi_0)$.
Finally, inserting (3) into (4) yields $b = \kappa_2/e^3N^2$, as promised.

EXERCISE 22.7-2

Miller's Rule

Consider the superposed waves $\mathcal{E} = \mathrm{Re}\,\{E(\omega_1)\exp(j\omega_1 t) + E(\omega_2)\exp(j\omega_2 t)\}$.
The first iteration (ignoring the nonlinear effect) gives a polarization density
$\mathcal{P} = \mathrm{Re}\,\{P(\omega_1)\exp(j\omega_1 t) + P(\omega_2)\exp(j\omega_2 t)\}$, where

$P_1(\omega_1) = \epsilon_0 \chi(\omega_1) E(\omega_1)$ (1a)
$P_1(\omega_2) = \epsilon_0 \chi(\omega_2) E(\omega_2)$ (1b)

In the second iteration, we have a driving force $\mathcal{F} = \mathcal{E} - b\,\mathcal{P}^2$, i.e.,

$$\mathcal{F} = \mathrm{Re}\,\{E(\omega_1)\exp(j\omega_1 t) + E(\omega_2)\exp(j\omega_2 t)\}$$
$$- b\,[\mathrm{Re}\,\{P_1(\omega_1)\exp(j\omega_1 t) + P_1(\omega_2)\exp(j\omega_2 t)\}]^2.$$

This force has many components, including a component $\mathrm{Re}\,\{F(\omega_3)\exp(j\omega_3)\}$ of frequency $\omega_3 = \omega_1 + \omega_2$ and complex amplitude $F(\omega_3) = -(b/2)P_1(\omega_1)P_1(\omega_2)$. This force creates a polarization density at frequency ω_3 with complex amplitude $P_2(\omega_3) = \epsilon_0\chi(\omega_3)F(\omega_3) = \epsilon_0\chi(\omega_3)(-b/2)P_1(\omega_1)P_1(\omega_2)$. Substitution from (1) yields
$P_2(\omega_3) = \epsilon_0^3(-b/2)\chi(\omega_1)\chi(\omega_2)\chi(\omega_3)$, from which (22.7-14) follows.

CHAPTER
23

ULTRAFAST OPTICS

23.3 PULSE PROPAGATION IN OPTICAL FIBERS

EXERCISE 23.3-1

Dispersion Compensation in Optical Fibers

a) The dispersion length $z_0 = \pi\tau_0^2/D_\nu$, where $D_\nu = -(\lambda_o^2/c_o)D_\lambda$, so that $z_0 = \pi\tau_0^2 c_o/\lambda_o^2 D_\lambda$. For the first fiber segment we have:
$D_\lambda = 20$ ps/km-nm $= 2\times10^{-5}\ \mathrm{s/m^2}$,
$\tau_0 = 10\ \mathrm{ps} = 10^{-11}\ \mathrm{s}$, and
$\lambda_o = 1.55\ \mu\mathrm{m} = 1.55\times10^{-6}\ \mathrm{m}$,
so that $z_0 = 1.96\ \mathrm{km}$.
At a distance $d_1 = 100\ \mathrm{km}$, the chirp parameter and the pulse width are, respectively,
$a = d_1/z_0 = 51$
$\tau_1 = \tau_0\sqrt{1+(d_1/z_0)^2} \approx 510\ \mathrm{ps}.$

b) The dispersion compensation condition is $d_1 D_\lambda + d_2 D'_\lambda = 0$ so that $d_2 = -d_1 D_\lambda/D'_\lambda$. If the dispersion coefficient of the second fiber segment is $D'_\lambda = -100$ ps/km-nm, we have $d_2 = 100$ km $\cdot\,(20/100) = 20\ \mathrm{km}$.

EXERCISE 23.3-2

Dispersion Compensation by Use of a Periodic Sequence of Phase Modulators

The effect of GVD on pulse propagation over the distance *d* between its minimum width (where it is unchirped) and its maximum width is described by the following equations (see Table 23.3-1):

Pulse width: $$\tau = \tau_0\sqrt{1+a^2} \tag{1}$$

Chirp parameter: $$a = z/z_0 \tag{2}$$

Dispersion length: $$z_o = \pi\tau_o^2/D_\nu\,. \tag{3}$$

The quadratic phase modulator does not alter the pulse width, but it changes the chirp parameter. A change by a factor of $-2a$ is obtained if

$$-2a = \zeta\tau^2\,. \tag{4}$$

This change guarantees that the pulse is modified periodically, as shown in Fig. 23.3-7. Substituting (1), (2), and (3) into (4) leads to (23.3-23).

CHAPTER

24

OPTICAL INTERCONNECTS AND SWITCHES

24.1 OPTICAL INTERCONNECTS

EXERCISE 24.1-1

Interconnection Capacity

Assume that the hologram is divided into L sub-holograms, each of which contains M spatial harmonic functions ($M^{1/2}$ in the x direction and $M^{1/2}$ in the y direction). The incident ray on each sub-hologram is directed into M simultaneous directions, so that each of L points is connected to M points. If $a \times a$ is the area of the hologram, then a^2/L is the area of the sub-hologram. A width $a/L^{1/2}$ corresponds to a spatial frequency uncertainty $\Delta\nu = L^{1/2}/a$ (or angular uncertainty $\lambda L^{1/2}/a$). The M harmonic functions on a sub-hologram must be separated from one another by a spatial frequency equal to the uncertainty ($L^{1/2}/a$) in each direction, so that the spatial bandwidth B in one direction must be at least $M^{1/2}L^{1/2}/a$. It follows that $B \geq M^{1/2}L^{1/2}/a$ or $(Ba)^2 \geq ML$.

If $B = 1000$ lines/mm and $a = 1$ mm, then $(Ba)^2 = 1000$. If every point at the input plane is connected to every point at the output plane, i.e., if $L = M$, then $M^2 \leq (Ba)^2$ or $M \leq \sqrt{(Ba)^2} = 31.6$. Thus, at most, each of 31 points at the input are connected to each of 31 points at the output.

EXERCISE 24.1-2

The Logarithmic Map

The local spatial frequencies are
$\nu_x = (1/2\pi)\partial\varphi/\partial x = (1/\lambda d)(\ln x + 1 - 1 - x) = (1/\lambda d)(\ln x - x)$,
$\nu_y = (1/2\pi)\partial\varphi/\partial y = (1/\lambda d)(\ln y - y)$.

The angles of deflection are therefore
$\theta_x = \lambda\nu_x = (1/d)(\ln x - x), \quad \theta_y = \lambda\nu_y = (1/d)(\ln y - y)$.

Rays originating at location (x, y) at the hologram thus reach the location (x', y') in a plane a distance d away via $x' = x + \theta_x d = \ln x, \quad y' = y + \theta_y d = \ln y$, thereby indicating that the transformation $x' = \ln x$ and $y' = \ln y$ is implemented.

The phase function $\varphi(x, y)$ specified in (24.1-9) is obtained by recognizing that $\int \ln(x)\, dx = x\ln(x) - x$.

24.4 PHOTONIC LOGIC GATES

EXERCISE 24.4-1

Nonlinear Transmittance Functions that Exhibit Bistability

a) $\mathsf{T}(x) = 1/[(x-1)^2 + a^2]$, $a = 0.1$.

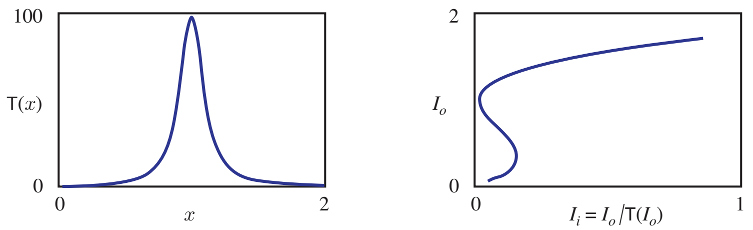

b) $\mathsf{T}(x) = 1/[1 + a^2 \sin^2(x+\theta)]$, $a = 5$, $\theta = \pi/4$.

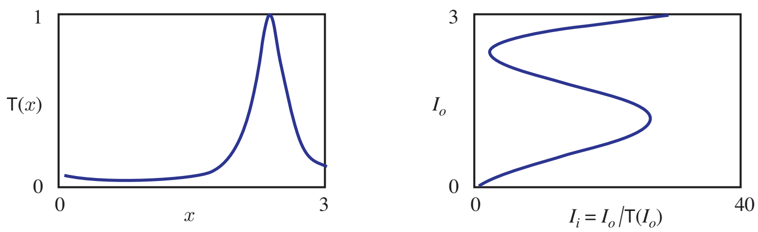

c) $\mathsf{T}(x) = (1/2)[1 + \cos(x+\theta)]$, $\theta = 3\pi/4$.

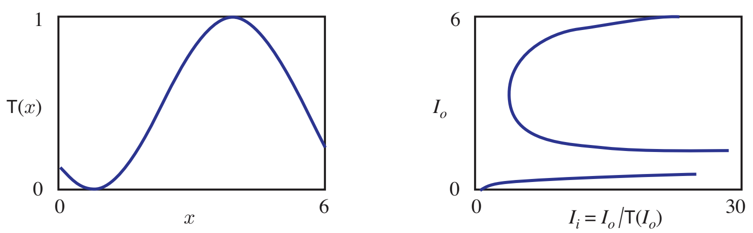

d) $\mathsf{T}(x) = \mathrm{sinc}^2[(a^2 + x^2)^{1/2}]$, $a = 2$.

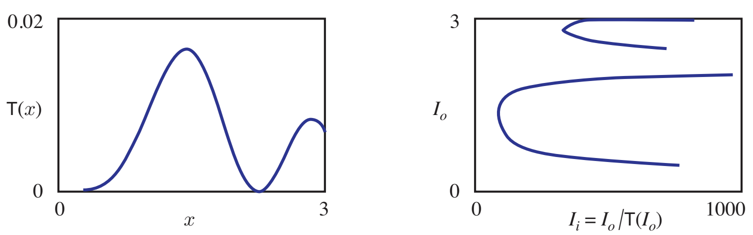

e) $\mathsf{T}(x) = (x+1)^2/(x+a)^2$, $a = -5$.